



NTNU – Trondheim
Norwegian University of
Science and Technology

Sedimentology and Diagenesis of Upper Triassic Sandstones, with Emphasis on the Snadd-Fruholmen Transition, Barents Sea

Marthe Auset

Petroleum Geoscience and Engineering

Submission date: June 2012

Supervisor: Mai Britt E. Mørk, IGB

Norwegian University of Science and Technology
Department of Geology and Mineral Resources Engineering

Abstract

Triassic and Jurassic sediments from two cores in the Nordkapp Basin, Barents Sea, were analyzed by sedimentological, petrographic, SEM and XRD methods. The objective of the study was to gain better understanding of the depositional environments of the Upper Triassic-Jurassic, Snadd-, Fruholmen- and Stø formations with emphasis a mineralogical shift in the transition between the Snadd and Fruholmen formations, and try to relate the differences to depositional environment, climatic changes and diagenesis.

The studied sediments of the Snadd and Fruholmen formations represent a transition from tidal flat, shoreline and inner shelf deposits. And the Stø Formation mainly represents inner shelf deposits, with exception of some fluvial deposits due to a local variation in one of the cores. The deposits represent an overall transgressive trend.

The diagenetic processes differ in the three formations due to dissimilar depositional environment. In the Snadd Formation rhizocretions have been observed in combination with rootlets, and high levels of iron and manganese indicate influence by fresh-water. XRD analyses of mudstones showed no great compositional differences the Snadd and Fruholmen formations supporting observations from sandstone compositions of similar provenance and environment above and below the formation boundary.

The largest compositional variation is seen between the Fruholmen and Stø formations, this is in accordance with other studies conducted in the Nordkapp Basin. The distinct increase in maturity may be due to extensive reworking connected with a regional transgression and sea-level rise.

Sammendrag

Sedimentene fra to kjerner fra Nordkappbassenget, Barentshavet, har blitt analysert ved hjelp av sedimentologi, petrografi, SEM og XRD. Målet med studiet har vært å øke forståelsen av avsetningsmiljøet i Snadd-, Fruholmen- og Støformasjonen, med hovedfokus på overgangen mellom Snadd- og Fruholmen. Dette har blitt gjort ved å analysere det mineralogiske skiftet mellom formasjonene, samt relatere ulikhetene til avsetningsmiljøet, klimaendringer og diagenese.

Sedimentene analysert i Snadd- og Fruholmenformasjonen representerer en overgang fra tidevannsflate, til strandsekvens, til indre-kontinentalsokkelavsetninger. Støformasjonen representerer i hovedsak avsetninger fra indre kontinentalsokkel, med unntak av noen fluviale avsetninger grunnet en lokal variasjon. Avsetningene i kjernene viser en generell transgressiv trend.

De diagenetiske prosessene er ulike i de tre formasjonene grunnet forskjellig avsetningsmiljø. Rhizolitter av sideritt har blitt observert, hvor sideritten har høye jern og mangan verdier og er trolig påvirket av ferskvann. XRD-analyser av leirstein fra Snadd- og Fruholmenformasjonen viser ingen endringer i sammensetning på tvers av formasjonsgrensen. Dette støtter opp om observasjonene gjort av sandsteinskomposisjonen, og tyder på tilsvarende proveniense og miljø over og under formasjonsgrensen.

Den største endringen i mineralogisk sammensetning kan sees mellom Fruholmen- og Støformasjonen, noe som samsvarer med tidligere studier fra Nordkappbassenget. Den markante økningen i modenhet kan skyldes omfattende omarbeiding knyttet til en regional transgresjon og havnivåøkning.

Acknowledgements

I want to thank my supervisor at NTNU, Professor Mai Britt Engeness Mørk, for great help and guidance during this thesis. I would also like to thank Atle Mørk at SINTEF Petroleum Research for assistance at Dora, Morten Peder Raanes, from the Department of Material Science and Engineering, for help on the SEM-lab. Further I would like to direct a thank you to PhD Candidate Kristian Drivenes, for finding the time to run and interpret the XRD analyses for this thesis.

Trondheim, June 22th 2012

Marthe Auset

Table of contents

Abstract	i
Sammendrag	ii
Acknowledgements	iv
1. Introduction	1
1.1 Objectives of the Study.....	1
1.2 Previous Work	1
2. Analytical Approach	3
2.1 Methods	3
2.1.1 Logging of Core	3
2.1.2 Optical Microscopy.....	3
2.1.3 SEM Analysis	4
2.1.4 XRD Analysis	4
2.2 Sources of Error.....	5
3. Geological Setting	7
3.1 Introduction	7
3.2 The Localities	11
3.2.1 The Nordkapp Basin	11
3.2.2 The Bjarmeland Platform -Lateral Comparison.....	11
3.2.3 The Formations	12
4. Sedimentology.....	15
4.1 Description of Cores	15
4.1.1 Core 7227/08-U-01	15
4.1.2 Core 7230/05-U-03	22
4.2 Facies Description	27
5. Petrography	33
5.1 Snadd Formation.....	33
5.1.1 Lithology and Texture.....	33
5.1.2 Detrital Grains.....	34
5.1.3 Diagenetic Minerals	34
5.2 Fruholmen Formation	38
5.2.1 Lithology and Texture in Core 7230/05-U-03	38
5.2.2 Detrital Grains in Core 7230/05-U-03	38

5.2.3 Diagenetic Minerals in Core 7230/05-U-03	39
5.2.4 Lithology and Texture in Core 7227/08-U-01	40
5.2.5 Detrital Grains in Core 7227/08-U-01	40
5.2.6 Diagenetic Minerals in Core 7227/08-U-01	41
5.3 Stø Formation	46
5.3.1 Lithology and Texture.....	46
5.3.2 Detrital Grains.....	46
5.3.3 Diagenetic Minerals	48
5.4 Modal Analysis.....	49
5.5 XRD Analysis.....	52
6. Interpretations and Discussion	53
6.1 Depositional Environment.....	53
6.1.1 Core 7227/08-U-01	53
6.1.2 Core 7230/05-U-03	59
6.2 Regional and Stratigraphic changes in mineral composition	61
6.2.1 Sandstones.....	62
6.2.2 Mudstones	64
6.2.3 Burial Diagenesis	64
6.2 Further work	66
7. Conclusion.....	67
References	69
Appendix A	II
Appendix B	XXII
Appendix C	XXVI

1. Introduction

This master thesis is written at the Department of Geology and Mineral Resources Engineering at NTNU, during the spring of 2012. The thesis is part of the 5 year master program in Petroleum geology.

This is a core study from shallow drilled cores 7227/08-U-01 and 7230/05-U-03 in the Nordkapp Basin, Barents Sea. Core 7227/08-U-01 was drilled in the central part of the southwestern basin segment, and core 7230/05-U-03 in the central eastern segment of the basin (Bugge et al., 2002). The emphasis of this thesis will be on the transition from the Snadd- to Fruholmen Formation. The thesis also incorporates data collected in the project thesis, from the shallow drilled core 7430/07-U-01 at the Bjarmeland Platform (Auset, 2011), for the purpose of lateral comparison (Fig. 3-1 and 3-2).

1.1 Objectives of the Study

The objective of this study is to gain better understanding of the sedimentology, petrography and diagenesis of the Upper Triassic-Jurassic, Snadd-, Fruholmen- and Stø formations with emphasis on the transition between Snadd and Fruholmen. The main focus will be to look for a mineralogical shift in the transition between the two formations, and try to relate the differences to depositional environment, climatic changes and diagenesis. An increased understanding of this could help further research and give insight that could be valuable for further investigations of the area.

1.2 Previous Work

Investigations of mineralogical composition of the Triassic-Jurassic have previously been done (Bergan and Knarud, 1992; Bugge et al. 2002; Mørk, 1999) and form part of the basis for this study. Bergan and Knarud (1992) also discussed the possible implications for paleodrainage and subsidence. Their article suggests significantly different mineralogy in the Triassic Ingøydjupet Group compared to the uppermost Triassic-Jurassic rocks of the Realgrunnen Group. Bergan and Knarud (1992) reports that the rocks of the Ingøydjupet Group contain 15-30% plagioclase feldspar whereas the rocks of the Realgrunnen Group contain less than 1% total feldspar. This dramatic shift in the mineral suit is believed to occur

throughout the Barents Sea and on the bordering land areas of Svalbard, Franz-Josef Land and the Timan-Pechora Basin (Bergan and Knarud, 1992).

Bugge et al. (2002) also report a mineralogical shift where the feldspar content in the underlying Triassic sandstones drop from 20-30% to approximately zero in the overlying Jurassic sandstones, while the quartz content increases. Bugge et al. (2002) also suggest that this abrupt change may in part be explained by reworking of Upper Triassic sediments in the Early Jurassic, as is evident from common redeposition of Upper Triassic fossils. It also coincides with a climatic change from a semi-arid environment characterised by caliche development in the Carnian–Norian, to more humid conditions in the Early Jurassic. This indicates a similar mineralogical shift, however, implies that it takes place at a later stage than previously suggested by Bergan and Knarud (1992).

A mineralogical shift was also reported by Mørk (1999) who investigated variations in composition of Triassic sandstones of the Barents shelf and that the Middle and Upper Triassic successions in the Barents Sea showed a tendency to increase in mineralogical maturity when compared to Lower Triassic sandstones. She reports that in the Nordkapp Basin, the increase in maturity may be connected with facies changes from fine-grained marine to medium-grained lagoonal and shoreface deposits. However, rounding of grains is poor (Mørk, 1999).

Bugge et al. (2002) also offer detailed descriptions of the depositional environments previously interpreted in the Nordkapp Basin, and the stratigraphy in this paper is based on their stratigraphy (Fig. 3-2)

2. Analytical Approach

2.1 Methods

2.1.1 Logging of Core

A macroscopic description was made of core 7227/08-U-01 and core 7230/05-U-03 by core logging, covering part of the Snadd-, Fruholmen- and Stø Formation in the Nordkapp Basin. When logging a sampled core there are many aspects to consider, some of the most prominent are lithology, texture, sedimentary structures, color and fossils. These should be recorded in as much detail as possible, so that you at a later stage can combine the attributes to define different facies. The facies is a product of a particular depositional environment or depositional processes in that environment. Given that this is a sampled core one does not have the privilege of considering the lateral differences within a given layer, hence the vertical variations in grain-size; the packaging and stacking patterns of units; and the presence of depositional cycles become even more important. The standard method for collecting data of sediments is to make a graphic log of the succession, this immediately give a visual impression of the complete section, and allow you to compare different sequences within the section in a convenient way. The vertical scale used in this study is 1:20, which gives a sufficient level of detail for this purpose. However, the graphic logs have been downscaled to fit the printing format. For this study a fairly detailed analysis of the core has been carried out. Extra equipment such as loupe (10x), needles and 10% HCl have been used to further investigate the qualities of the sediments, and identify calcite. Measuring bands, grain size scales and stereo microscope have also been applied. In the process of logging new samples for thin section preparations were drilled and collected, as well as samples for XRD-analysis.

2.1.2 Optical Microscopy

There were 56 thin sections from the SINTEF shallow drilling project; in addition 13 thin sections were made for the purpose of this project. These thin sections have been examined mainly to calibrate the grain size used in the graphic logs, but also to identify diagenetic processes such as caliche and to get a better understanding of the depositional environment. For this purpose a polarization microscope was applied. The thin sections were analyzed in transmitted light using Nikon Optiphot. Modal analysis was carried out using Pelcon Point Counter program, the analysis was based on 300 points in each thin section. The modal analyses were carried out mainly to map any differences in mineralogical maturity between the formations. In order to separate pyrite aggregations from organic fragments a secondary source of light was directed towards the thin section at an angle.

2.1.3 SEM Analysis

Four polished thin sections, three from well 7227/08-U-01 and one from well 7230/05-U-03 were analyzed with a Scanning electron microscope (SEM). The scanning electron microscope is a valuable instrument when heterogeneous materials are to be characterized on a micro-scale. The area investigated is scanned by a thin focused electron beam. The beam can either be stationary or scanning a raster over the sample surface. When the focused beam hit the sample surface, it generates signals that can be detected. These signals can give information regarding chemical composition, topography, crystallography, average atomic number etc. The most common signals detected in SEM are x-rays, backscattered and secondary electrons (Hjelen, 1989). SEM was used for the purpose of identifying features as diagenetic cement, authigenic clay matrix and detrital grains difficult to classify by optical light microscopy. The SEM analysis included backscattered electron images (BEI), based on the differences in intensity of minerals reflecting their average atomic number. Thus, heavy minerals like pyrite will appear brighter than quartz, and K-feldspar lighter than quartz in grey-scale. This is used to study textural relations and chemical zonation. The BEI was used in combination with energy dispersive spectra's (EDS), where the peak position reflects energy and peak intensity is proportional to element concentration, in order to verify the presence of specific minerals. There was also conducted x-ray element mapping on one of the samples; element maps show the spatial distribution of elements in a sample and paint a complete 2D picture of the internal chemical zonation within a mineral. This was used to distinguish between areas of dolomite cement, quartz and albite as they had the same color in the BEI. A quantitative microprobe analyzer was used to classify carbonate mineralogy in a few selected samples. The instrument used to carry out these analyses was a JXA-8500F Electron Microbe.

2.1.4 XRD Analysis

Six of the collected samples were selected for standard bulk analysis. This was done in order to identify clay minerals. By using X-rays that are diffracted according to Bragg's Law the d-spacing of the sheet silicates is determined.

$$n\lambda = 2d\sin \varphi \quad (\text{Bragg's Law})$$

Here λ is the wavelength, φ is the angle of incidence and d is the distance between the lattice sheets. The samples were prepared by mortaring the material as gently as possible to obtain a coarse grinding (three of the samples were too resistant and therefore crushed in a single pot

Herzog swing mill). The fine powder was then packed into sample holders, assuring a flat sample surface, and placed inside the XRD instrument, D8 Advance. The results were then interpreted using Diffrac^{Plus} Evaluation connected to the PDF2 database. After removing the amorphous background noise, this program was used to make semi quantitative analysis of the mineralogical composition of the samples.

2.2 Sources of Error

There are several possible sources of error in this analysis. The logging of the core is highly dependent on the final interpretations after studying the details that can tell more about the depositional environment, here there are possibilities for human error or misinterpretations.

For the SEM analysis a possible error is that the standardization for quantitative mineral chemical analysis is not calibrated correctly. If the thin section is too thin the electron beam might burn a hole in the sample, this could also give inaccurate results.

The XRD requires an experienced person to interpret the result as the software programs often misinterpret the mineral patterns, it is therefore important to never rely on the software alone. This opens for human error, and can affect the results of the analysis. Problems in the sample preparation can also reduce the accuracy of the determinations. XRD has less sensitive detection limits than either XRF or optical methods of analysis, and as a result minerals present in quantities less than 2000 ppm may not be detected. If a sample is over grinded when milling, the original crystal structures might get destroyed and make them amorphous. If this happens XRD cannot be applied to detect the minerals as they will become invisible to the technique (Thornhild, 2011).

The modal analysis is merely a statistical approach where data is collected from 300 points on a thin section, this gives a good approximation of the lithology in the sandstone, however, opens for statistical errors. The point counted minerals and porosities may not be representative for the whole sample, particularly for accessory minerals. Some of the thin sections have bad quality and made it challenging to conduct petrographic analysis. Another source of error is that much of the feldspar was dissolved and a greater percentage should probably have been counted as porosity, it was also in many cases hard to differ between feldspar and lithic fragments due to dissolution and discoloration, this could also have resulted in higher results for feldspar.

3. Geological Setting

3.1 Introduction

The Barents Sea is limited by the Norwegian northern coastline and the northeastern Russian coastline, Novaya Zemlya to the East, Franz Josef Land, Svalbard in the North and the eastern margin of the Atlantic Ocean in the West (Fig. 3-1). It covers an area of approximately 1.3 million km² and the average depth is about 300 meters. This makes the Barents Sea one of the largest areas of continental shelf in the world (Johansen et al., 1992; Doré, 1995).

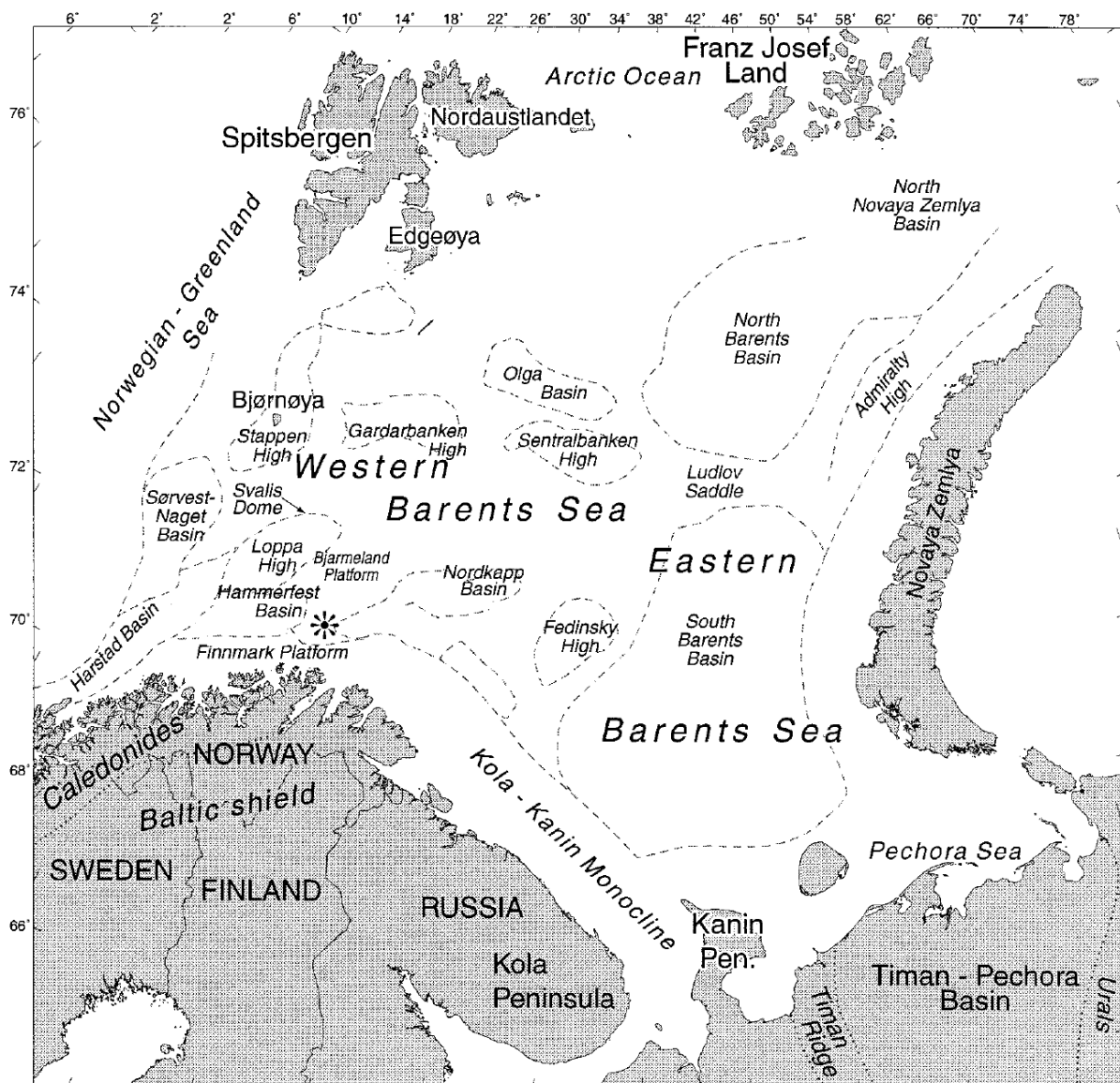


Figure 3-1: The Barents Sea area. Modified from Mørk, 1999.

The Barents Sea area was formed by two major continental collisions, and then split apart by continental separation at a later stage. This led to the complex variety of platform areas and

basins we can see today. The first collision event, the Caledonian orogeny, includes events that occurred from the Ordovician to Early Devonian, and ended about 400 million years ago (Fossen et al., 2006). This mountain building episode was caused by the closing of the Iapetus Ocean, a major seaway that occupied a position quite similar to the modern northeast Atlantic, as the Laurentian plate (Greenland, North America) and Baltic plate (northern Europe and western Russia) collided and merged into one continent, Laurasia (Doré, 1995). As the continents started to drift apart the mountain lost its support and started to collapse. The western part of the Barents Sea consisted of complex systems of highland, alluvial and fluvial planes, marshes and deltas prograding to the east. The sedimentary system was probably dominated by active horst-graben and basin formation (Smeror et al., 2009). In the Devonian to Early Carboniferous extensional movements reactivated faults following Caledonian structural features, these movements were controlled by extensional movement that started already 415-422 million years ago (Faleide et al., 1984; Gudlaugsson et al., 1998). This period was also characterized by exhumation and extensive erosion of the hinterlands, leading to accumulation of Old Red Sandstone deposits in the western part of the Barents Sea. The western margin of the Barents Sea, including Bjørnøya and western parts of Spitsbergen, was dominated by horst-graben formation with an N-S oriented fault trend, but further to the east there was a NE-SW oriented fault trend (Faleide et al., 1984; Smelror et al., 2009). As time passed the rifting ended, and combined with transgression this led to the formation of large shallow marine areas with carbonate and evaporate deposits. In the Carboniferous and Permian the area was exposed to some dramatic climatic changes. The Barents shelf drifted through several climatic zones, from the tropical to the temperate. At the same time the collision between Laurasia and Gondwanaland, with the Uralian orogeny was a final element in the fusion of most of the world's landmasses into a single supercontinent, Pangea, in Permian- Triassic times (Faleide et al., 1984; Nøttvedt and Worsley, 2006). The tectonic history of the Late Paleozoic and Mesozoic of the Barents Sea is dominated by extensional tectonic movements.

The Barents Sea drifted north from latitude of 20°N in the Carboniferous to 55°N in the Triassic and then continued to drift further north to about 75°N where it is situated today (Worsley et al., 1986, Doré 1995). The Triassic was a tectonically calm period in the western part of the Barents Sea. Regional subsidence resulted in deposition of thick Triassic sequences, locally 6-8 km in the east (Doré, 1995). Generally, the lower Triassic deposits are shallow marine, and mark the end of carbonate deposition. The sediment source in the Triassic was mainly in the east; both Fennoscandia and the Uralian mountains were important

sources of sediment to the NE-SW oriented paleo-coastline (Mørk, 1999; Smelror et al., 2009; Glørstad-Clark et al., 2011; Riis et al., 2008). In the Mid- and Late Triassic dark grey/black, phosphatic, organic rich mudstones were deposited. These can be seen both in Svalbard and in the Barents Sea, and they have proven to be good source rocks. In Svalbard these layers are called the Botneheia Formation, and in the Barents Sea they are called the Steinkobbe Formation. Throughout the Triassic alternating mud and sand layers were deposited, due to sealevel fluctuations, together with river channels deposited in regressive periods (Nystuen et al., 2006). The rifting continued throughout the Cenozoic and the opening of the ocean between Norway and Greenland. Faults in the western part of the Barents Sea were reactivated by shear movement and faulting. This resulted in subsidence on the western margin of the Barents shelf, tilting it to the west. Several platforms and basins were formed in this period in the western part of the Barents Sea (Faleide et al, 1984). From mid Jurassic the tectonic activity increased. The structural development of the southern part of the Barents Sea can be divided into two main steps; (1) the Mid Kimmeridgian rifting phase, and (2) the Late Kimmeridgian tectonic phase. The Mid Kimmeridgian rifting phase from the middle Jurassic was controlled by the breaking up of central parts of the Atlantic moving north towards the south western parts of the Barents Sea. The rifting resulted in normal faults and a series of basins due to extensional movement in the crust. West in the Barents Sea the Harstad-, Bjørnøya-, and Tromsø basins developed. During the Jurassic, transgression resulted in anoxic conditions in the rift basins causing deposition of organic rich clay. During the Late Kimmeridgian tectonic phase (Late Jurassic and Early Cretaceous), deep normal faults formed along altered zones in the Caledonides. In this period there was also a varying degree of subsidence. The late Kimmeridgian phases only lead to internal changes and horst-graben formation (Faleide et al., 1984; Faleide et al., 1993)

The subsidence in the Cenozoic was ended in the Eocene by periods with elevation and denudation. The eroded material was deposited along the western margin of the Barents Sea. Periods with ice lead to increased erosion, and big lateral variations in erosion can be seen in the Barents Sea. The Quarternary was dominated by several glacial periods with ice covering vast parts of the Barents Shelf, eroding and affecting the area. The eroding ice has resulted in large prograding sequences along the western continental margin (Vorren & Mangerud, 2006). In some basins the stratigraphy is well preserved and mainly Tertiary deposits are eroded away. In comparison considerable parts of the Mesozoic deposits are eroded away in the areas with the most erosion (Dimakis et al., 1998; Vorren & Mangerud, 2006).

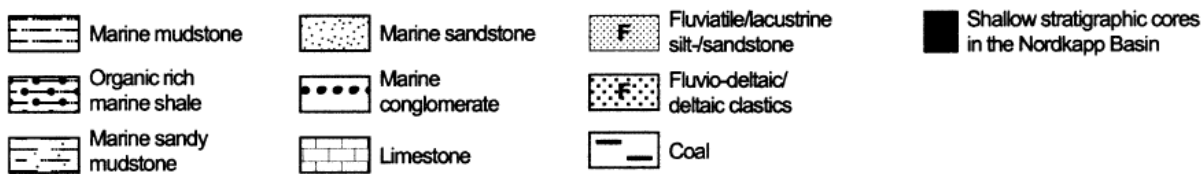
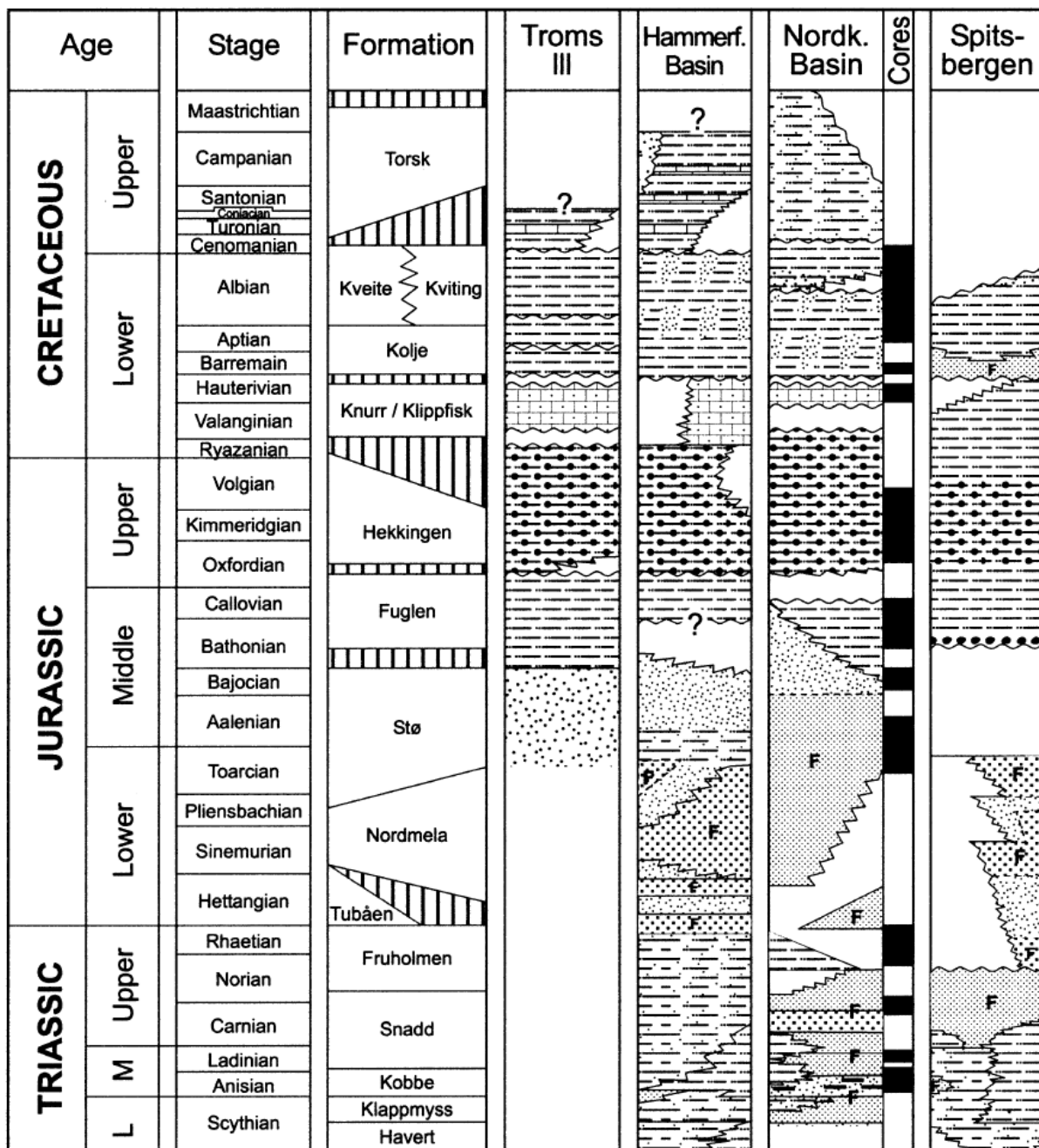


Figure 3-2: Regional stratigraphy of the Barents Shelf and Spitsbergen. The cored intervals in the Nordkapp Basin are shown. Bugge et al., 2002.

3.2 The Localities

3.2.1 The Nordkapp Basin

Wells 7227/08-U-01 and 7230/05-U-03 are both located in the Nordkapp Basin (Fig. 3-3). The Nordkapp Basin is a Late Palaeozoic rift basin characterised by its many salt diapirs. The basin is a half-graben, bound by a major fault on one side, following the NE-SW trend of the Caledonides. The basin is over 300 km long and 30-80 km wide, and was a major site for Triassic deposition (Gabrielsen et al., 1990; Jensen and Sørensen, 1992). During the Late Carboniferous- Early Permian there was a considerable deposition of salt in the basin, the salt has later been mobilized a number of times. Upper Palaeozoic and Mesozoic sediments that later filled in the basin, were uplifted by salt diapirism in the Early/Middle Triassic, Late Jurassic, Late Cretaceous and Tertiary (Bugge et al., 2002). Regional uplift and erosion in the Early Tertiary and extensive glacial erosion in the Late Pliocene/Pleistocene removed up to 1200 m of the Mesozoic and Cenozoic strata and left them heavily tilted and truncated around the salt diapirs, only covered by a thin sheet of glacial sediments. During much of the Triassic and Jurassic the Nordkapp Basin was a large marine embayment, open to the ocean in the southwest (Bugge et al., 2002)

3.2.2 The Bjarmeland Platform -Lateral Comparison

In this study well 7430/07-U-01 has been used for the purpose of lateral comparison of the Snadd Formation. This well is located at the Bjarmeland platform, in the southern part of the Barents Sea (Fig. 3-3). The Bjarmeland Platform represents the stable area between the Hammerfest and Nordkapp basins to the south and south east and the Sentralbanken and Gardbanken highs to the north. As a result of uplift during the Tertiary the platform sediments are dipping gently towards the south and the sediments that subcrop towards the angular unconformity under the Quarternary deposits get progressively older. The platform has not undergone any big tectonic events since the Late Paleozoic (Gabrielsen et al., 1990).

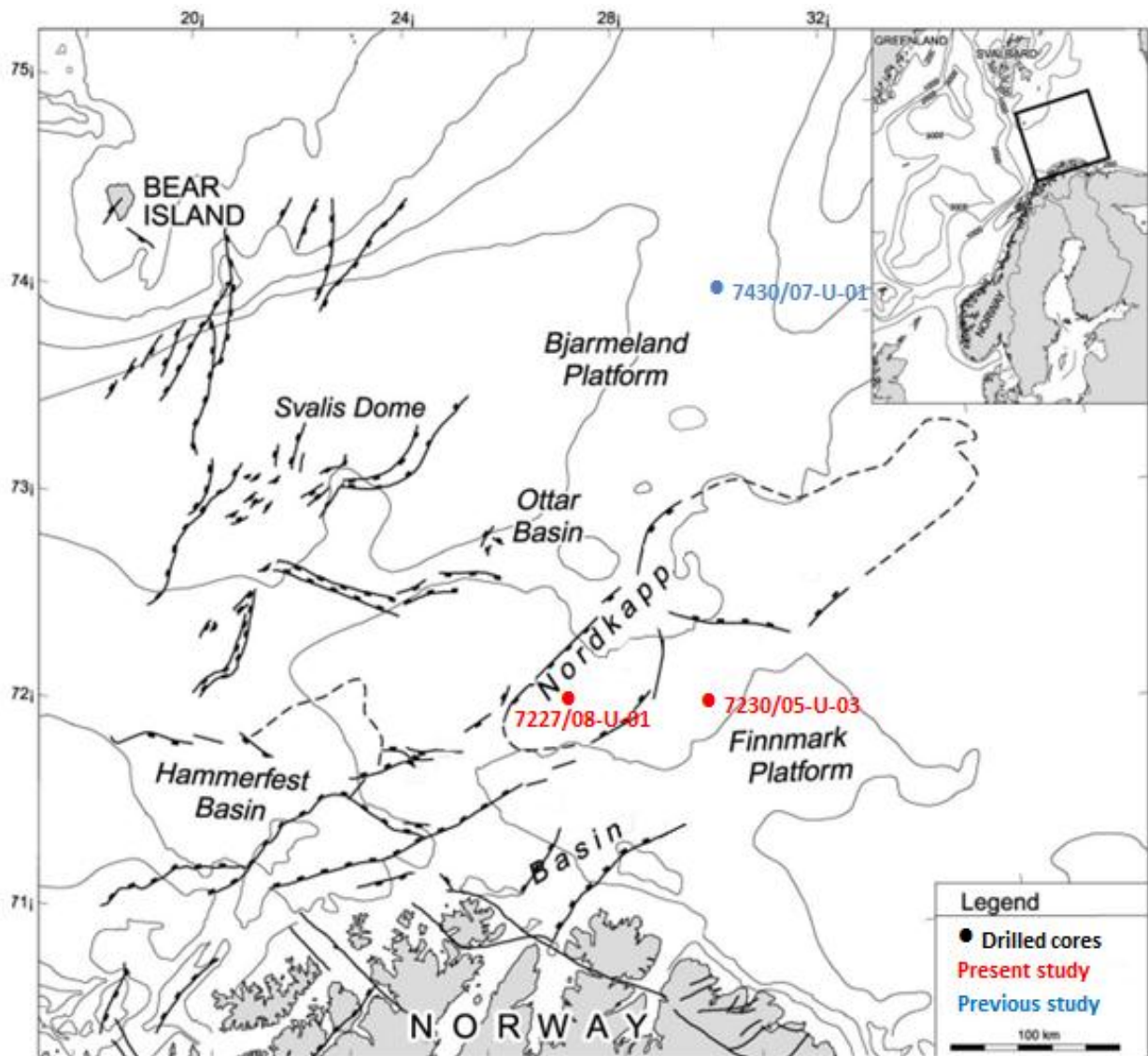


Figure 3-3: The Nordkapp Basin is a rift basin in the south western Barents Sea, and is located southeast of the Bjarmeland Platform. The figure shows the location of the drilled cores studied in this paper, as well as the location of the drilled core studied in the project assignment used for the purpose of lateral comparison. Modified from Bugge et al., 2002.

3.2.3 The Formations

Ingøydjupet Group

The Snadd Formation is middle to late Triassic, and the Ladinian sequence represents fairly distal marine deposits (Fig. 3-2). The Carnian is marked by large-scale progradation of deltaic systems over the entire region (Worsley et al., 1988). The Snadd Formation shows great similarities in age and development to the lower and middle part of the Kapp Toscana Group of Svalbard (the Tschermakfjellet- and De Geerdalen Formation). The lithology of the lower part of the Kapp Toscana Group is dominated by shale and claystone occurring in upward-coarsening sequences to include siltstone and sandstone beds in the upper parts of the

formations (Worsley et al. 1988). The Snadd formation has also been interpreted by Bugge et al. (2002) to incorporate shoreface and coastal plain deposits, and overall represent a regressive development (Bugge et al., 2002).

Realgrunnen Group

The Fruholmen Formation is of late Triassic age, and throughout most of this period the Barents Sea area was covered by fluvial plains (Fig. 3-2). Fruholmen is present in the Nordkapp Basin where the sandstones have previously been interpreted to originate from braided river delta fronts and pro-delta environments (Bugge et al., 2002). Fruholmen has also been studied in other localities, for example the Troms I area, where the deposits are characterized as marine shales in the lowermost deposits, gradually changing to coastal and fluvial sandstones, also in the Hammerfest Basin these deposits are described as marine shales (Worsley et al. 1988).

The Stø Formation represents the end of the Early Jurassic to the Middle Jurassic deposition in the Barents Sea (Fig. 3-2). During the Early Jurassic the coastal plains were flooded due to subsidence. These deposits are mainly characterized as shallow marine sand (Johannessen and Nøttvedt, 2007). These marine sands have been interpreted to be deposited in an upper inner shelf environment, and are intensively bioturbated (Worsley et al., 1988; Bugge et al., 2002). Shallow marine sandstones have also been observed in this formation; in addition to sandstones which may have been deposited in a tidal bar complex or a delta mouth bar (Bjørngen, 1985). The sediments have also been interpreted to include some deltaic sandstones and fluvial deposits indicating an overall regressive trend for this formation (Bugge et al., 2002)

4. Sedimentology

4.1 Description of Cores

A sedimentological analysis of the transition between the Snadd- and Fruholmen Formation has been done to make an interpretation of the depositional environment, and its effects on the maturity of the deposited sediments. A thorough description was made of well 7230/05-U-03 and 7227/08-U-01 by core logging. Both of the cores also include the transition from Fruholmen- to the Stø Formation; however this is not the main objective of this study. The characteristic properties of the formation have been subdivided into facies and described in section 4.2. The different depositional environments interpreted from the core are described in section 4.3. The description is presented as graphic core logs, logged in scale 1:20 which are included in Appendix A.

4.1.1 Core 7227/08-U-01

Core 7227/08-U-01 is approximately 41.6 meters long. The core is complete, and only smaller sections are missing in comparison to the full length of the core. The core represents a continuous section between 30-71.62 meters below sea bed, and can be seen in Figure 4-1. The core incorporates deposits from the Snadd-, Fruholmen- and Stø formations, and has been described in that order.

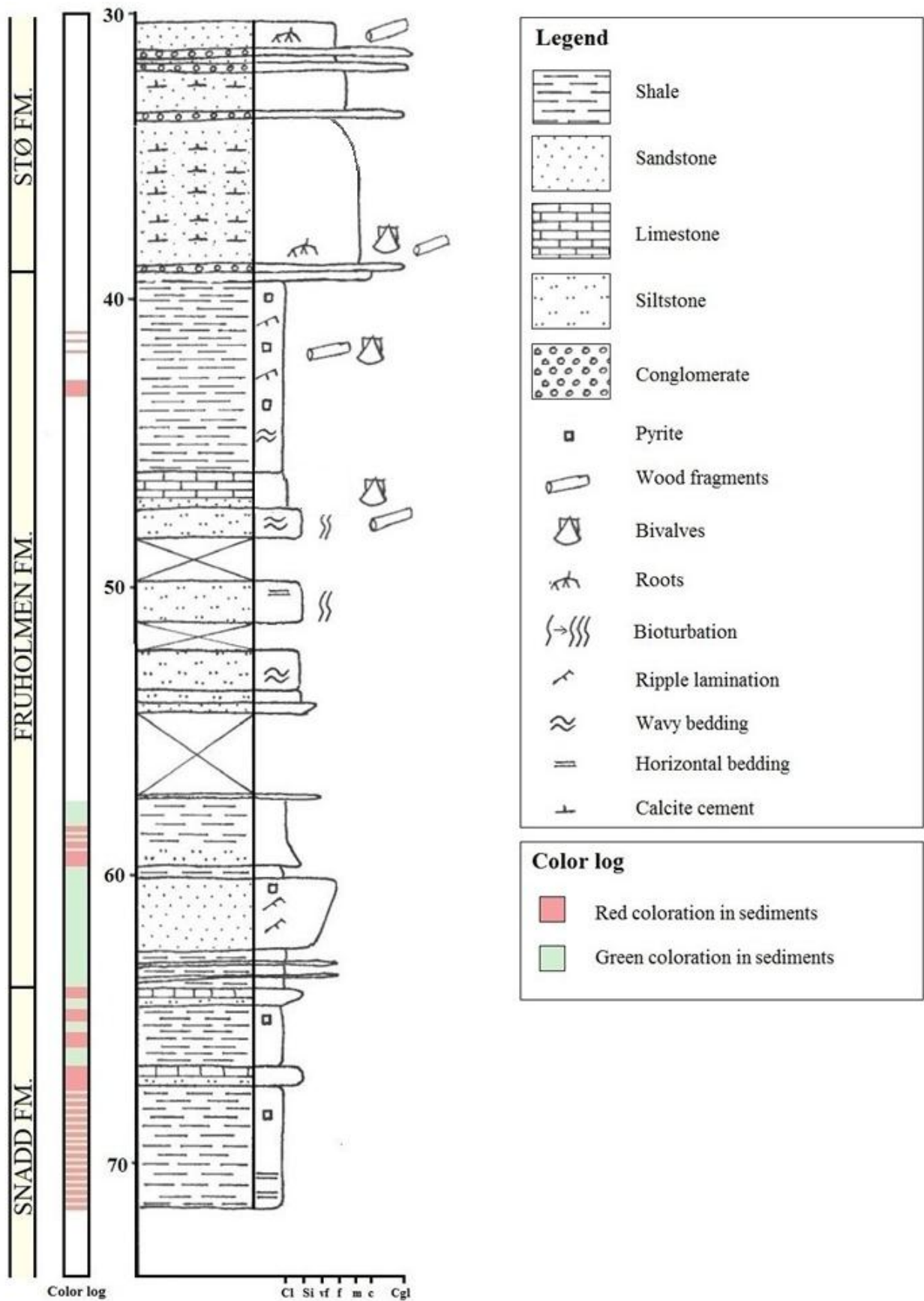


Figure 4-1: Logged core 7227/08-U-01 from the Nordkapp Basin.

Snadd Formation: 71.62-64.00 meters

The lower 7.04 meters of the core are deposits from the Snadd Formation, and the deposits have many of the typical characteristics for this formation. The lowest part of the core consists of one continuous, 4.2 meters thick, layer of mudstone with a distinct color distribution, but no visible depositional structures. The color of the core alternates between green and red, and show evidence of differential permeability in the mudstone resulting in variations in the degree of iron reduction (Fig. 4-2, a). In the upper part of this layer variegated mottled mudstone can be observed (Fig. 4-2, b). This layer is followed by a slightly coarser silty-mud layer, in the transition between the two layers there is a lamina with pyrite (Fig. 4-2, c). The upper part of this layer is calcite cemented, and some siderite can also be observed in the core. Following this is a new layer of mudstone with similar characteristics as that described first, the general trend is that it gets less red in color moving up the core. At 65.3 meters depth the characteristics of the mudstone changes somewhat, and it has a much more intense reddish color. There is pyrite mineralization as well as calcite filled cracks (Fig. 4-2, d). The upper part of the mudstone layer is greenish with pyrite mineralization throughout the layer, <0.5 cm in diameter. The upper 20 cm of the Snadd Formation starts with alternating layers of silt and very-fine sand and parallel bedding, some vertical burrows filled with coarser sediments can also be seen in this layer (Fig 4-3, a). The layer also has some pyrite mineralization, <0.2 cm in diameter. After this follows a layer where the lower part of the layer is very rich in siderite and the upper part of the layer is followed by calcite cemented fine-grained sandstone.

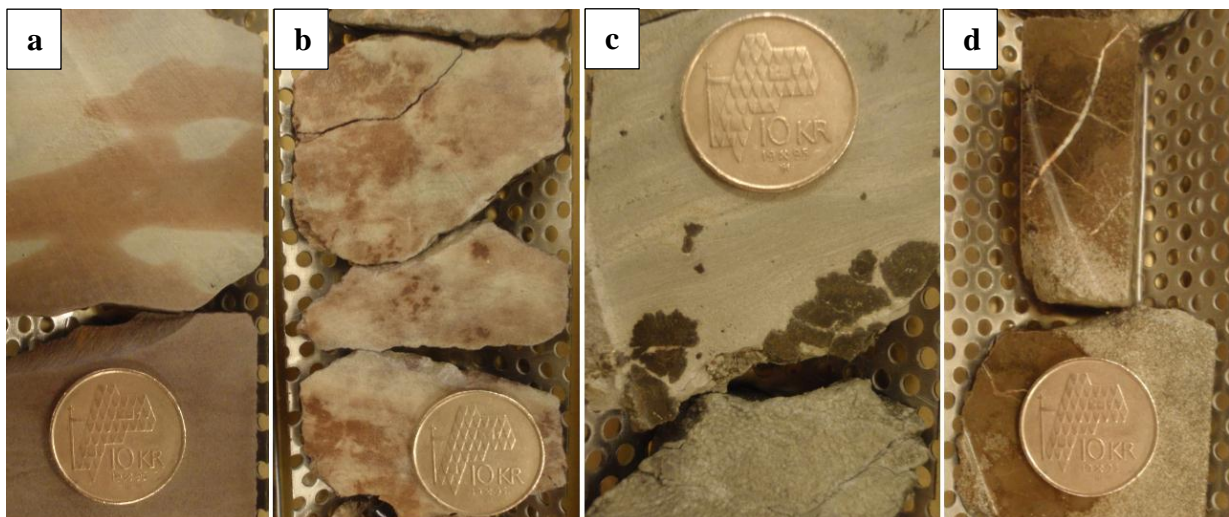


Figure 4-2: (a) Distinct color pattern in the mudstone due to differences in the permeability, 68.4 meters depth. (b) Variegated mottled mudstone, 67.54 meters depth. (c) Pyrite mineralization in the transition between two layers, 67.3 meters depth. (d) Siderite rich area with calcite cemented cracks, 65.15 meters depth.

Fruholmen Formation: 64.00-39.20 meters

From 64-62.5 meters depth a series of alternating mudstone- and fine-grained sandstone layers with an average thickness of approximately 30 cm follows. There are no characteristic depositional structures in these layers. The following layer, however, has clear depositional structures. The layer goes from 62.5-60.2 meters, and is coarsening up from silt to fine-grained sand. Moving up the layer the silt/sand ratio increases, and the bedding has changed from wavy- bedding to some visible ripples, towards the top of the layer there are almost no visible structures (Fig. 4-3, b and c). Throughout this layer pyrite can be seen (Fig. 4-3, b). This layer is followed by a 50 cm thick mudstone layer, with a greenish color, and a 2.35 meter thick, fining up, layer going from silt- to mudstone which is very contorted and lacking depositional structures.

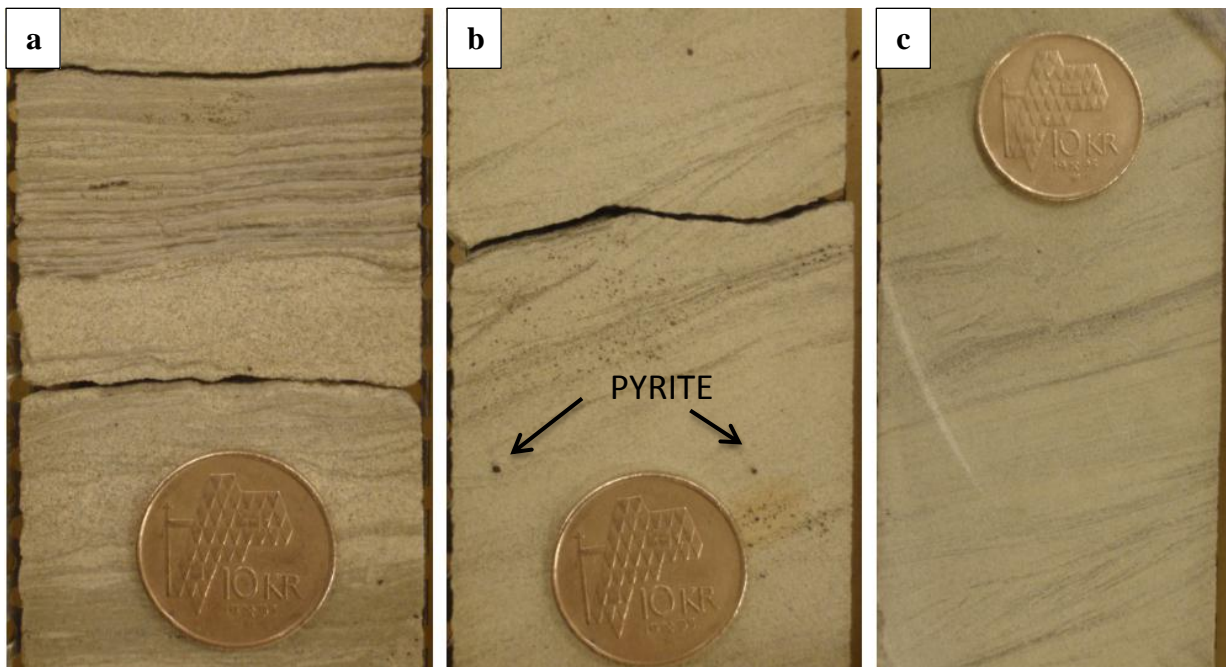


Figure 4-3: (a) Parallel bedding with alternating silt and very fine sandstone, 64.45 meters depth. (b) The black arrows are pointing to some pyrite mineralization, ripples can also be observed, 62.1 meters depth. (c) Wavy bedding structures with some apparent ripples, 61.7 meters depth.

There is approximately 2.8 meters of missing core, and it starts again at 54.38 meters depth, with a brown colored, coarsening up layer. The layer is 38 cm thick, and goes from silt- to very-fine sandstone. On top of this layer there is a silt layer with a thickness of about 0.5 meters, in this layer burrows with coal linings can be seen (Fig. 4-4, a). On top of this layer there is a sand layer with a big siderite concretion, the layer is also characterized by the bioturbation, and burrows are both vertical and horizontal. From 52.2-51.3 meters depth there is some core missing. Over the missing data there is 1.4 meters of alternating mud-, silt- and very fine-grained sandstone. The layers are quite well mixed together in some parts due to

bioactivity, but in other places small scale graded bedding can be seen. At 50.5 meters depth there is a mineralization/concretion that with some crystallization that was not possible to identify without further analysis, an XRD analysis of the concretion was therefore conducted (Fig. 4-4, b). From this analysis it was found that the concretion mainly contained pyrite, the XRD spectra is included in Appendix C. This layer is followed by yet another 1.2 meters of missing core. The layer on top of the missing data bears resemblance to the layer below, with burrows and alternating silt and mudstone layers. There are also many good examples of syneresis to be found here within the preserved original depositional structures (Fig. 4-4, c). From 47.44-46 meters depth there is a dark colored mudstone, with some red almost horizontal sections with a thickness of 1-2 cm (Fig. 4-4, d). There are no apparent depositional structures in this layer.

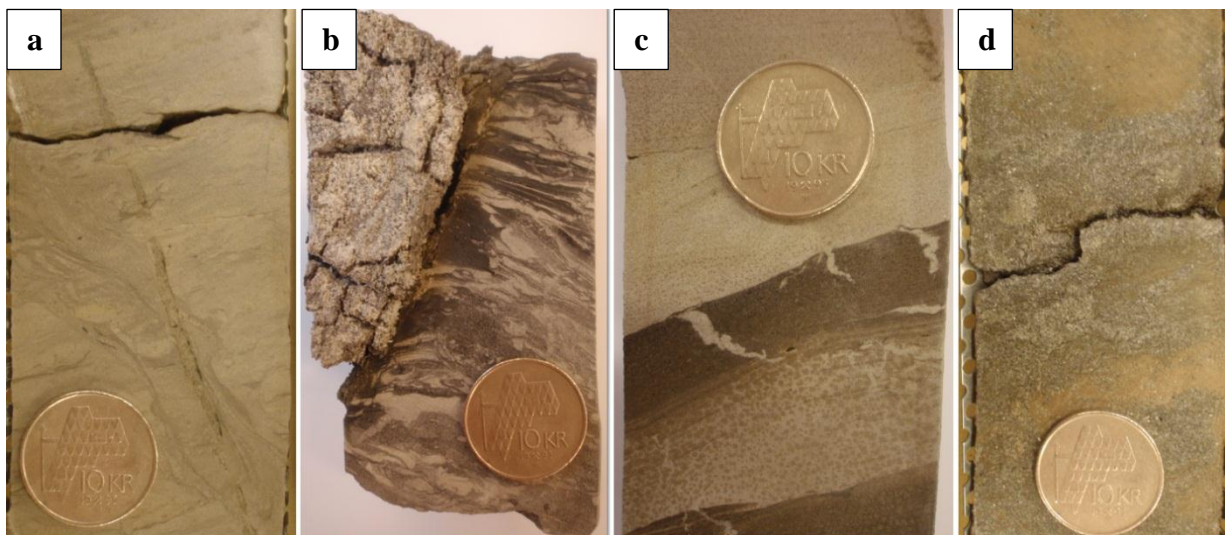


Figure 4-4: (a) Vertical burrow with coal lining, at 53.4 meters depth. (b) Pyrite concretion, at 50.5 meters depth. (c) Syneresis structures, at 48.1 meters depth. (d) Wacke sandstone with red sections, at 46.6 meters depth.

On top of this layer there is a 2.5 meters thick homogenous siltstone layer, with some pyrite mineralization, (Fig. 4-5, a). 13 centimeters of missing data, before a very similar layer continues further up to 39.48 meters depth. From about 43 meters depth and up some ripples are still preserved, and some horizontal burrows can also be seen, (Fig. 4-5, b). On top of this layer, some organic debris and coal laminae are seen in two layers with a grain-size of respectively fine- and coarse grained sandstone, (Fig. 4-5, c).

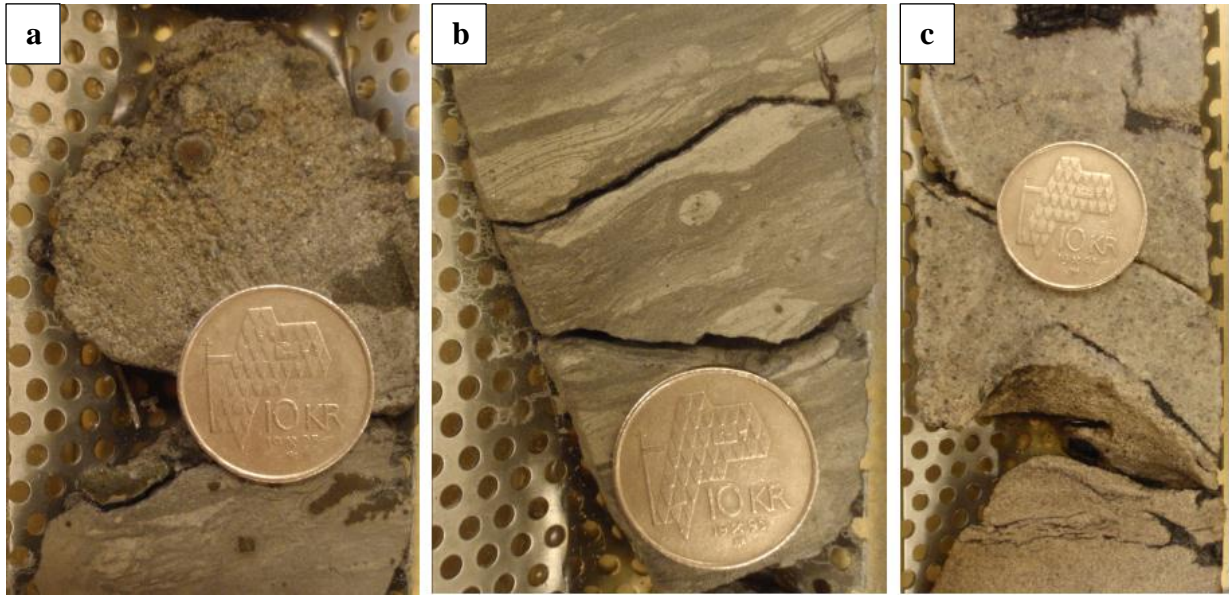


Figure 4-5: (a) Pyrite concretions that can be seen throughout the layer, 42.8 meters depth. (b) Horizontal burrows and some preserved ripples, 41.50 meters depth. (c) Organic debris and coal lamina, 39.4 meters depth.

Stø Formation: 39.20- 28.0 meters

The Stø Formation starts off with some of its very characteristic conglomerate, making the border between the Fruholmen and the Stø Formation easy to recognize (Fig. 4-6, a). The base of the Stø Formation is marked by a 20 centimeter thick layer of polymict conglomerate overlying an erosional surface. The cobbles are well rounded with a diameter of 0.5-10 centimeters, the cobbles are granitic. On top of this lies a 5.5 meters thick layer. The lower part of the layer is completely calcite cemented, and organic debris can be observed (Fig. 4-6, b). Further up in the layer the calcite cementation is less complete, but characteristic round areas have been carbonate cemented (Fig. 4-6, c). This continues throughout the rest of the layer, with only a few coal laminas inbetween. From 33.7-33.5 meters depth a new layer of conglomerate can be seen, also this conglomerate is polymict, however, the pebbles are much smaller, <5 cm in diameter (Fig. 4-6, d). On top of this layer of conglomerate there is a 0.5 meter thick layer of medium-grained sandstone with a thin (2 cm thick) carbonate cemented layer within. Then a 12 cm thick layer of coarse sandstone, and on top of that another layer of medium-grained sandstone. At 32.24 meters depth there is another 14 centimeter thick layer of conglomerate overlying a thin layer with medium-grained sand and then a 10 centimeters thick layer with conglomerate. On top of these thin layers with conglomerate there is a 1.6 meters thick layer of fine-grained sandstone with a brown color and some coal laminations, which ends at 30.30 meters depth. The top 30 centimeters of the core are not taken into consideration as they are polluted by the drilling process.

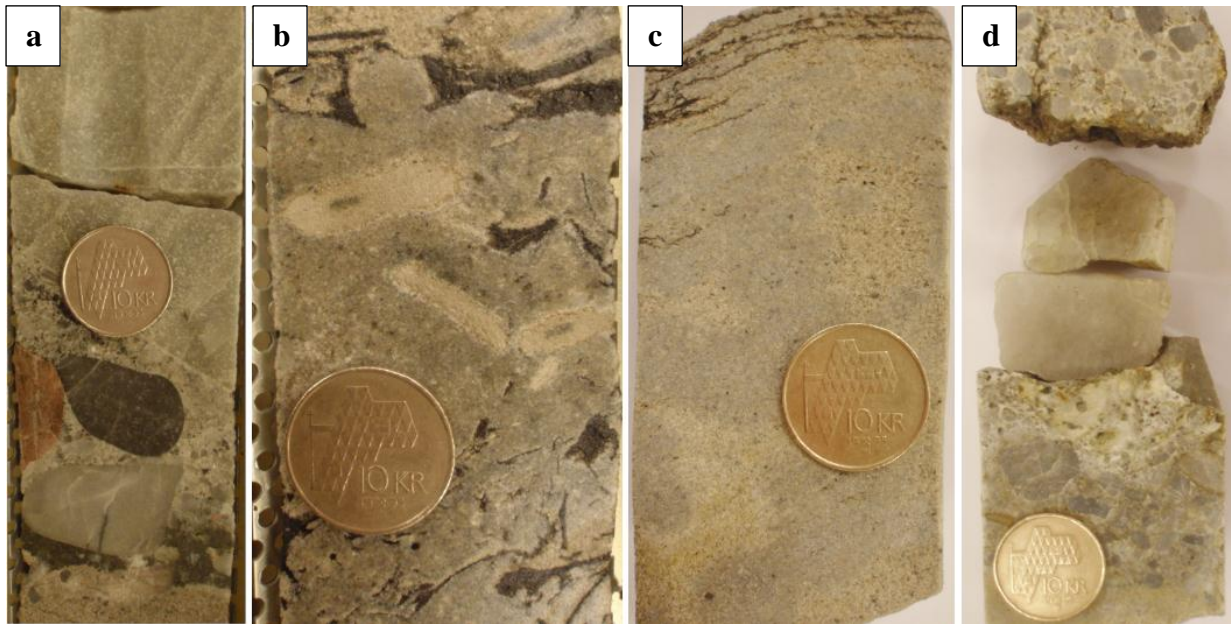


Figure 4-6: (a) Polymict conglomerate, 39.10 meters depth. (b) Almost completely carbonate cemented sandstone with some lenses of non-cemented sandstone and some organic debris/wood fragments, 38.55 meters depth. (c) Grey carbonate cemented areas in the sandstone and some coal laminae, 35.10 meters depth. (d) Polymict conglomerate, 33.60 meters depth.

4.1.2 Core 7230/05-U-03

Approximately 87.5 meters of core has been examined, described and interpreted in the study of this core. The core is complete, and only smaller sections are missing in comparison to the full length of the core. The core represents a continuous section between 28-115.5 meters below sea bed, and can be seen in Figure 4-7. The core consists of sediments from three different formations; Snadd, Fruholmen and Stø, described respectively below.

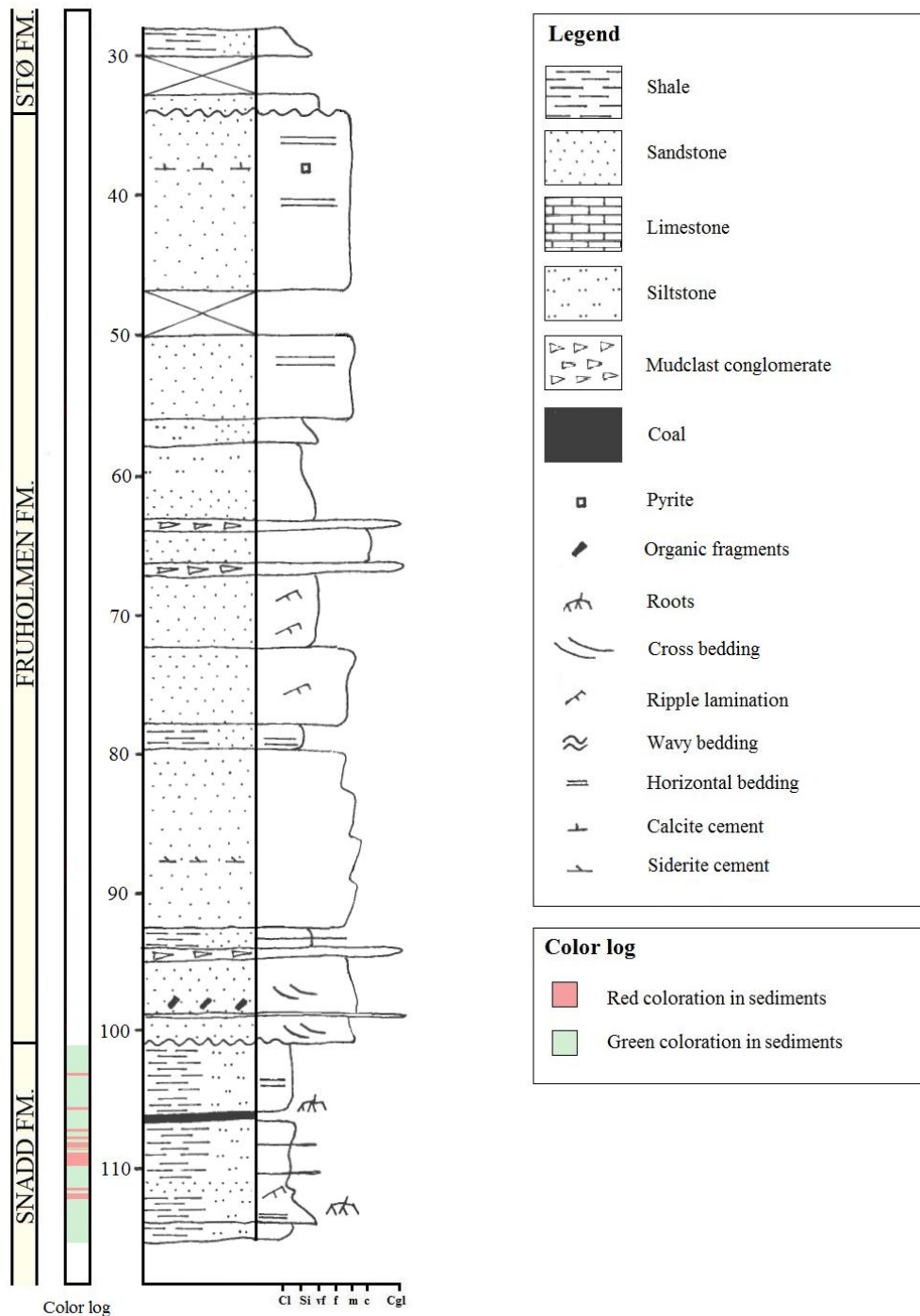


Figure 4-7: The logged core 7230/05-U-03 in the Nordkapp Basin.

Snadd Formation: 115.5-101.86 meters

The Snadd Formation in this core is mainly represented by mudstone deposits with a characteristic play of colors, alternating between red and green, represented in the color log. However, some internal variations can be seen. The lower 40 cm of the core consists of parallel bedded mudstone with a greenish color, (Fig. 4-8, a). From 115.10-112.22 meters depth a fining upwards layer, going from very fine-grained sandstone to mudstone, is deposited. The layer has no recognizable primary bedding. Towards the top of the layer some siderite concretions can be observed. From 111.78-111.68 meters depth a bleached layer of mud has been accumulated, followed by two mud layers showing alternating lenticular and parallel bedding (Fig. 4-8, b). From here a thick mudstone layer follows, this layer is characterized by sections of variegated mottled mudstone (Fig. 4-8, c). Sections of red siderite-rich mud typically found near caliche are found up to 105.54 meters depth (Fig. 4-8, d). The massive mud layer is only interrupted by a 4 cm thick coal layer at 106.5 meters depth (Bugge et al., 2002). The layer is overlain by another thick mudstone layer with some horizontal laminations in the lower part.

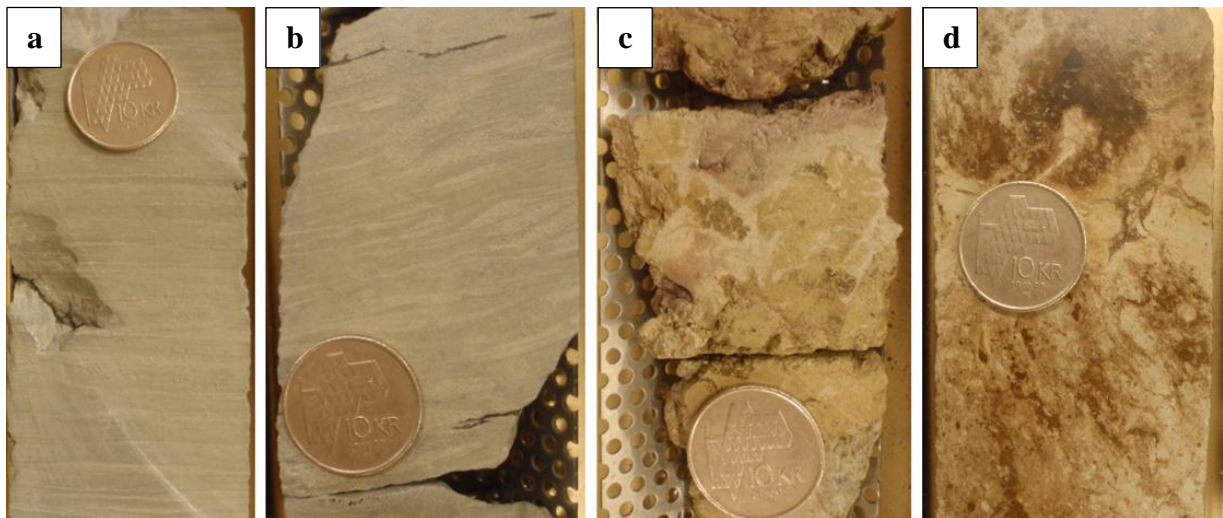


Figure 4-8: (a) Parallel bedded silty mud with a greenish color, 115.30 meter depth. (b) Lenticular bedding, and ripple lamination in silty mud with a greenish color, 110.85 meters depth. (c) Variegated mottled mudstone, 109.50 meters depth. (d) Siderite patterns typical for caliche profiles, 108.40 meters depth.

Fruholmen Formation: 101.86-34.08 meters

The Fruholmen Formation in this core mainly consists of medium-grained sandstones interbedded with a few meters thick siltstone beds. From the abrupt facies change at the unconformity a two meters thick, fining upwards, sandstone layer can be seen (Fig. 4-9, a). The layer is overlain by a 30 cm thick layer of conglomerate with coal laminations and mudclasts (Fig. 4-9, b).

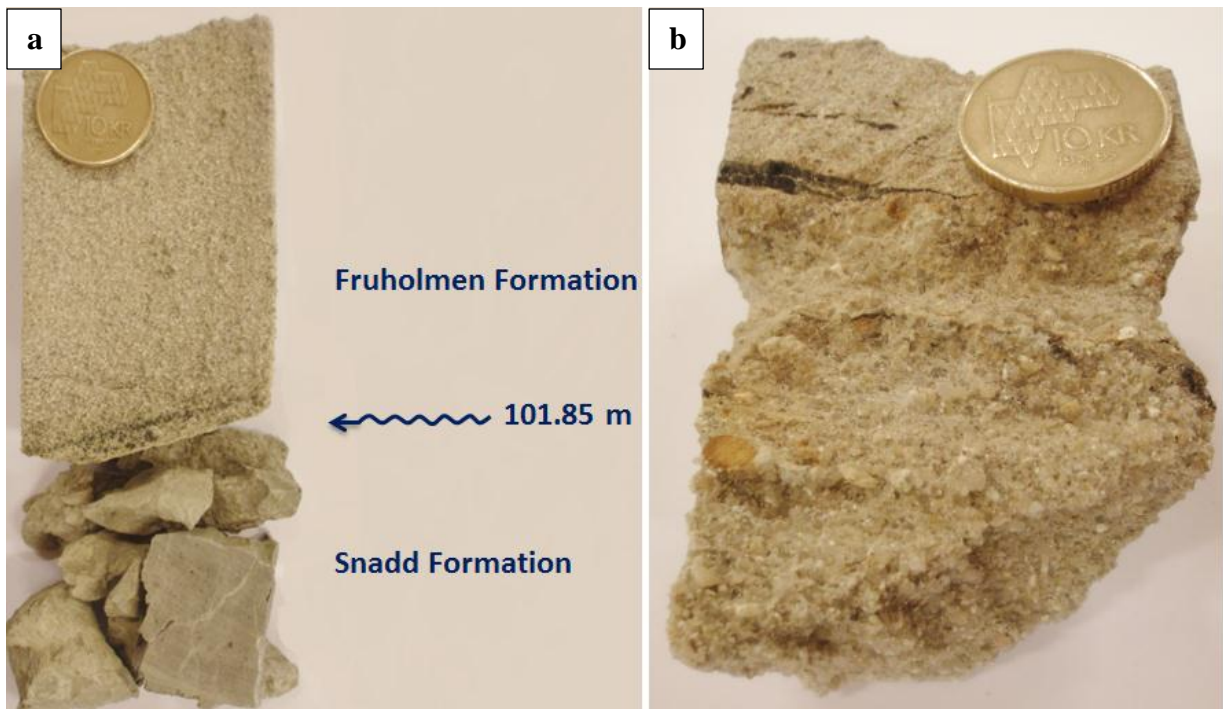


Figure 4-9: (a) The transition from Snadd to Fruholmen, 101.85 meters depth. (b) Conglomerate with coal laminations, 99.53 meters depth.

Following the conglomerate is another fining up sandstone layer with coal fragments and some cross laminations. At 95.12 meters depth this sand layer is interrupted by a silt layer. The silt layer is overlain by a 46 cm thick layer of mudclast conglomerate (Fig. 4-10, a). The mudclast conglomerate is overlain by alternating mud and very fine sand with some horizontal lamination in the lower part and some escape burrows in the upper part (Fig. 4-10, b). At 93 meters depth a new coarsening upwards layer follows, overlain by yet four other coarse-grained sandstone layers without any recognizable original depositional structures, up to 82.20 meters depth. From here several thinner sandstone layers follow, overlain by parallel laminated silty sandstone. The parallel laminated layer is followed by a layer with piled load-casted ripples/ball-and-pillow structures (Fig. 4-10, c) (Reineck and Singh, 1980). This layer is overlain by a medium-grained sandstone layer with coal laminae, and ripples (Fig. 4-10, d). This layer is overlain by several thinner sandstone layers without any visible depositional structures.

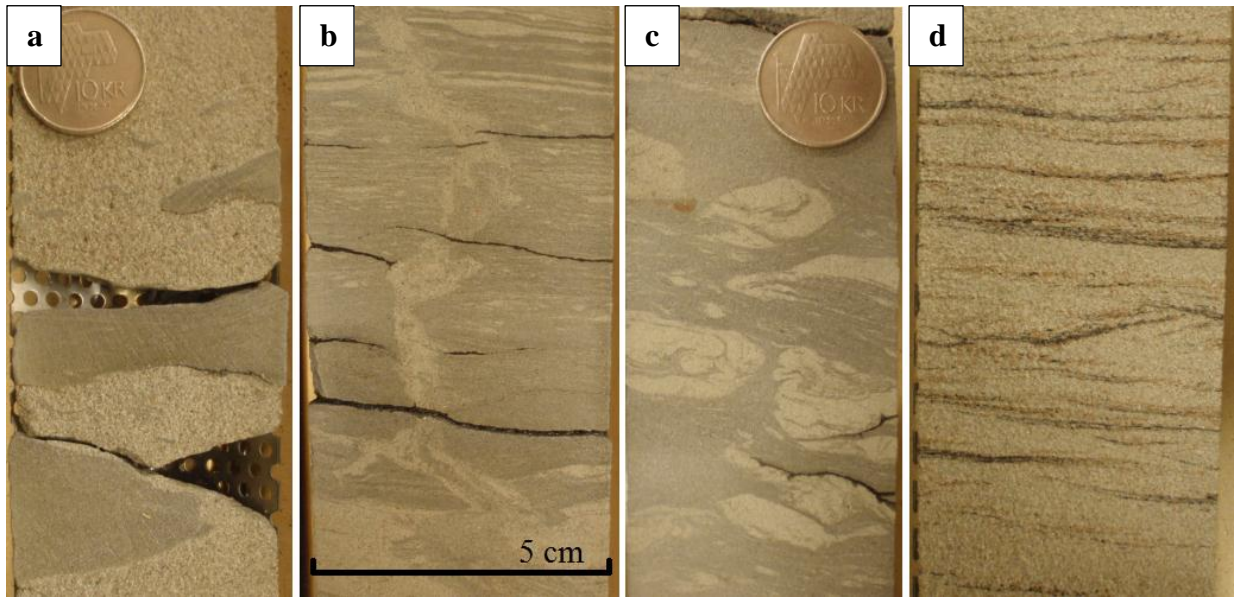


Figure 4-10: (a) Mudclast conglomerate, at 94.55 meters depth. (b) Escape burrow, 93.3 meters depth. (c) Ball-and-pillow structures, 77.95 meters depth. (d) Coal lamina, 74.55 meters depth.

At 72.7 meters depth a fining upwards layer with flaser bedding in the lower part and lenticular bedding in the upper follows. The layer has very-fine to silty grain size. This layer is overlain by another fining upwards layer showing the same characteristics. Above the second fining up layer a coarsening upwards layer can be observed, this layer also show flaser bedding and some coal laminae can be seen towards the top of the layer. The layer stops under a layer of mudclast conglomerate which is then followed by numerous thin sandstone layers gradually fining upwards from medium-grained sandstone at 66.70 meters depth to very-fine grained sandstone at 60.2 meters depth. Overlaying these sandstone layers is yet another siltstone bed observed. The bed show similar characteristics to the previously described siltbeds, with ball-and-pillow structures. The loading structures are followed by a two fining upwards layers going from very-fine grained sandstone with wavy bedding to parallel bedded siltstone. The layers are overlain by a new interval with medium-grained sandstone. This interval with medium-grained sandstone stretches from 55.90-34.10 meters depth, and show similar characteristics in the different sand layers. The layers have horizontal coal laminae, and pyrite can be seen (Fig. 4-11, a and b).

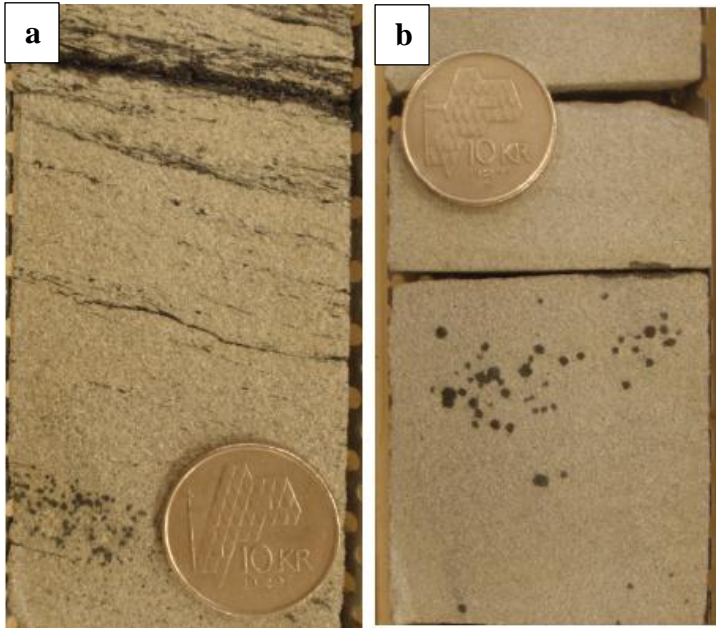


Figure 4-11: (a) Horizontal coal laminae, 46.20 meters depth. (b) Pyrite, 52.38 meters depth.

Stø Formation: 34.08- 28.0 meters

The lower part of the Stø Formation has some silty deposits. These are overlain by sandstone deposits with coaly lamination, the grain size shifts from silty sand to fine-grained sand with some cross bedding (Fig. 4-12, a). At 29.40 meters depth an 80 centimeter thick layer of silty mud and sand could be observed, here there were no original structures left (Fig. 4-12, b). The upper 38 centimeters of the core are not considered as they are disturbed from the drilling.

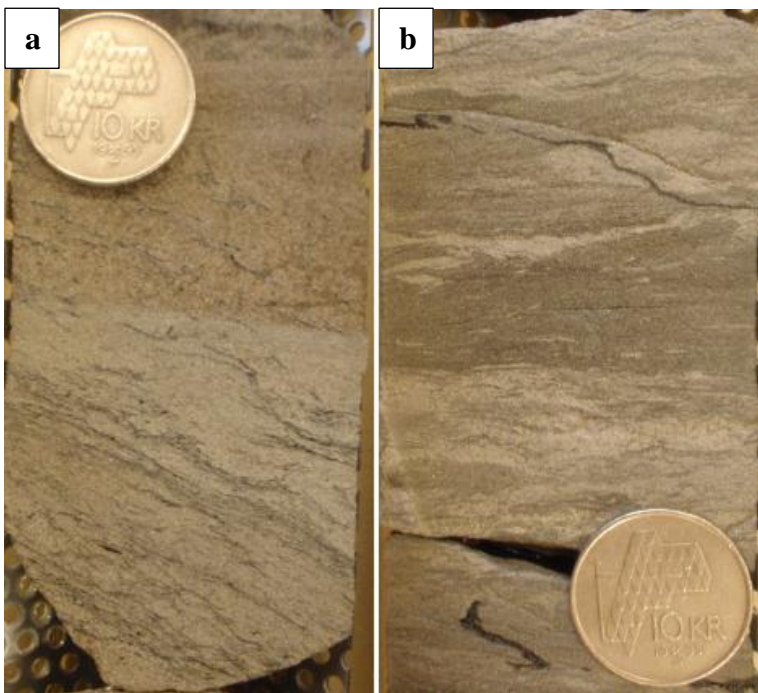


Figure 4-12: (a) Coal laminations, 33.8 meters depth. (b) Silty sandstone, 29.20 meters depth.

4.2 Facies Description

Facies 1: Alternating Mud and Sand Layers

Observations:

In the Fruholmen formation in core 7227/08-U-01 characteristic sections of alternating silty mud- and sandstone can be seen. Dark-colored muddy layers (clayey silt) alternate with light-colored fine sandy layers (silty fine sand to strongly fine sandy silt). In these layers synaeresis structures have been observed several places (Fig. 4-4, c). Escape burrows were observed in some places.

Interpretation:

The alternating silt and sandstone layers bear witness of varying depositional energy. This is typically found in tidal areas where the tidal variations will give different energy at different times during deposition; however, the lack of ripples indicates that this could be due to a different environment. This facies is also typical for the delta front slope. Pro delta deposits are characteristically fine-grained to muddy sediments i.e. clay and silty clay. The sediments show layering due to both differences in grain size and coloring. Occasional ripple bedding and small-scale graded bedding are common. Bioturbation can also be present, but usually restricted to certain zones. The escape burrows observed indicate rapid deposition, which suggest that some of the sand and clay layers are storm deposits (Reineck and Singh, 1980).

The shrinkage cracks can appear subaqueously as a result of a rapidly flocculated clay layers that have developed shrinking structures due to compaction. Synaeresis cracks are also indicative of an increase in the salinity, this is important in coastal lagoons and inland sabkhas where salinity of water increases markedly (Reineck & Singh, 1980; Reading, 1978). An illustration of the formation of synaeresis in can be seen in Figure 4-13

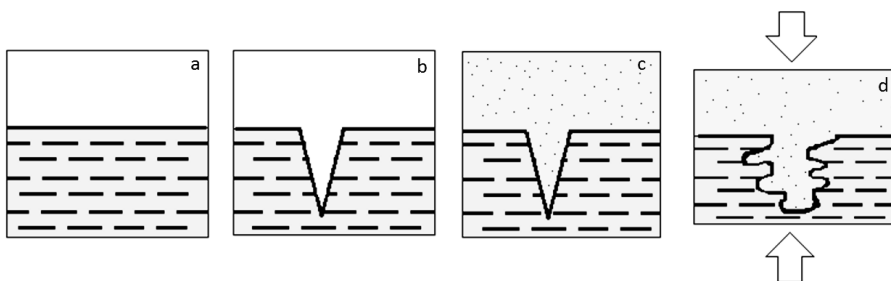


Figure 4-13: The synaeresis cracks in the package might initially have been preserved as small cavities (b), which then later were filled with silt and sand from the overlying beds and laminae (c). Later compaction has given the cracks a distinct shape with small bulges down on each side (d) (Auset, 2011).

Facies 2: Lenticular Bedding

Observations:

In several places in the core lenticular bedding can be observed in the Snadd Formation and in the Fruholmen Formation, for details see Appendix A. This stratification structure occurs as inter-bedded clay and sand, with well-preserved ripple-shaped sand lenses with cross-laminated internal structures. The sand occurs as lenses which are isolated in the clay both vertically and horizontally in the lower part of the sequences, but upwards in the section the sand/clay relationship increases and thicker connected ripple-bedded lenses can be observed (Fig. 4-8, b). Most of the lenses show ripples of the original current direction. However, as the samples are not oriented the current direction cannot be interpreted. Lenticular looking bedding also occur in the combination with the alternating clay and sandstone layers of facies 1, however, here the internal ripple structures are not always apparent.

Interpretation:

The lenticular bedding is formed when the clay content exceeds the sand, examples of this can be observed at several levels in the Snadd Formation in both cores. This matches the theory presented by Reineck and Singh (1980), they suggest that the lenticular bedding is commonly formed in environments with deposition of more mud than sand. The lenticular bedding is formed together with wavy and flaser bedding (facies 3 and 4) in environments that provide conditions for alternating supply of sand and mud. These types of environments can be listed up as tidal flats, subtidal environments, marine delta-front environments, lake environments and on the shallow marine shelf (Boggs, 2006).

Facies 3: Wavy Bedding

Observations:

Wavy bedding can be seen several places together with lenticular bedding in this core. In wavy bedding sand and mud alternate and form continuous layers. Bioturbation can also be found in this type of bedding.

Interpretation:

What separates wavy bedding from flaser bedding (facies 4) is that this bedding requires conditions that allow for deposition and preservation of both mud and sand (Reineck & Singh, 1980). The different environments that supply both sand and mud can be found in the interpretation of facies 2.

Facies 4: Flaser Bedding

Observations:

Flaser bedding is a type of ripple bedding that also can be observed at several levels in the boxed cores. It is often seen as a transition from wavy- or lenticular bedding (facies 2 and 3) as the sand/mud ratio increases. This facies can also in some places be observed as thin interbedded packages of sand where the lenticular bedding is the main facies.

Interpretation:

As mentioned above the flaser bedding is formed where you have a higher sand/mud ratio, the sand content is considerably higher than the mud content in these sections of the core. Reineck and Singh (1980) proposed that flaser bedding commonly forms in environments where the deposition and preservation of sand is higher and more favorable than mud, this fits to the distribution of sediments found in these units. Mud flasers form in periods of quiescence, whereas the sand is deposited in periods of higher energy conditions. Both ripple and cross lamination can be observed within these layers. Flaser bedding in addition to lenticular bedding is formed in environments where there are conditions for alternating supply of sand and mud. These environments are listed in the interpretation of facies 2 (Boggs, 2006).

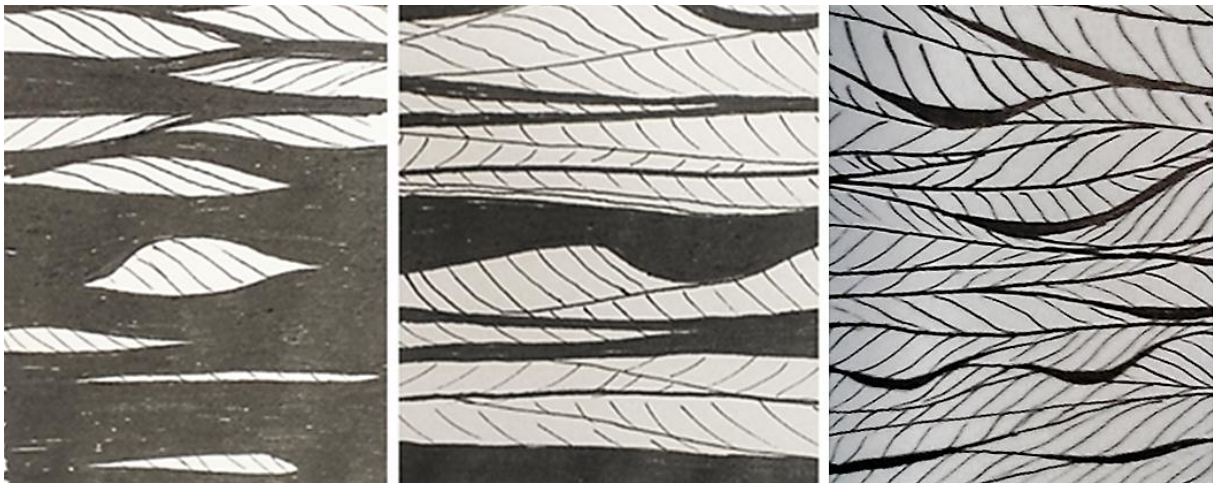


Figure 4-14: Drawing a,b and c shows how lenticular-, wavy-, and flaser bedding are defined in this study, respectively (Auset, 2011).

Facies 5: Fining Upwards Sandstone

Observations:

In the lower part of the formation some fining upwards layers of sandstone, going from fine-grained to medium-grained, can be seen in Fruholmen in core 7230/05-U-03. These sediments show some faint crossbedding.

Interpretation:

Fining upwards units of medium-fine-grained sandstone are typically found in delta front environment where distributary channels can be found. A distributary channel is a natural stream which leads part of the sediment and water discharge of a major stream into the sea. Near the upstream part of the channel current direction is persistent downstream. However, as the channel flares out downstream, current direction becomes variable and current velocity is reduced and deposition of sediments is increased (Reineck and Singh, 1980). The most common sedimentary structures are cross-bedding, current-ripple bedding, scour-and-fill structures and erosional surfaces. Another feature is cross bedding with overturned foresets (Reineck and Singh, 1980).

Facies 6: Homogenous Sandstone with some Horizontal Coal Lamination

Observations:

In core 7230/05-U-03 the upper part of the Fruholmen Formation medium-grained sandstone with some faint horizontal bedding can be observed. There are also some horizontal coal laminations. These sandstones also comprise some coarsening upwards layers.

Interpretation

Homogenous sands can occur in several environments, one possible reason for the homogenous deposits of sand might be shoreline. In these environments the fine material might get washed away. As the sediment is transported, the fine and coarse material is sorted out, resulting in a homogenous sand package with homogenous grain size. The package could also have been disturbed by bioturbation, erasing any original structures in the deposit (Reineck & Singh, 1980). The horizontal lamination, however, suggest high energy during deposition. This could also be distributary mouth bar deposits. This is the place with the highest depositional rate in the delta, and the homogenous appearance of the sandstone could be due to constant reworking of the sediments due to continuous reworking. Thin laminations of plant debris are often present (Reineck and Singh, 1980).

Facies 7: Mud Clast Conglomerate

Observations:

At several depths, in core 7230/05-U-03, sandstone containing big mud clasts are seen. These are found in connection with the coarsening upwards sandstone. Bioturbation is completely lacking in these sediments, indicating unfavourable living conditions.

Interpretation:

In combination with distributary channels clay fragments are often incorporated in the sediments (Reading, 1978). Intraformational conglomerates similar to those observed in this core have previously been interpreted to represent channel deposits, possibly within a deltaic depositional system. The mudclasts cannot have been transported far as they would have broken down (Riis et al., 2008).

Facies 8: Conglomerate

Observations:

There are several layers of conglomerates observed in core 7227/08-U-01, and it occurs in the upper formation in the core, the Stø Formation. The conglomerates are polymict orthoconglomerates with a sand matrix. The clasts are well rounded, cobble-sized and appear to be extraformational. The size of the conglomerate clasts get smaller for each successive layer of conglomerate seen in the core. At the bottom of the lowest conglomerate package there appears to be an erosional surface.

Interpretation:

As mentioned above the surface between the conglomerate and the underlying mud package appears to be erosional. The lowest conglomerate package observed in core 7227/08-U-01 probably represents the erosional surface between Fruholmen and Stø formations. Conglomerates are typically found at the base of fluvial deposits where the bottom of the fluvial deposits cut into younger sediments. The series of conglomerates could be interpreted to be a meandering river moving back and forth cutting into previously deposited river sediments. It could also be several generations of channel deposits (Reineck and Singh, 1980).

Facies 9: Reduced Silty Mudstone

Observations:

The lower part of the cores shows thick silty mud packages. There is a recognizable pattern of color variations within the mud layers; this could be paleosol which is an early diagenetic process. In some of the mud packages typical traces from rootlets are observed, and it is also possible to find independent organic fragments in some of the layers. The packages also show red coloration.

Interpretation:

Silty mud is normally deposited in calm conditions where the fine material is allowed to settle, this is the case in several environments. Thick mud layers can be indicative of deep marine deposits, below storm base level where the sediments are allowed to settle. It is also possible that the sediments are deposited in shallow water lagoons. In general lagoons accumulate fine-grained sediments deposited from suspension. The clays and silt are commonly structure less due to extensive bioturbation. In humid and temperate lagoons, the muds are often rich in organic matter including plant debris washed in by rivers (Reineck and Singh, 1980). The red coloration is typical for strata which have been exposed or undergone pedogenic processes (Worsley et al., 1988).

Facies 10: Siltstone with Ball and Pillow Structures

Observations:

In core 7230/05-U-03 the medium-grained sandstone deposits are interrupted by packages of muddy-siltstone and very fine sand displaying penecontemporaneous deformation structures (Fig, 4-10, c). These sediments also display some ripples, and between the load structures wavy bedding can be observed.

Interpretation:

The load structures are most likely produced by piled load-casted ripples. Load structures are not restricted to any environment, however, they are occasionally found in shallow-water environments, especially in areas normally having rapid mud sedimentation, interrupted by occasional sand deposition. In other words these structures rather point to rapid sedimentation in the areas they are associated with (Reineck and Singh, 1980). The wavy bedding observed in between is described in facies 3.

5. Petrography

5.1 Snadd Formation

5.1.1 Lithology and Texture

The lower 7 meters of core 7227/08-U-01 and the lower 13.6 meters of core 7230/05-U-03 are both part of the Snadd Formation. And for both core 7227/08-U-01 and core 7230/05-U-03 the grain-size can be described as silty mud (Fig. 5-1). The mud matrix is mica-rich, and fragments of muscovite and biotite can be seen. The matrix also contains some thin laminas of organic matter seen as thin dark lines in the optical microscope. Some of the thin sections merely consist of mudstone, these are less mica-rich.

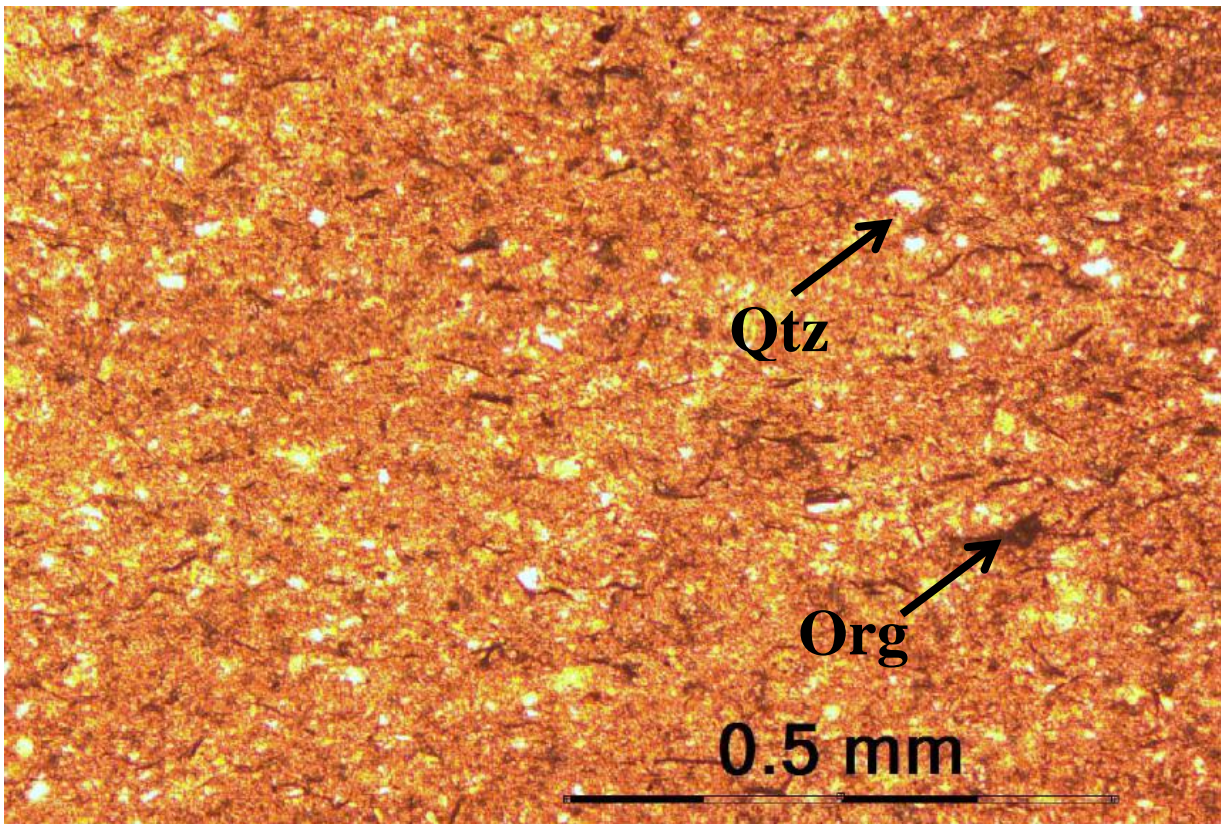


Figure 5-1: Typical silty mudstone texture found in the Snadd Formation. Organic matter (Org) can be seen as thin dark lines, and detrital quartz grains (Qtz) are white in plane polarized light, 69.8 meters depth (7227/08-U-01).

5.1.2 Detrital Grains

Quartz is the dominant detrital mineral in the silty mudstones, and the quartz consists merely of monocrystalline grains (Fig. 5-1). Some of the samples have some organic fragments. Muscovite and biotite are recognized in the mica-rich matrix. Traces of heavy-minerals have also been observed, among others garnet and tourmaline. SEM analysis also showed trace amounts of albite (thin section 64.25 meters depth, 7227/08-U-01).

The Snadd Formation also comprise some pure mudstones with no recognizable detrital grains, these thin sections do, however, show interesting diagenetic structures.

5.1.3 Diagenetic Minerals

Siderite

In several of the thin sections in the Snadd Formation, concentric carbonate nodules were observed in the mud matrix. The siderite concretions looked chemically zoned, and SEM was applied to verify the chemical zonation (Fig. 5-2). Ten electron microprobe analyses were also carried out and the results are presented in Table 5-1. The first six analyses were collected from the concentric siderite shown in Figure 5-2, b, taken from the core and out. Similarly, analyses were collected from the zoned siderite seen in Figure 5-3. The analysis shows a high content of manganese in the core of the siderite, with a gradual leaching of manganese towards the border of the crystals. The outer layer in both samples show a significantly higher magnesium content (Tab. 5-1).

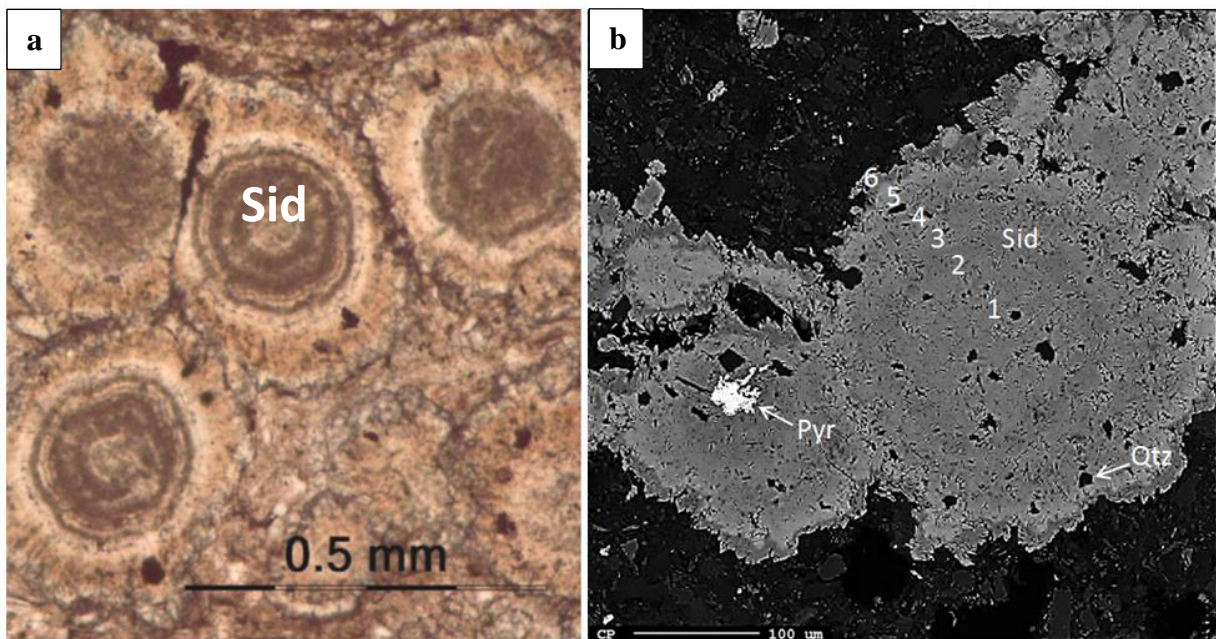


Figure 5-2: (a) Concentric siderite nodules seen in planar light, the siderite appear zoned (b) The backscattered electron image shows that the siderite nodules are actually chemically zoned. The thin section is from 64.25 meters depth, 7227/08-U-01.

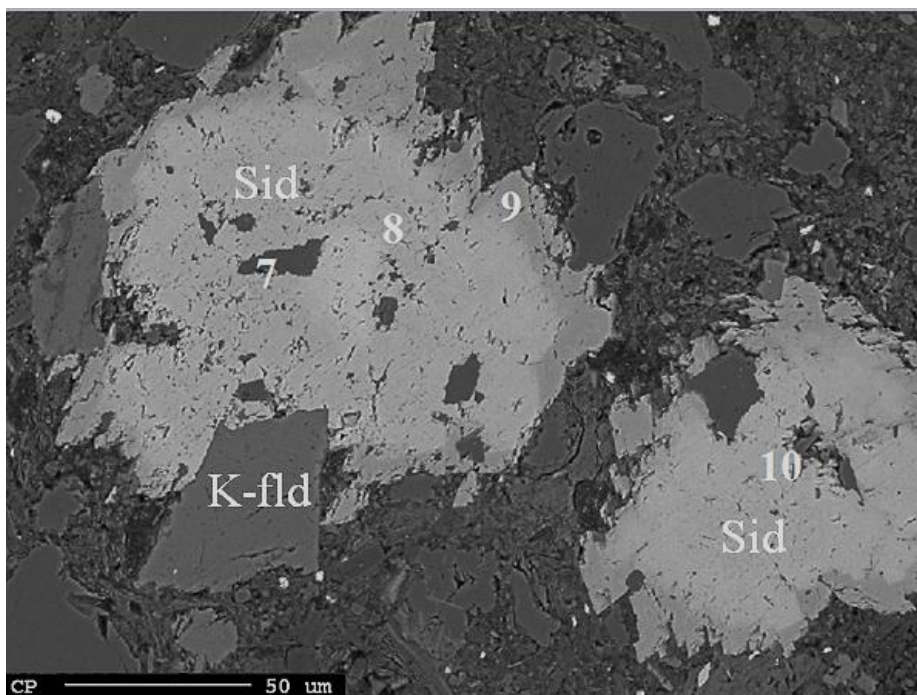


Figure 5-3: BEI image of siderite nodules (Sid) showing the locations for carbonate analysis 7 through 10, a potassium-feldspar grain (K-flid) is also indicated on the picture, 109.87 meters depth, 7230/05-U-03.

Table 5-1: Carbonate mineral compositions for the ten analyses from the Snadd Formation.

Carbonate mineral composition (cation proportions):						
Well	Depth	No	Fe	Mn	Mg	Ca
7227/08-U-01	64.25	1	69.1	24.4	2.4	4.2
7227/08-U-01	64.25	2	53.3	37.6	4.1	5.0
7227/08-U-01	64.25	3	81.7	10.3	2.9	5.1
7227/08-U-01	64.25	4	84.5	6.1	3.5	5.9
7227/08-U-01	64.25	5	91.4	2.1	2.6	3.8
7227/08-U-01	64.25	6	61.6	0.6	27.9	9.9
7230/05-U-03	109.87	7	89.0	3.4	3.2	4.5
7230/05-U-03	109.87	8	93.4	4.8	1.0	0.8
7230/05-U-03	109.87	9	65.6	0.4	23.3	10.7
7230/05-U-03	109.87	10	78.0	15.0	3.2	3.8

Pyrite

Pyrite occurs in the Snadd Formation in both cores, the pyrite appear as euhedral crystals (Fig. 5-4). The crystals occur in clusters or as single crystals. The color of pyrite in plane-polarized light is dark brown to black. The pyrite normally occurs in the detrital matrix.

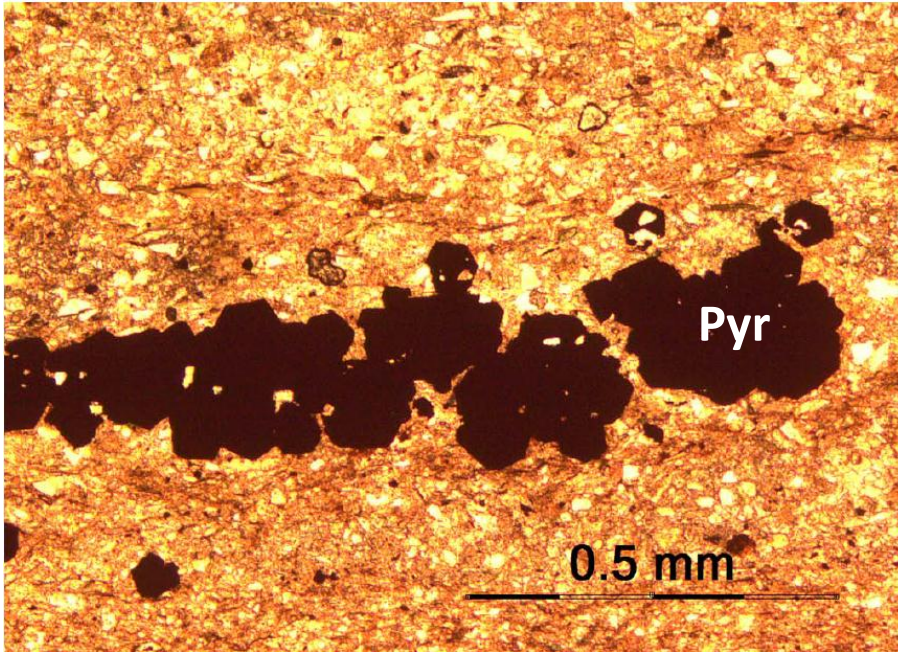


Figure 5-4: Clusters of euhedral shaped pyrite (Pyr) in the detrital matrix, 66.85 meters depth, 7227/08-U-01.

Clay Minerals

Both SEM and XRD analysis of the matrix indicate that it contains mainly illite and kaolinite. The kaolinite showed characteristic vermicular structures, as well as booklet structures (Fig. 5-5). The illite structures were harder to detect with SEM, but could be separated in the backscatter images as slightly lighter color than the kaolinite due to its high molecular weight. The XRD analysis also showed that the clay also probably contains some smectite (Appendix C).

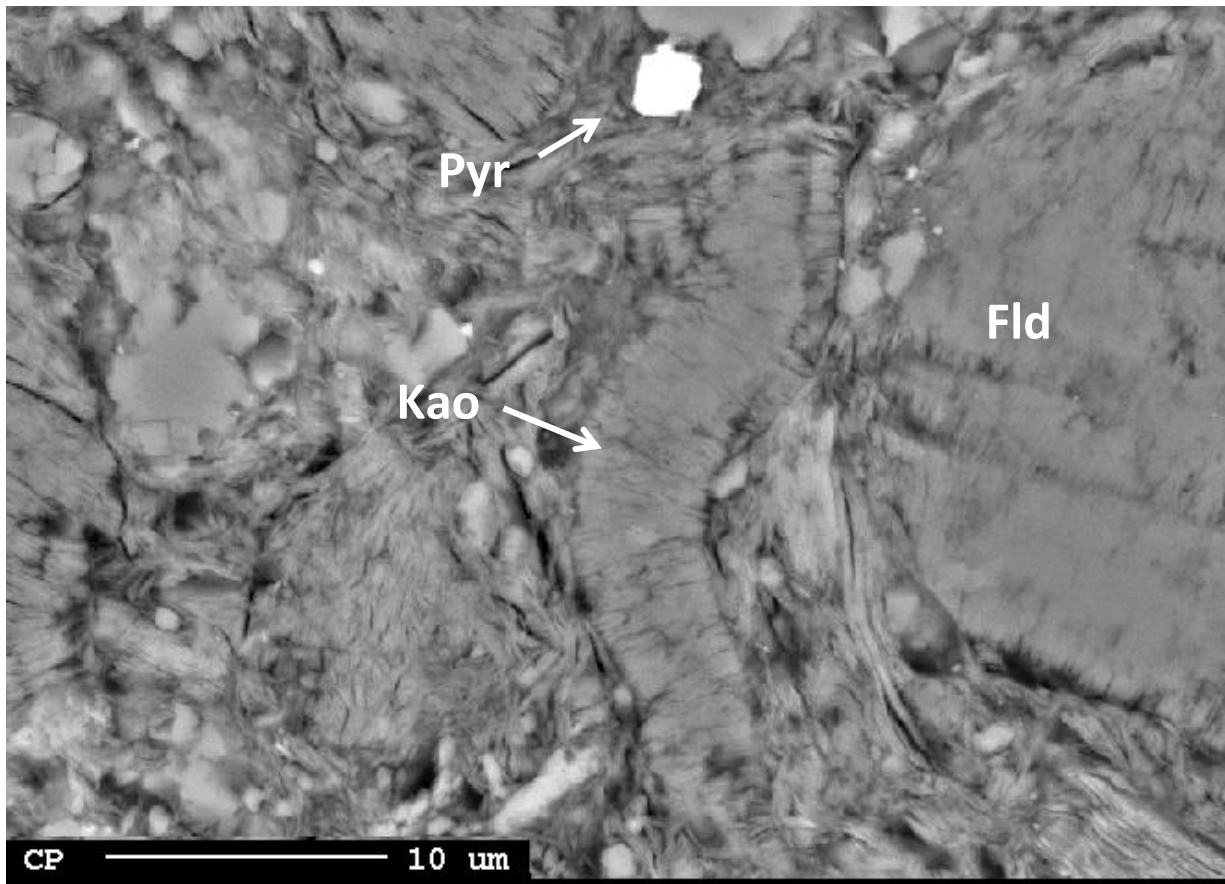


Figure 5-5: Vermicular kaolinite (Kao), kaolinitized feldspar (Fld) and pyrite (Pyr), 64.25 meters depth (7227/08-U-01)

5.2 Fruholmen Formation

In the Fruholmen Formation the facies is quite different in the two wells and will therefore be described separately.

5.2.1 Lithology and Texture in Core 7230/05-U-03

For the most part core 7230/05-U-03 can be described as medium-grained sandstone (Fig. 5-6). However, variations in grain size goes from fine to medium-grained sandstone. The fragments are sub- angular and not very well sorted. The formation also comprises some very fine-grained sandstone and silt layers. Throughout the upper 20 meters of the formation horizontal coal laminas can be observed.

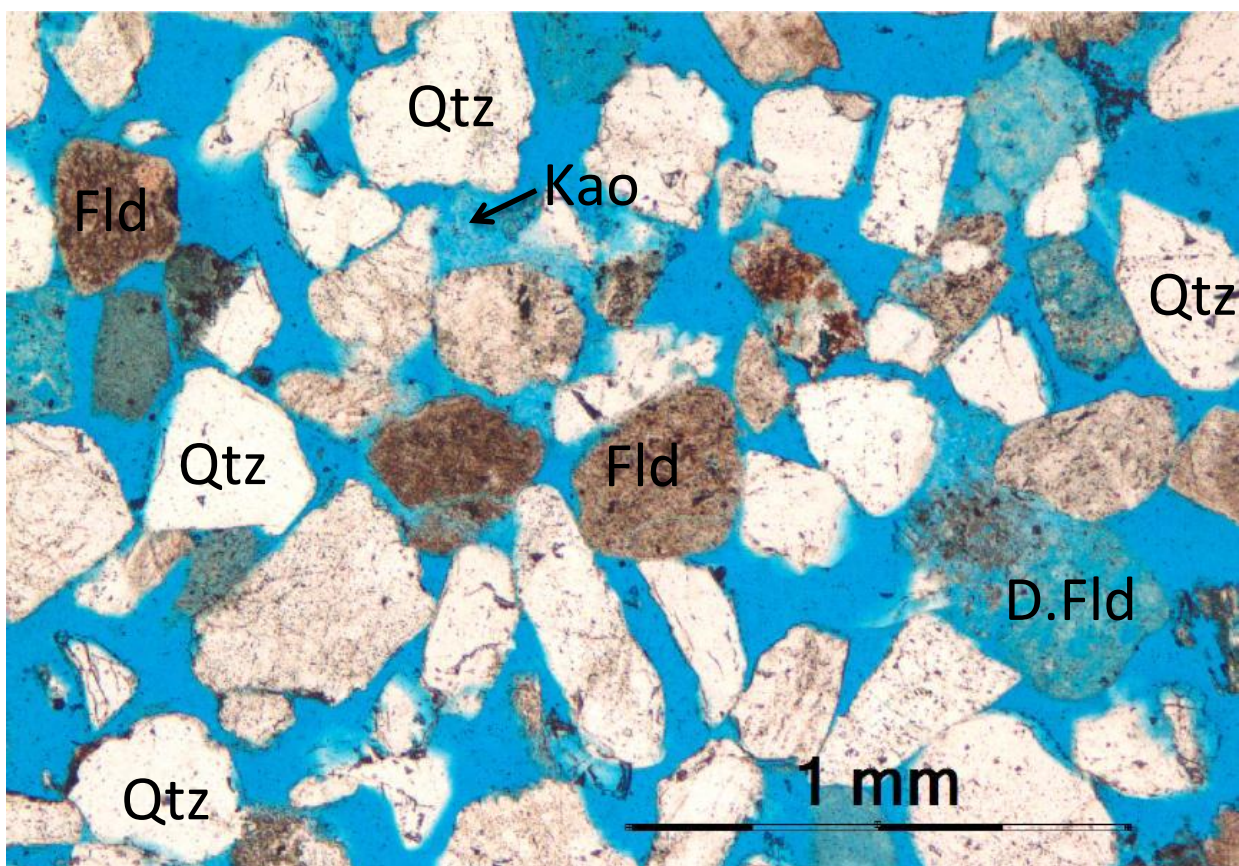


Figure 5-6: Typical thin section from Fruholmen in core 7230/05-U-03, The picture shows medium-grained sandstone with a high content of feldspar (Fld) in the core. The dominant detrital grain is quartz (Qtz), and it is possible to see some replacing kaolinite in the pore space, some of the feldspar is very dissolved (D.Fld). Porosity has been colored blu by epoxy (Kao), 98.33 meters depth.

5.2.2 Detrital Grains in Core 7230/05-U-03

In the Fruholmen Formation the dominant detrital grain is quartz. Chert and volcanic fragments can also be observed. Feldspar is also abundant, however, due to dissolution it is hard to separate K-feldspar from Plagioclase, it is hard to say whether the dissolution took place before or after deposition. Some muscovite grains can also be observed with the detrital

grains. In the coal laminae plant fragments with cellular structures have been observed in combination with other organic debris (Fig. 5-7). Traces of heavy minerals have been observed, some of the observed minerals were tourmaline and zircon.

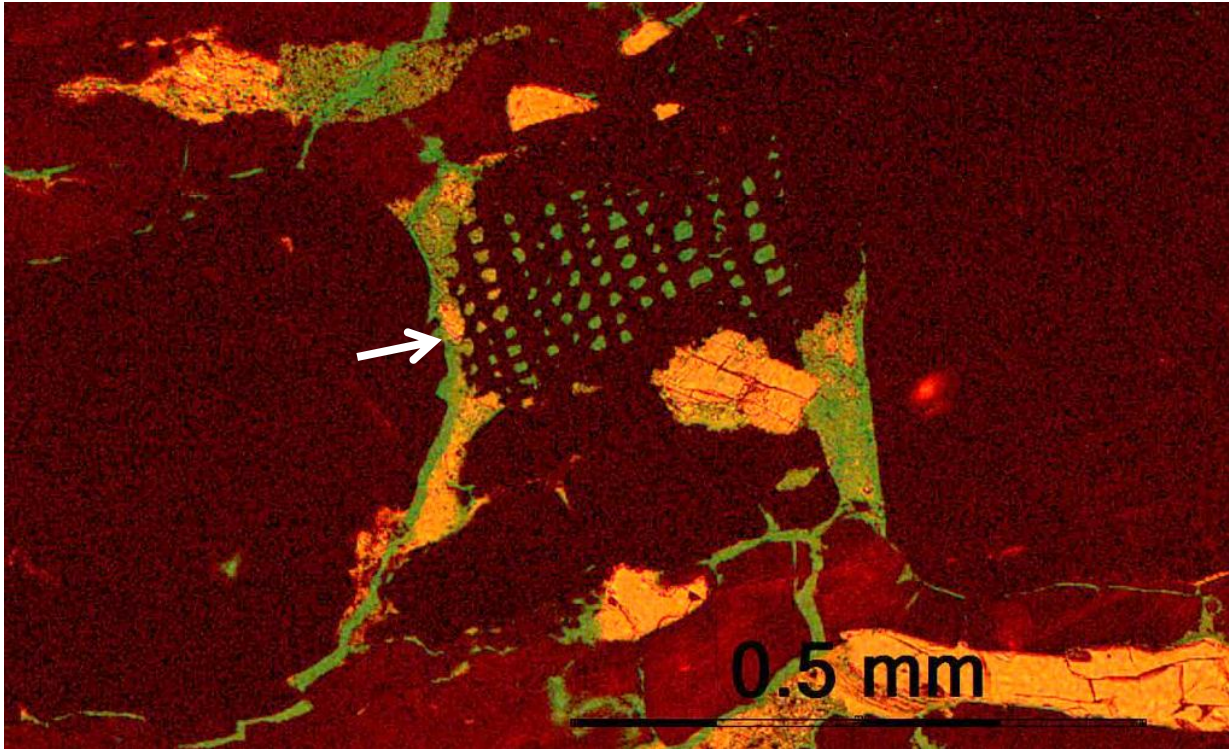


Figure 5-7: The arrow points to a plant fragment with original cellular structures still intact, 45.92 meters depth.

5.2.3 Diagenetic Minerals in Core 7230/05-U-03

Clay Minerals

The kaolinite minerals in the pore space are small, but they can easily be identified in optical microscope. The kaolinite shows characteristic booklet structures, and appear as clusters of plate shaped crystals. The kaolinite appears as pore fill or replacement of detrital minerals. They display perfect cleavage and white color in plane polarized light and low order grey to black interference colors (Fig. 5-8, a and b).

Similarly to the Snadd Formation XRD analysis of the matrix indicate that it contains mainly illite and kaolinite. XRD also indicate that there is some smectite in the samples from the Fruholmen Formation (Appendix C).

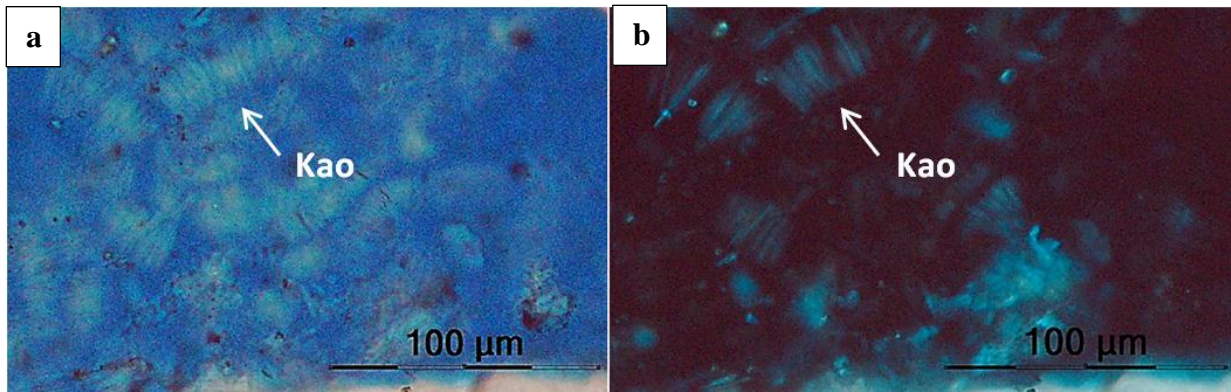


Figure 5-8: (a) Typical booklet structures in kaolinite (Kao), white color in plane polarized light. (b) Same thin section showing the interference colors of the kaolinite minerals displaying perfect cleavage, 98.33 meters depth.

Glauconite

Glauconite was observed in the formation, displaying the characteristic kidney shape. Glauconite is green in plane polarized light and dark green/grey with crossed nichols.

5.2.4 Lithology and Texture in Core 7227/08-U-01

The Fruholmen Formation in core 7227/08-U-01 mostly consist of silty mudstone, which is documented in the thin sections collected from the core. The lithology varies from very fine-grained sandstone to mudstone. Figure 5-9 shows the typical lithology found in the Fruholmen Formation in this core.

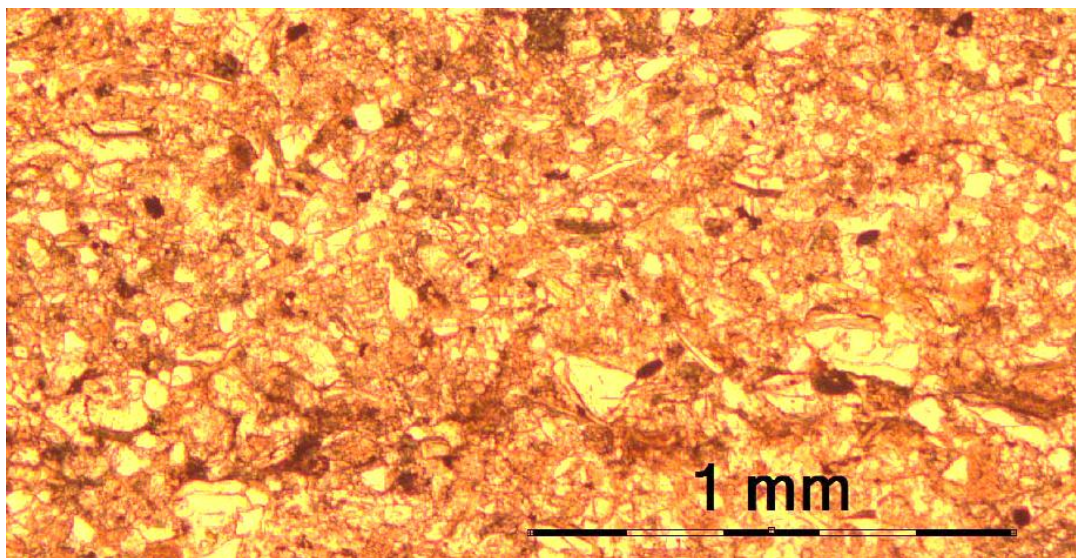


Figure 5-9: Very fine-grained sandstone with silty-mud matrix, the quartz grains are white, and the mud matrix has a brown color, 66.85 meters depth.

5.2.5 Detrital Grains in Core 7227/08-U-01

Also in this formation quartz is the dominant detrital mineral in the silty mudstones, and the quartz mainly consists of monocrystalline grains (Fig. 5-9). The mudstones often contain a lot

of organic material and shell fragments like juvenile bivalves (Fig 5-10). Fruholmen also comprises some pure mudstones with no recognizable detrital grains, these thin sections do, however, show interesting diagenetic structures.

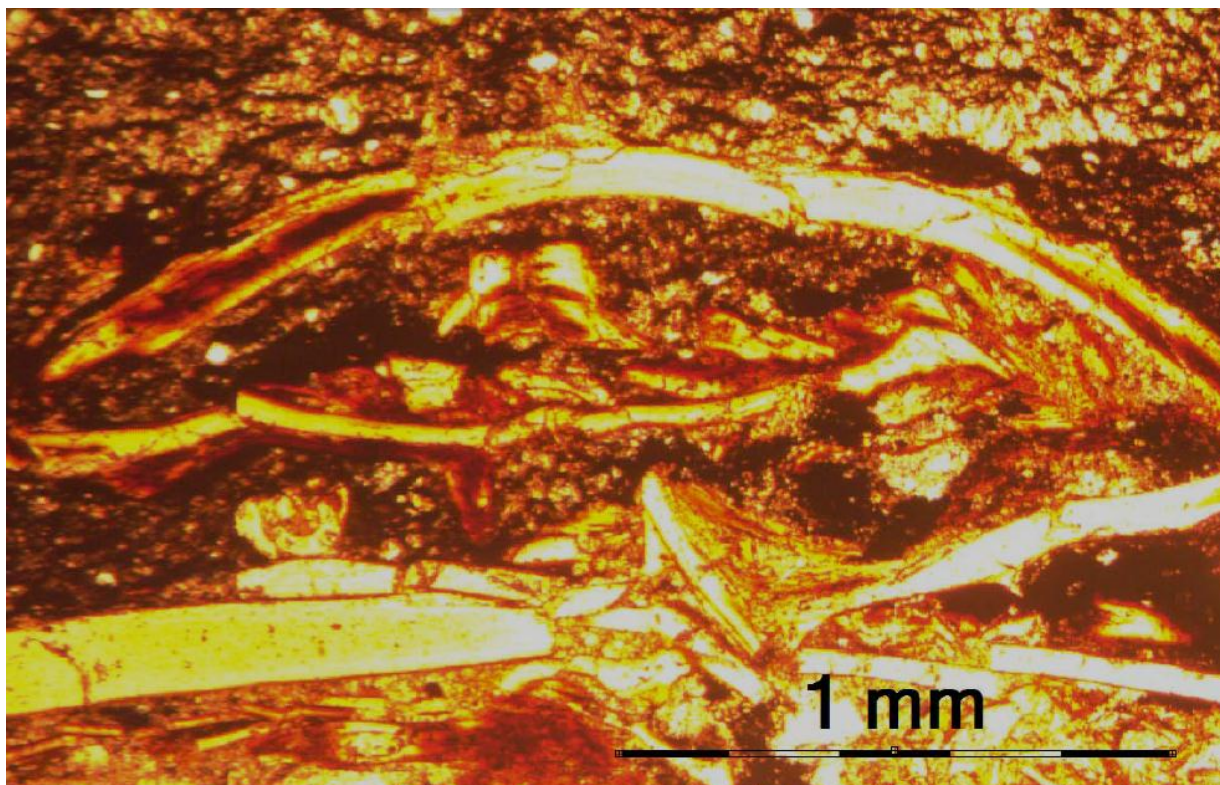


Figure 5-10: Juvenile bivalves in a silty mudstone, 35.9 meters depth.

5.2.6 Diagenetic Minerals in Core 7227/08-U-01

Dolomite

By doing SEM x-ray element mapping of the thin section it is apparent that a lot of the cement is actually dolomite cement (Fig. 5-13). The dolomite can be seen quite well in the Mg-mapping in Figure 5-13. The pink areas in the Mg-map are those rich in magnesium, and combined with the green areas of the Ca-mapping they represent the areas where it is most likely dolomite cement. Rhombic dolomite has also been observed in some of the thin sections from this formation (Fig. 5-11). EDS of the dolomite is included in Appendix B.

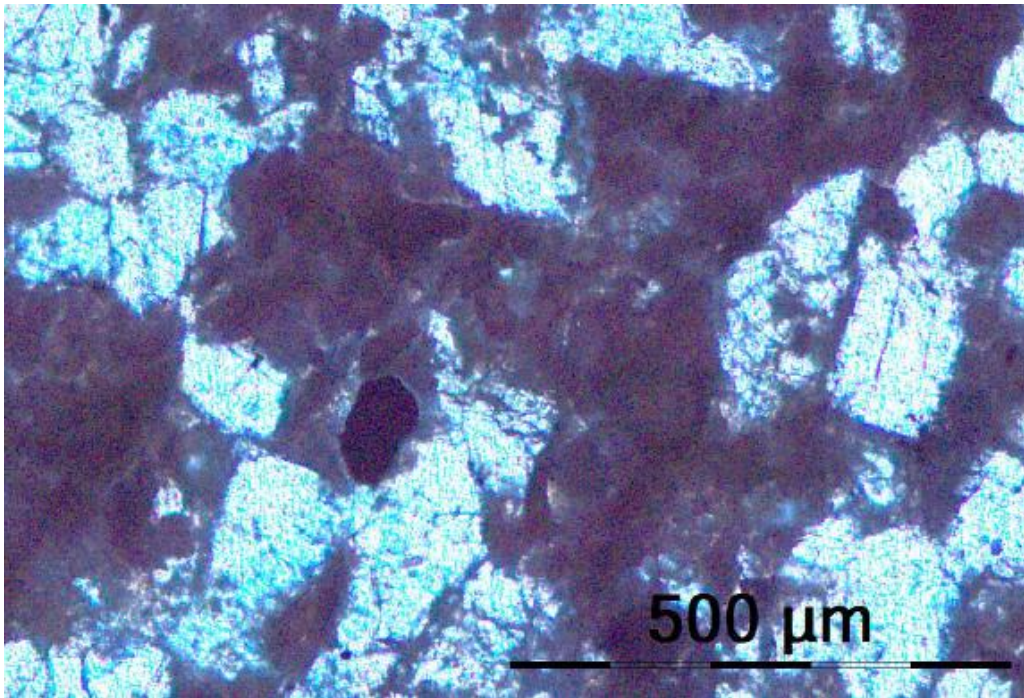


Figure 5-11: Rhombic dolomite crystals in mudstone, 46.75 meters depth

Calcite Cement

Several of the thin sections are completely or partly cemented. In the mudstones with silt laminae the coarser grained areas are more cemented than the rest. There have also been observed carbonate nodules similar to the sphaerosiderites observed in core 7227/08-U-01.

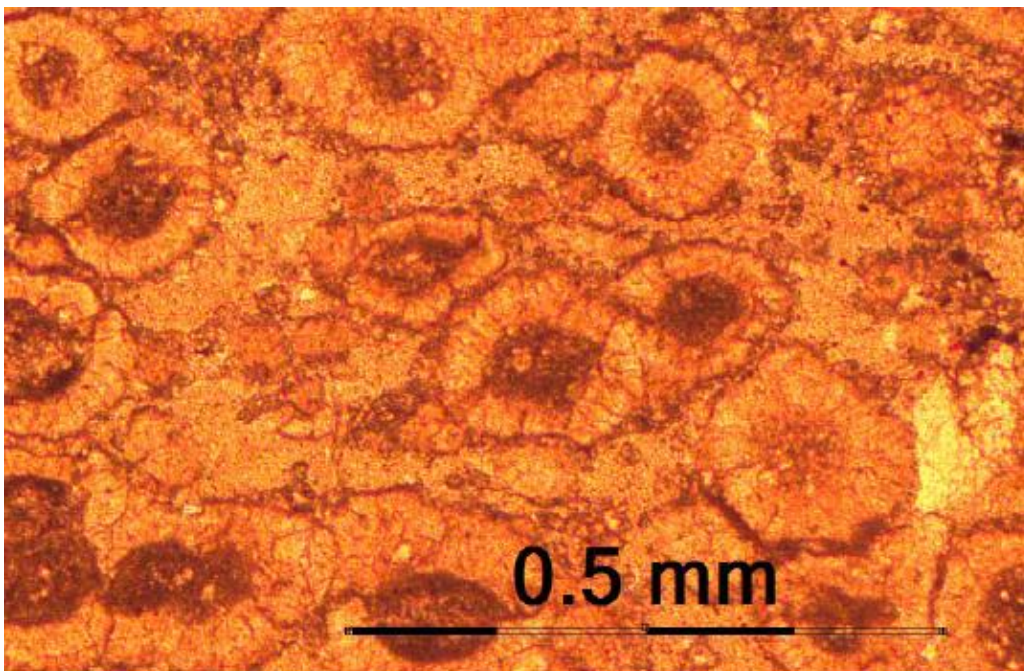


Figure 5-12: Carbonate nodules in mudstone, 45.75 meters depth.

Phosphatized Shell Fragments

A shell fragment similar to that seen in Figure 5-10 was also mapped. The P- mapping shows elevated levels of phosphorus in the shell fragment indicated that it has been phosphatized (Fig. 5-13).

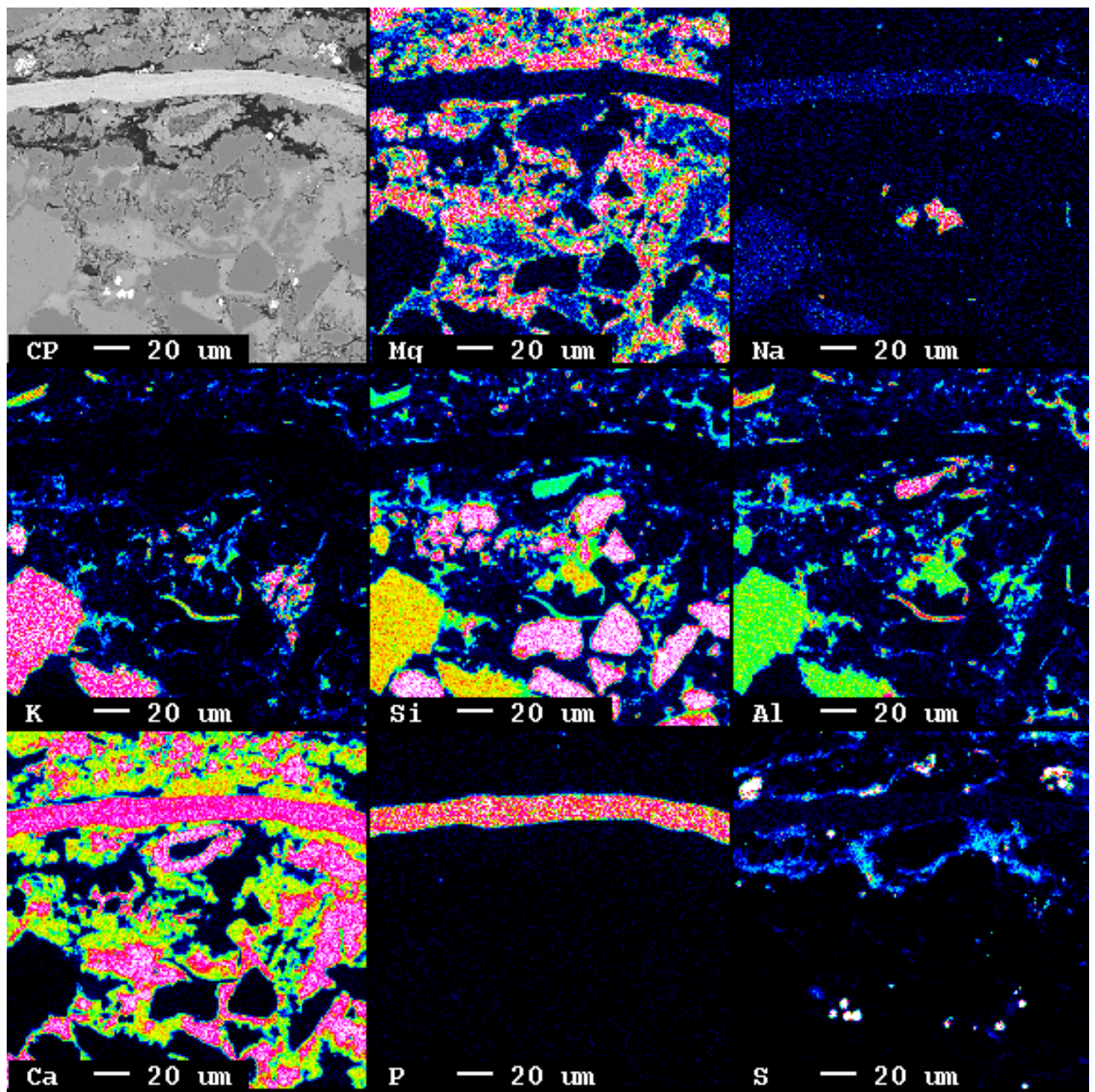


Figure 5-13: Element mapping of a thin section allows us to map the concentration of each element in the thin section. The scale goes from white at the highest concentrations, through pink, red, yellow, green blue and finally black where the thin section does not contain any trace of the element being mapped. This figure shows the BEI image in the upper right corner, and then the mapping of Mg, Na, K, Si, Al, Ca, P and S.

Pyrite

The pyrite in Fruholmen appears as cubically shaped crystals, but also framboidal as seen in Figure 5-13. The crystals occur in clusters or as single crystals. The color of pyrite in plane-polarized light is dark brown to black. The pyrite normally occurs in the detrital matrix. In Figure 5-13 the pyrite is most easily detected as small white dots in the BEI image, and light-pink/white dots in the S-mapping.

Barium Sulphate

By applying SEM the mineral filling the micro fractures in a limestone was determined. By analyzing the energy dispersive spectras collected from the sample, it was found that the mineral was barium sulphate, BaSO₄ (Fig. 5-14).

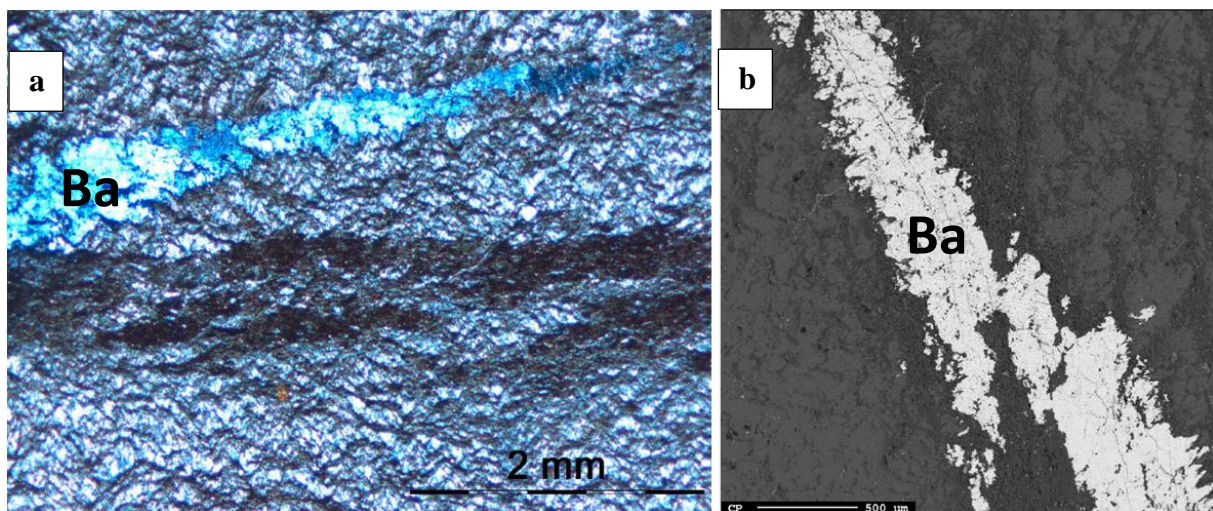


Figure 5-14: Barium Sulphate (Ba) filled micro fractures in the Fruholmen Formation, (a) shows fracture filled with barium sulphate seen with an optical microscope with crossed Nichols. (b) The fracture seen in BEI, the barium sulphate has a much higher molecular weight than the surrounding illite and calcite matrix, and therefore appears white. The slightly lighter colors areas in the matrix mainly consist of illite, the scalebar shows 100 μm. The thin section is from 48.9 meters depth.

Illite and Kaolinite

Both SEM and XRD analysis of the matrix indicate that it contains mainly illite and kaolinite. Neither the typical illite nor the kaolinite structures were detected with SEM, but could be separated in the backscatter images as slightly lighter color than the kaolinite due to its high molecular weight. EDS was used to identify the different autigenic clay minerals in the matrix (Fig. 5-15 and 5-16). Here the two clay minerals were separated by the mineralogical fingerprint of each mineral. This is displayed in the EDS spectras presented below, for more details see Appendix B.

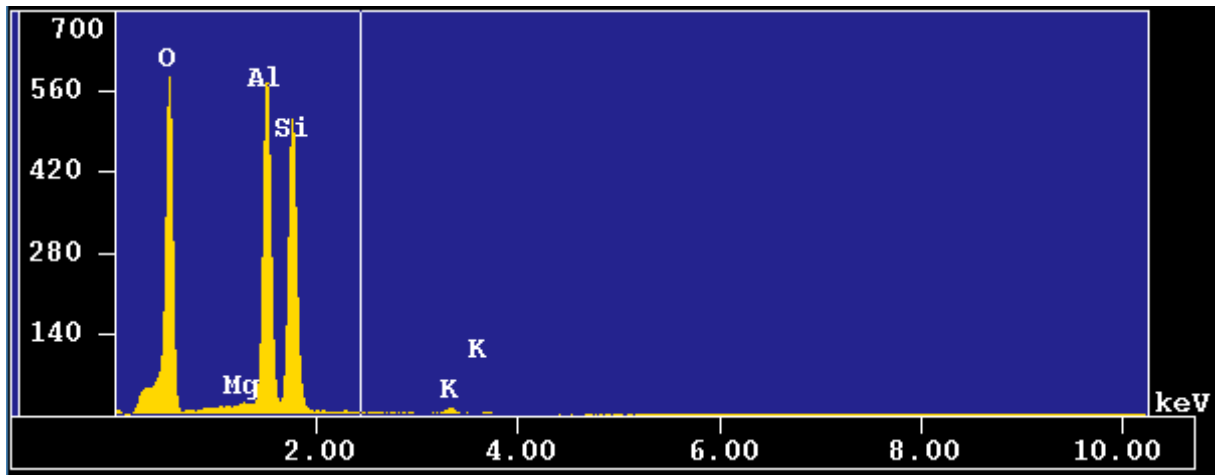


Figure 5-15: This EDS spectra shows the composition of kaolinite.

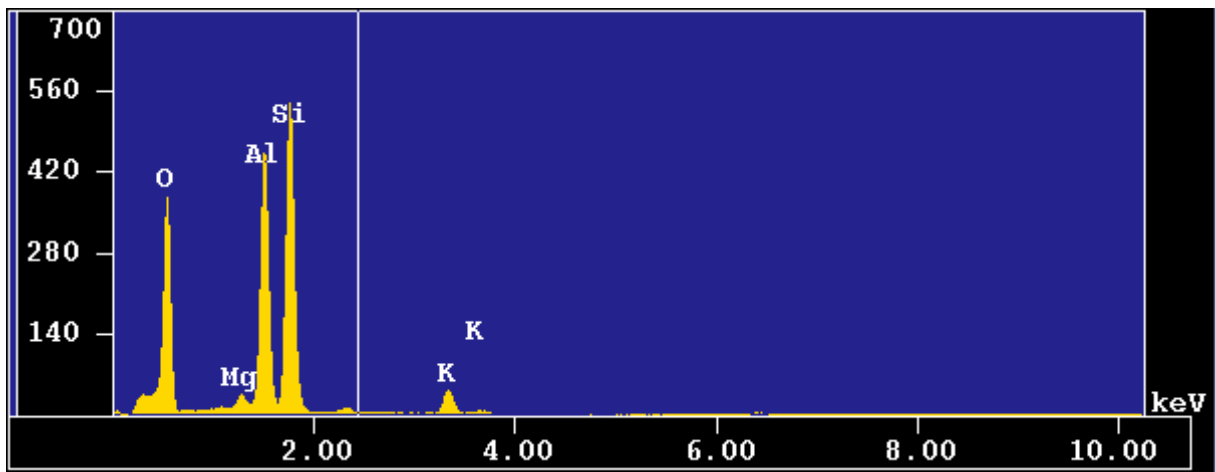


Figure 5-16: The EDS spectra for illite has a higher Kalium content separatin it from the kaolinite fingerprint.

Glauconite

The upper part of the sediments in the Fruholmen Formation displays immature glauconite, with several partly glauconitized grains. There was also observed some more developed glauconite grains in the core. The glauconite mineral is a hydrous potassium iron aluminosilicate which has a green color in plane-polarized light.

5.3 Stø Formation

5.3.1 Lithology and Texture

The Stø Formation shows a much more mature texture. The grain size varies from very-fine- to medium (Fig. 5-17). In core 7227/08-U-01 Stø comprises two different types of facies. However, the upper part of the core shows a similar facies to that seen in core 7230/05-U-03 and they are therefore presented together.

5.3.2 Detrital Grains

Quartz is the dominant detrital grain in the Stø Formation in both wells. Quartz mostly occurs as monocrystalline grains with uniform extinction. However, some of the grains have undulating extinction indicating intercrystalline deformation. Quartz also occurs as polycrystalline grains, and as part of rock fragments. Feldspar and muscovite appear in sparse amounts, some of the feldspars show albite and gridiron twinning (Fig. 5-18). Heavy minerals like garnets, zircon and rutile have been observed in trace amounts (Fig. 5-19 and 5-20).

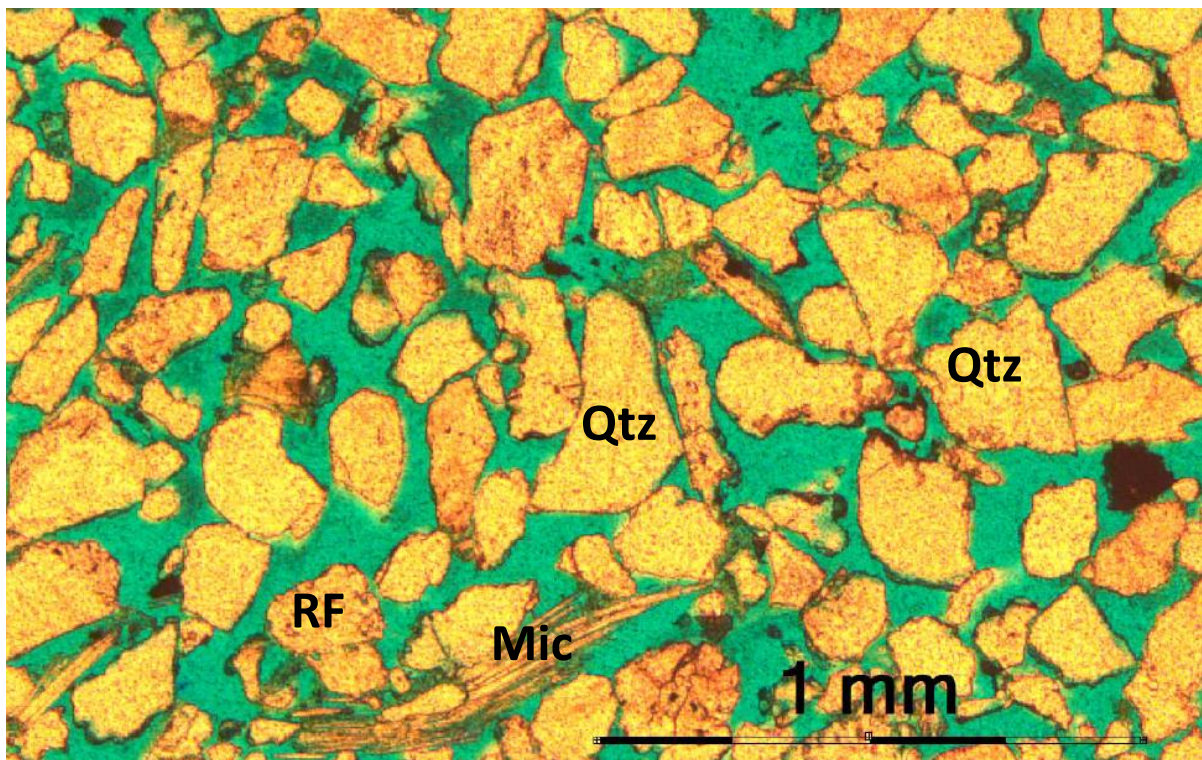


Figure 5-17: The texture seen in the Stø Formation here from core 7230/05-U-03. The sample shows the typical detrital grains found in the formation. The dominant detrital grain is quartz (Qtz), but the formation also has a considerable amount of rock fragments (RF), muscovite is also seen in sparse amounts (Mic). The porosity in the thin section has been colored blue with epoxy, 32.8 meters depth (7230/05-U-03).

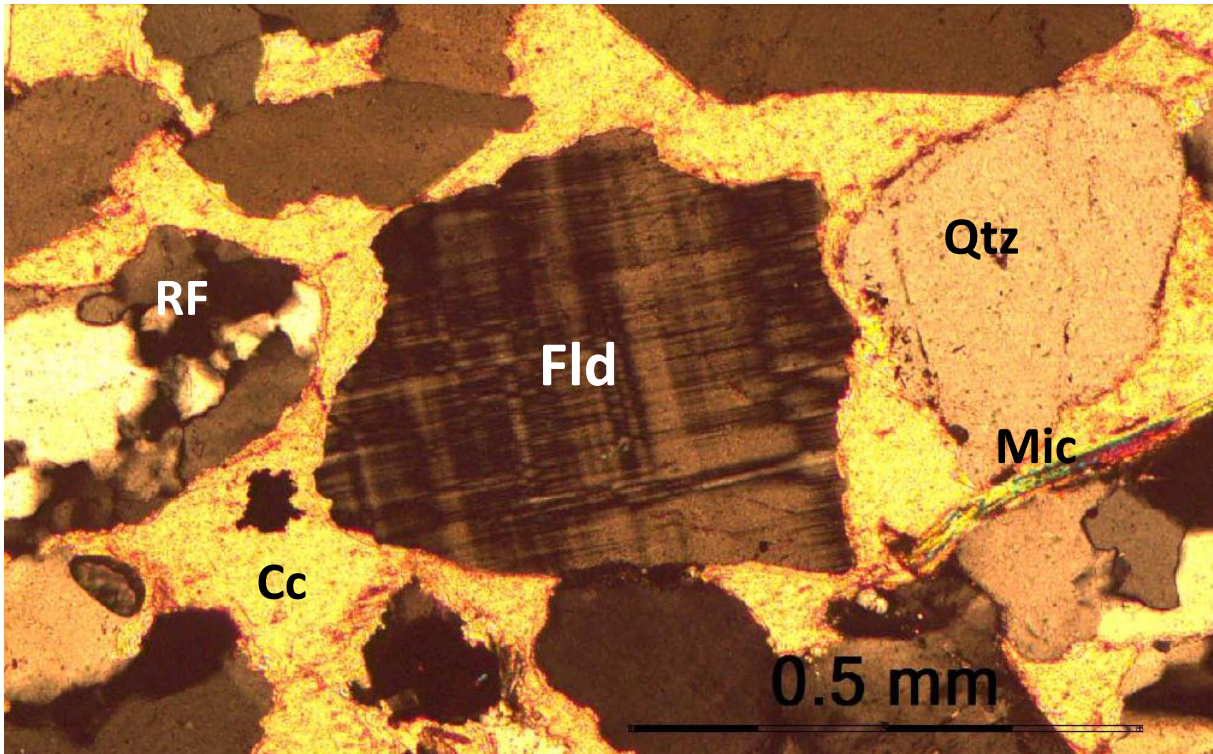


Figure 5-18: Some of the detrital grains found in the Stø Formation, The most dominant is quartz (Qtz), they also contain moderate amounts of rock fragments (RF), Some feldspar (Fld) can be seen here showing crosshatched twins, and some mica (Mic) here it is muscovite, The pore space is filled with calcite cement (Cc). 36.0 meters depth (7227/08-U-01)

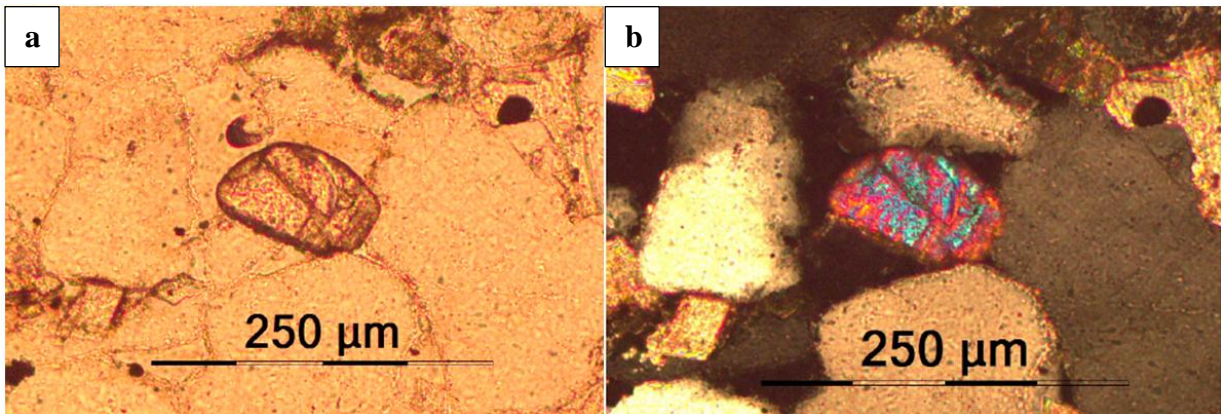


Figure 5-19: (a) Zircon displaying high relief in plane polarized light. (b) The zircon has high order interference colors with crossed nichols. The thin section is from 31.55 meters depth (7227/08-U-01).

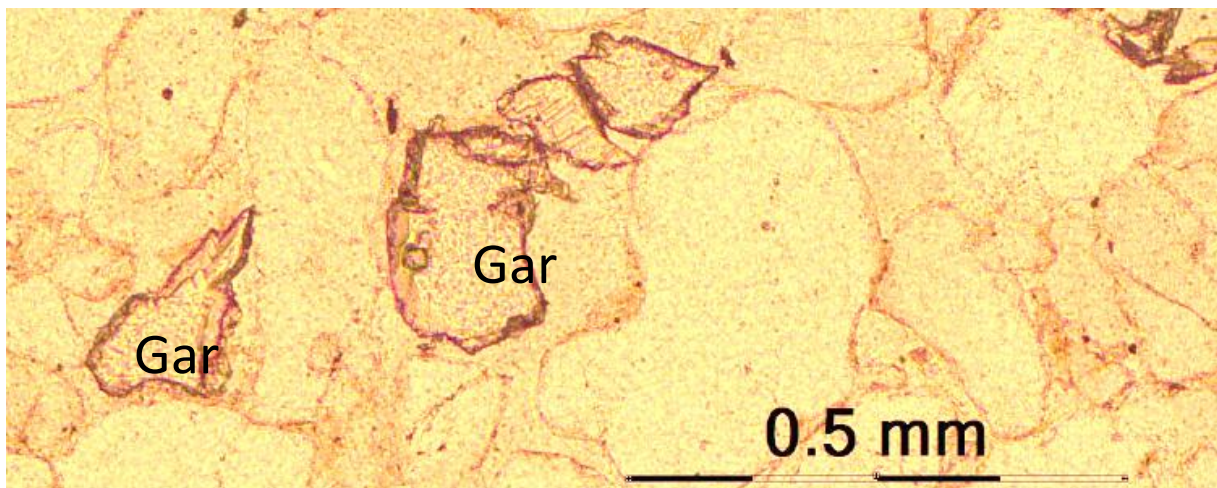


Figure 5-20: Garnet fragments (Gar) displaying high relief and isotropic extinction, 36.0 meters depth (7227/08-U-01).

5.3.3 Diagenetic Minerals

Glauconite

Glauconite has been observed in several of the thin sections in the upper part of the formation. The glauconite is rounded, and it does not display the typical kidney shape one would expect. The glauconite is green in plane polarized light, with lower order green and grey interference colors.

Carbonate Cement

Carbonate cement is particularly dominating in the lower part of the Stø Formation in core 7227/08-U-01. The calcite cement appears as round cemented areas in the core. In the thin sections it is pore filling cement (Fig. 5-18).

Pyrite

The pyrite in the Stø Formation appears as pore filling cement in small patches randomly distributed in the thin sections (Fig. 5-21). The color of pyrite in plane-polarized light is dark brown to black. When hit by a secondary light source golden colors can be observed in the microscope.

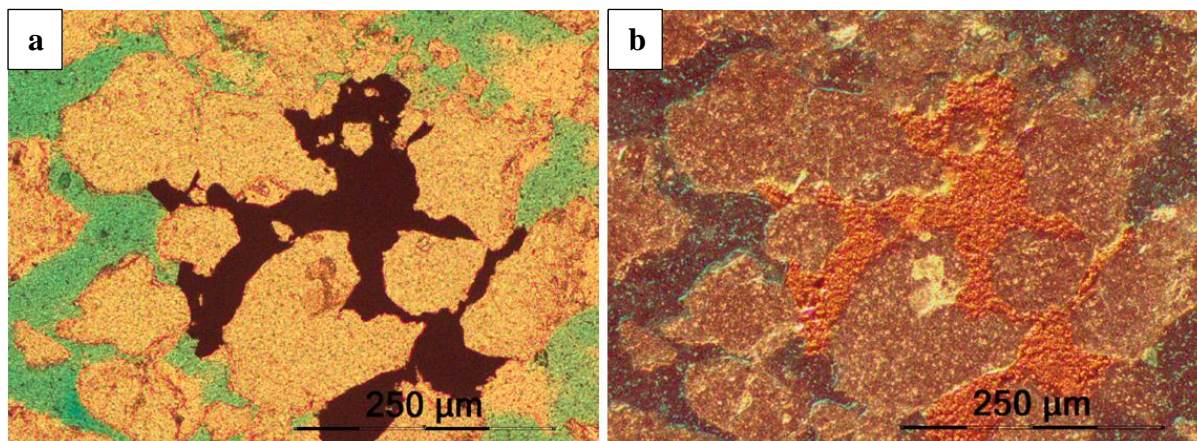


Figure 5-21: (a) Pyrite cement seen in planar polarized light. (b) The same pyrite cemented are with a secondary light source directed towards it making it display golden colors. The thin section is from 33.68 meter depth (7230/05-U-03).

Illite and Kaolinite

Both illite and kaolinite have been verified in the matrix using SEM.

5.4 Modal Analysis

Neither core 7227/08-U-01 nor core 7230/05-U-03 comprised sandstone suitable for modal analysis, as the lithology mainly consisted of silty-mudstones. In order to compare the mineralogical maturity across the formation boundary between the Snadd and Fruholmen formations a third well was used. As mentioned previously well 7430/07-U-01 will be used for the purpose of lateral comparison of the Snadd Formation. Well 7227/08-U-01 and 7230/05-U-03 both include short sections from the upper Snadd Formation. By comparing the facies of these sediments with those seen at the Bjarmeland Platform the deposits can be correlated (The location of the core is marked as “*previous study*” in figure 3-3). Core 7430/07-U-01 comprises shale, sandstone and siltstone, forming a series of stacked upwards coarsening subunits, often overlaid by coal beds. The modal analysis in this study is mainly used to see the difference in feldspar content in the different formations. Due to very generally fine grained deposits in both cores, 12 thin sections suitable for modal analysis were selected from the three cores. The content and distribution of detrital grains, matrix, diagenetic minerals and porosity is presented in Table 5-2. From the modal analysis it was found that the sediments in the Snadd and Fruholmen formations contained arkosic arenite, and the Stø Formation contained quartzarenite and sublitharenite.

Modal analysis was carried out mainly for the purpose of comparing the variation in the mineralogical maturity between the three formations, with the main focus on the transition between Snadd and Fruholmen formations. Maturity can be compositional and expressed in chemical or mineralogic terms. A pure quartz concentration is the ultimate sand. This is because quartz is the only physically and chemically durable constituent of plutonic rocks common enough to be accumulated in great volume (Pettijohn, 1954). A measure of mineralogical maturity, therefore, is given by its quartz content. As most quartz was originally plutonic and closely associated with feldspar, the maturity may also be expressed by the disappearance of feldspar (Dott, 1964). The modal analysis in this study show no great difference in mineralogical maturity between the Snadd and Fruholmen formations, however, a great difference from the underlying Triassic Snadd and Fruholmen formations to the Jurassic deposits in the Stø Formation. The sandstones in Snadd and Fruholmen are classified as arkosic arenite, and they both plot in the same area in the QFL-plot (Fig. 5-22). The sandstones in the Stø Formation are classified as sublitharenites, and quartz arenite. The data collected in the modal analysis conducted for this report reflects the same findings as Bugge et al. (2002), with feldspar concentrations between 24-39% for Snadd and Fruholmen, and 0-6% in the Stø Formation.

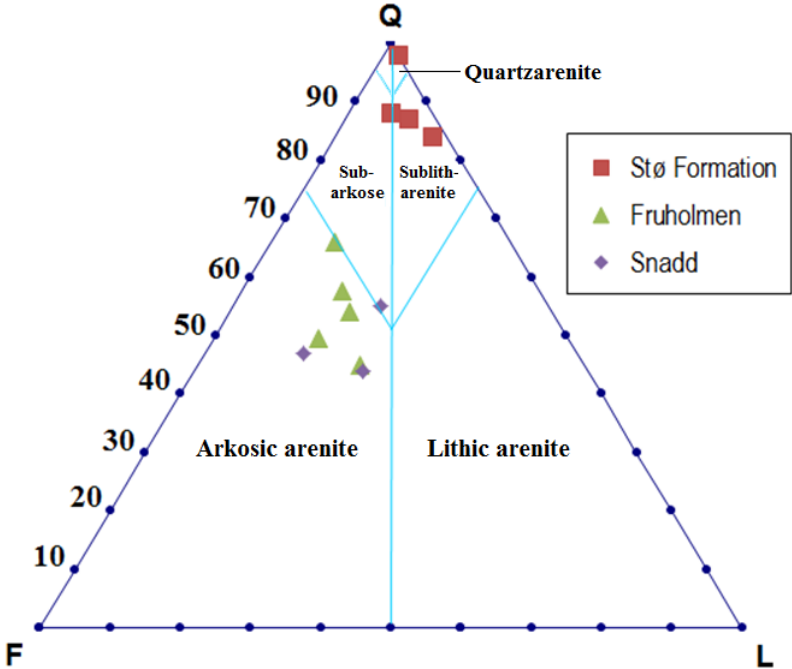


Figure 5-22: Quartz-Feldspar-Lithics (QFL) plot of the sandstones in the three different formations. “L” includes mica, accessory heavy minerals, and the polygranular rock fragments (Pettijohn et al. 1972, Dott 1964).

5.5 XRD Analysis

Core 7227/08-U-01 and core 7230/05-U-03 both have clay deposits above and below the Snadd-Fruholmen formation boundary. In order to further investigate the theory of a change in mineralogical composition samples from both Snadd and Fruholmen formations were collected, from both cores, in order to make a comparison of the clay composition in the two formations. The samples were collected from mudstone sections above and below the boundary to avoid that the facies affected the results. Strongly cemented samples were excluded from the study to reduce the impact of diagenetic influence on the semi quantitative analysis. According to Bergan and Knarud (1992) a transition in the mineralogical composition may give information about changing paleodrainage and subsidence patterns of the depositional basin, section 1.2. The dominant mineral in the samples was quartz, the samples also contain a considerable amount of feldspar, both K-feldspar and plagioclase, there was also found trace amounts of anatase and clinocllore. The two dominant autigenic clay minerals identified in the samples are illite and kaolinite (Appendix C).

The results from these XRD analyses, however, show no great differences in the mineralogical composition above and below the formation boundary. Sample 1 show very different values from the remaining five, and will not be used for comparison as this sample was collected to check the mineral contents of an unknown concretion. Sample 2-6, however, show very similar mineral composition with small variations. The wide bulge to the right of the Illite peak is probably the result of a mixed-layer mineral. The wide peaks at 4.47 Å and 2.56 Å are a good match for smectite (montorillonite), but the 001 reflection has lower angles, and it is therefore probable that there is some mixed layer illite/smectite present (I/S). The samples all have high quartz content, and have a matrix consisting mainly of illite and kaolinite. Sample 2 and 5 do not have any Plagioclase present; this could be due to local variations within the facies. Sample 2 and 3 have some Anatase.

The kaolinite and illite in the matrix could also be an indicator of the environment. Diagenetic clay minerals occur in sediments by direct precipitation from pore fluids, alteration of detrital silicates, mechanical clay infiltration and compaction of ductile argillaceous grains (Ketzer et al., 2003)

6. Interpretations and Discussion

6.1 Depositional Environment

The interpretation of depositional environment has been carried out based on the sedimentological logs (Appendix A), the core and facies description in Chapter 4 and the petrographic observations presented in chapter 5. The cores will be interpreted separately.

6.1.1 Core 7227/08-U-01

Snadd Formation

The Snadd Formation comprises several mud layers with a dusky red color. The dusky red color has been interpreted to be due to exposure and pedogenic processes. In several places variegated mottled mudstone appeared. This facies has been interpreted to be part of a developing soil. According to Reading (1978) a heterogeneous distribution of Eh leads to patchy transformation and color-mottled textures involving red, green, brown, ochre, and bleached patches. The permeability of the host sediment also controls the distribution of ferric and ferrous pigments. The formation also contains several layers which display siderite nodules, or sphaerosiderite. For the purpose of further investigating the depositional environment in the Snadd Formation, carbonate analysis of these chemically zoned siderite nodules were conducted.

In both cores SEM was used to carry out carbonate analysis on siderite nodules found in the Snadd Formation, the results of these analysis were presented in section 5.1. The results were further interpreted and are displayed in ternary $\text{CaCO}_3\text{-MgCO}_3\text{-FeCO}_3$ and $\text{CaCO}_3\text{-MgCO}_3\text{-MnCO}_3$ plots below (Fig. 6-1, a and b). The concentration of the major elements is relatively constant throughout a single sphere and does not show any signs of extensive alteration or chemical zoning, except for the outer zone in the two measured siderite nodules. According to a previous study conducted by Mozley (1989) siderites from fresh water environments are often very pure, and can contain as much as 90% FeCO_3 . Siderites from marine environments on the other hand are usually impure, and show extensive substitution of magnesium and to some extent calcium for iron in the crystal lattice. In addition marine siderite generally contains less manganese and has a higher Ca/Mg-ratio than fresh water (Mozley, 1989).

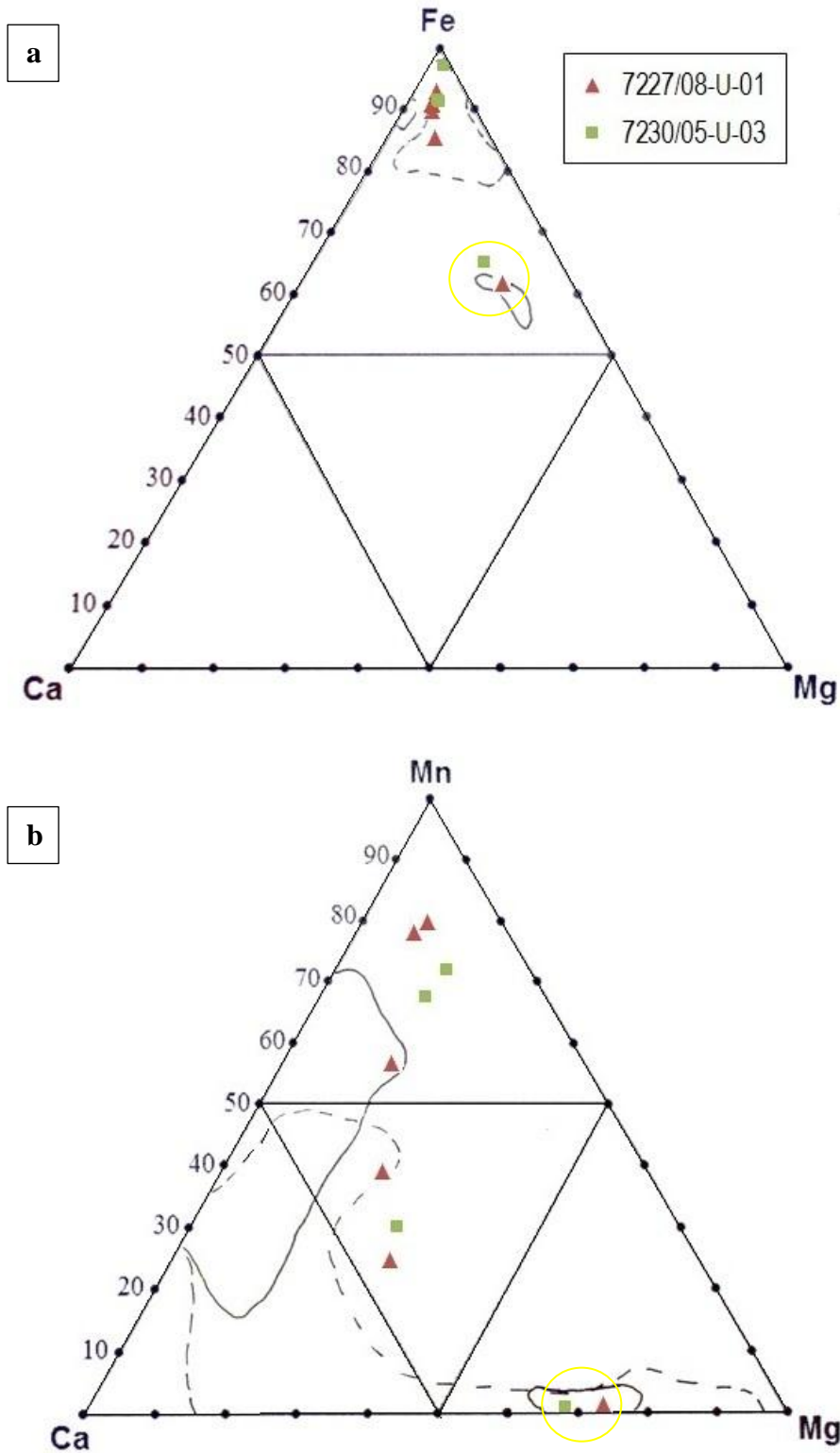


Figure 6-1: Ternary $\text{CaCO}_3\text{-MgCO}_3\text{-FeCO}_3$ (a) and $\text{CaCO}_3\text{-MgCO}_3\text{-MnCO}_3$ (b) plots for siderite taken in the Snadd Formation in core 7227/08-U-01 and 7230/05-U03 with an electron microscope. The circled areas are from Peters Mozley's paper (1989) and indicate his results collected for fresh-water siderite. The yellow circles indicate the results for the outer layer in each of the two siderite nodules.

The analysis carried out on the sphaerosiderite found in the Snadd Formation show similar characteristics to the plotted results for fresh-water siderites found in Mozley (1989), he reports that there are no documented cases of marine siderite ever approaching end-member composition.

Marine sediments also generally contain relatively low concentrations of manganese (<1%) (Mozley, 1989). The plot below shows a high FeCO_3 content, where most of the data points are plotted by the end-member (>90% FeCO_3). The same tendency can be seen in the other plot which shows a relatively high content of manganese (25-80%). This indicates that these siderites developed in fresh-water conditions, which further supports the interpretation of subaerial conditions and fits well with the previous interpretation of paleosol. The two analyses done in the outer layer in each of the sphaerosiderites, however, show a lower iron content (~60%), with a considerable substitution of magnesium and very low levels of manganese (<1%). These results are indicated with a yellow circle in the plots. These results could possibly indicate that the outer layer in the siderite nodules were developed at a later stage after the sediments were exposed for marine conditions, but as they are placed in an overlap zone between marine and fresh-water conditions no definite conclusion can be drawn.

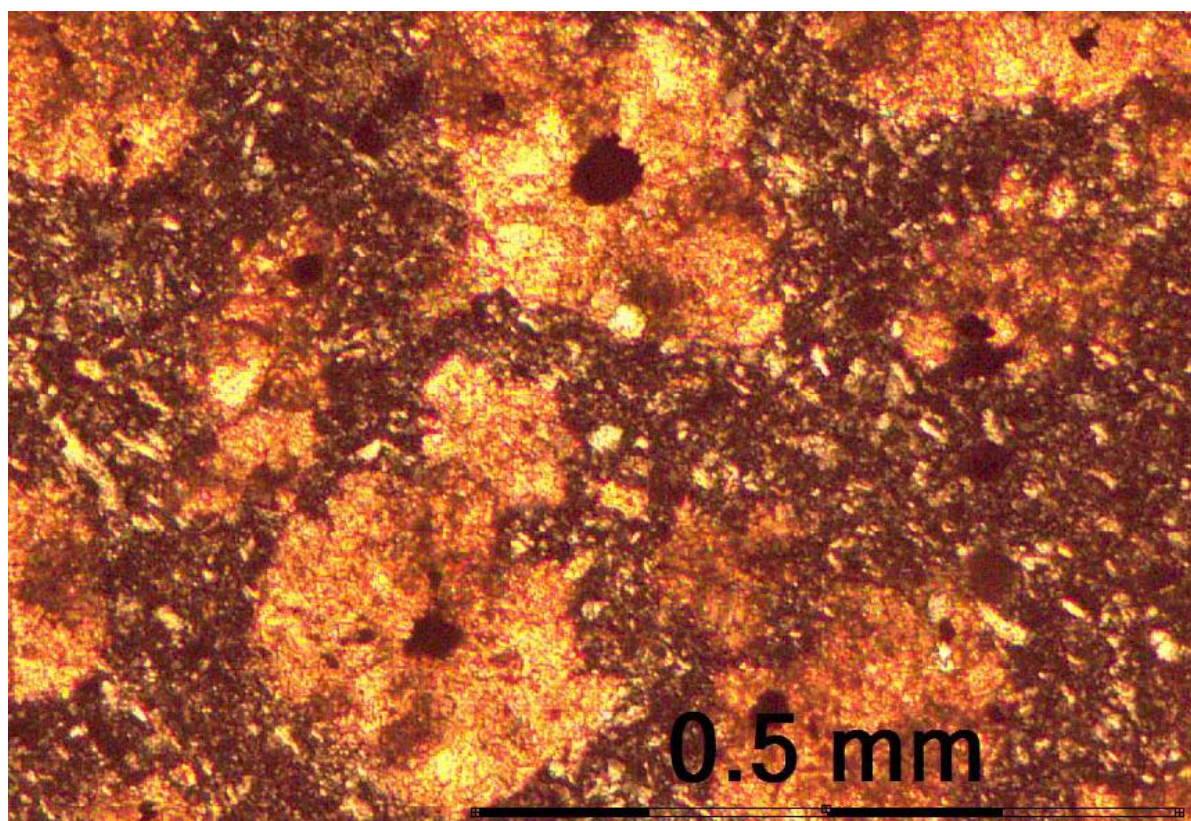


Figure 6-2: Siderite rhizocretions with organic residue in the center, 65.1 meter depth (7227/08-U-01).

Another factor to consider is that well-preserved sphaerosiderites typically exhibit smooth exteriors, spherulitic crystalline microstructures and relatively pure (>95% FeCO₃) compositions. Diagenetically altered sphaerosiderites typically exhibit corroded margins, replacement structures and increased crystal lattice substitution of Ca²⁺, Mg²⁺ and Mn²⁺ for Fe²⁺ (Ufnar, 2004). The sphaerosiderites investigated in this study did not have smooth surfaces, which could indicate that they have been diagenetically altered at a later stage.

The results from the carbonate analysis also support the theory that these sphaerosiderite could be siderite rhizocretions (Fig. 6-2). Rhizocretions are generally considered an indicator of fresh-water conditions (Adams et al., 2006). In fresh-water systems, where sulphate concentrations are limited, Fe(III) reduction commonly results in the production of Fe(II)-rich carbonate minerals (Curtis and Spears, 1968). Siderite formed in fresh pore water is commonly related to wetland soil environments (Ufnar et al., 2001). Carbonate accumulations close to the surface are prominent in a number of different soils, and their origin has been studied extensively. In particular, the role of roots, both indirectly and directly as channels for evapotranspiration, in pedogenic caliche formation has been found to be significant (Klappa, 1980). For these reasons, siderite present in association with rootlets is commonly assumed to be directly associated with soil-forming processes (Adams et al. 2006). The Snadd Formation in core 7227/08-U-01 has been classified as delta plain/tidal flat deposits (Fig. 6-4)

Fruholmen Formation

The Fruholmen Formation comprises a series of alternating silt and sandstone layers, these beds often show characteristic syneresis structures, and to some extent burrows in some sections. The deposits are disturbed in many places, and bear witness of varying depositional energy. This facies is typical for the delta front slope. Pro delta deposits are, as mentioned in section 4.2, characteristically fine-grained to muddy sediments i.e. clay and silty clay. The sediments show layering due to both differences in grain size and coloring. The presence of small scale graded bedding also supports this interpretation. The escape burrows observed indicate rapid deposition, which suggest that some of the sand and clay layers are storm deposits (Reineck and Singh, 1980). The shrinkage cracks are most likely the result of rapidly flocculated clay layers that have developed syneresis structures due to compaction (Reineck & Singh, 1980; Reading, 1978). The coarsening upwards unit at the base of the formation suggests that delta deposits can have prograded into the fine-grained pro delta deposits.

Some glauconite was also observed in this formation, glauconite has for a long time been considered as diagnostic of a specific systems tract of a depositional sequence. However, Amorosi (1995) points out the importance of separating between autochthonous and allochthonous glauconite. In this core only a low concentration of allochthonous glauconite was observed, this is most commonly observed in wave-, tide- and storm dominated deposits of the transgressive system tract (TST) and high stand system tract (HST) (Amorosi, 1995). This coincide with the interpretation that these deposits are storm influenced deposits.

In the upper part of the formation the color of the deposits get darker and red coloration can be seen in the sediments. In thin section carbonate nodules, similar to the sphaerosiderite observed in Snadd can be seen (Fig. 5-12). And dolomite crystals confined in mud can be seen (Fig. 5-11). In the interpretation of Snadd these diagenetic structures are interpreted to be early caliche processes, and diagnostic of subaerial environment. In order for carbonate nodules to develop the soil needs to be exposed for subaerial conditions for a considerable period of time. The dolomite nodules are interpreted to be diagenetically altered sphaerosiderites with increased crystal lattice substitution of Ca^{2+} , Mg^{2+} and for Fe^{2+} . The Fruholmen. Formation deposits have been classified as inner shelf deposits (Fig. 6-4).

Stø Formation

The deposits observed in the Stø Formation have been divided into two separate main facies. The lower six meters consist of slightly fining upwards coarse-grained sandstones with concentric carbonate cemented patches. The slightly fining upwards trend combined with the conglomerates suggests that this could be fluvial deposits. It should also be considered that the sandstones are both overlain and underlain by polymict conglomerates. As mentioned in section 4.2 conglomerates are commonly associated with fluvial deposits. The deposits could coincide with those found in braided rivers, which consist of thick fining upwards sequences, starting with well-rounded conglomerate. Such coarse conglomerates are restricted to very high energy channels. In mass flow deposits the degree of rounding of clasts evident in this core will not occur. (Reineck and Singh, 1980). The wood fragments also suggest proximity to continental environment. The concentration of the cementation varies throughout the layer, and in some places the sandstone is completely cemented. These calcite cemented patches were first interpreted to be caliche deposits (Fig. 6-3). In general it has been stated that calcrete is formed near-surface in stable geomorphic areas, where for a certain period of time there is negligible sediment deposition due to terrace development or distant avulsion of the

river (Reineck and Singh, 1980). CaCO_3 accumulation develops due to repeated wetting and drying of the upper surface, involving evaporative precipitation of CaCO_3 . The main source of Ca^{2+} is rainwater (Reineck and Singh, 1980). Development of calcrete is a very time consuming process, and based on calcrete formation in Holocene it has been suggested that many nodules, and internodular filling, similar to that seen in this core, would take 6000-10000 years to develop (Leeder, 1973). However, due to the sparry cement in the deposits it was considered less plausible. The common cement types in caliche are vadose micritic cement, blocky calcite cement and meniscus cement. Microsparry fabrics are common (Flügel, 2009). So for this to be true the micrite must have been altered into sparry cement. These concentric calcite cemented areas are therefore believed to be caused by dissolution and redeposition of shell fragments in the original deposits. This interpretation is also supported by the observed juvenile bivalves in thin section.



Figure 6-3: The concentric calcite patches as they are observed in the core. The arrow shows the upwards direction of the cores. This section is from 35-37 meters depth.

The upper part of the core mainly consists of thin sandstone layers with a brown color with some organic matter. The sediments contain laminae enriched with skeletal fragments. These deposits have been interpreted to be storm deposited sediments from the inner shelf.

Small volumes of authigenic kaolinite is present in almost all the samples, this could indicate near surface meteoric water flushing causing feldspar dissolution and precipitation of the dissolved feldspar as kaolinite (Bjørlykke et al., 1979).

The lower part of the deposits in the Stø Formation has been interpreted to be coastal deposits, and the upper part has been interpreted to be inner shelf (Fig. 6-4).

6.1.2 Core 7230/05-U-03

Snadd Formation

In core 7230/05-U-03 the Snadd Formation comprises similar sediments as those described in core 7227/08-U-01. The dusky red coloration and soil profiles can also be recognized in this core. Variegated mottled mudstone can be observed at several depths, which is typically found in developing soils. In addition siderite cementation in rootlet looking patterns indicate early stages of caliche development (Fig. 4-8, d) Carbonate analysis of siderite nodules were also conducted in this formation, the results were presented in section 6.1.1.

Fruholmen Formation

The lower part of the Fruholmen Formation consists of several fining upwards units going from medium- to fine-grained sandstone. These sections show faint cross bedding described in section 4.1.2. These deposits have been interpreted to be distributary channel deposits. The homogenous sand packages with some horizontal coal laminations have been interpreted to be distributary mouth bar deposits. In mouth bars thin laminations of plant debris and coal are often present, and plant fragments showing cellular structures have been observed in this core (Fig. 5-7). The homogenous appearance of the remainder of the sediments could be due to the constant reworking of these sediments, however, some coarsening upwards layer have also been observed in the core. This is the place with the highest depositional rate in the delta, and as a consequence syndepositional deformation structures could develop in these types of environments. But due to the fine-grained nature of the layers showing piled load-casted ripples it could also be interdistributary bay deposits, which are open water bodies surrounded by levees and marshes, but open or connected to the sea by tidal channels. These sediments can have some lenticular bedding and current ripples in the coarser sediments brought in by crevasse channels, the fast deposition of coarser material over the silty mud could also result in the ball-and-pillow structures observed in the core.

The traces of pyrite cement seen in the thin sections from this formation appear to be late diagenetic because of the framboidal morphology indicating precipitation due to microbiological sulphate reduction close to the sediment surface (Berner, 1970).

Low concentrations of immature allochthonous glauconite were observed in this formation. According to Amorosi (1995) this type of glauconite is most commonly observed in wave-, tide- and storm dominated deposits of the transgressive system tract (TST) and high stand system tract (HST) (Amorosi, 1995). This coincide with the interpretation that these deposits are tidal influenced delta deposits.

These deposits are interpreted to be delta front deposits (Fig. 6-4).

Stø Formation

The Stø Formation comprises a series of alternating silt and sandstone layers. The deposits are disturbed in many places, and bear witness of varying depositional energy. This facies is typical for the delta front slope. Pro delta deposits are, as mentioned in section 4.2, characteristically fine-grained to muddy sediments i.e. clay and silty clay. Shell remains are common throughout; wood fragments are also present (Reinech and Singh, 1980).

Small volumes of authigenic kaolinite is present in almost all the samples, this could indicate near surface meteoric water flushing causing feldspar dissolution and precipitation of the dissolved feldspar as kaolinite (Bjørlykke et al., 1979).

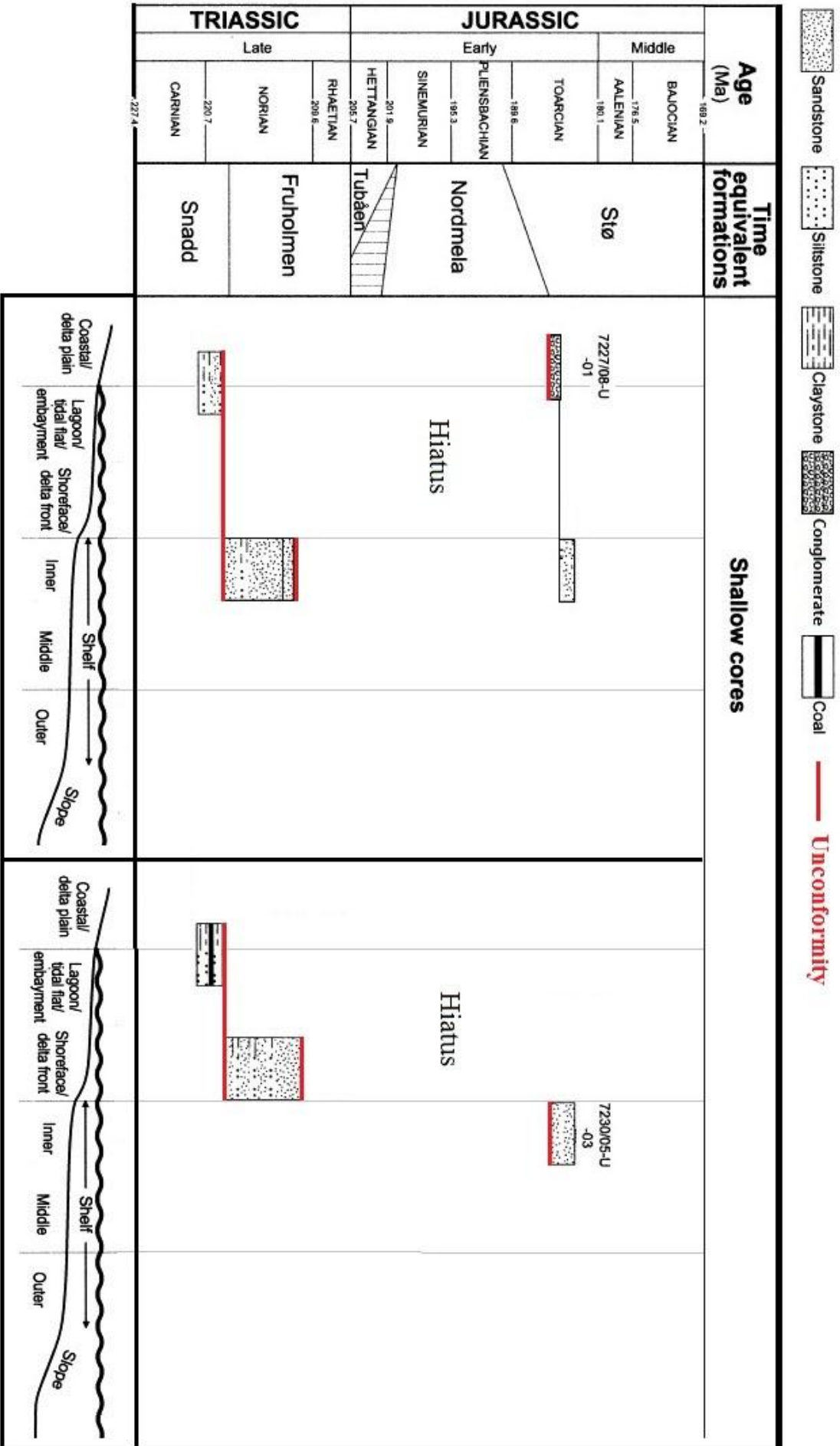


Figure 6-4: Interpreted depositional environment in the two cores, and the assigned lithology. The vertical axis does not show true stratigraphic thickness. The results tally with the interpretations done by Bugge et al. (2002). Modified from Bugge et al., 2002.

6.2 Regional and Stratigraphic changes in mineral composition

6.2.1 Sandstones

The depositional environment is peremptory for any mineralogical shift in the sediments. The interpretation of the depositional environment in the three formations is therefore crucial to better understand the reason for a mineralogical shift in the sandstones.

The sediments in the Snadd Formation are mainly low energy shoreline deposits, lagoon and coastal plain mudstones with early caliche formation. They were deposited in a lower delta plain setting where neither fully continental nor elevated delta conditions developed. This could indicate that the studied area was part of a westward prograding paleo coastline stretching from the south-western part of the Barents Sea, across the Bjarmeland Platform and up to Svalbard (Riis et al., 2008). The interpretation of the Fruholmen Formation as delta front shoreface and inner shelf also correlates well with the interpretation of Bugge et al. (2002). However, in the present study the upper part of the Fruholmen Formation in core 7227/08-U-01 has been interpreted to have been exposed for subaerial conditions for a considerable period of time. This interpretation is mainly owing to the carbonate nodules in the silty-mudstone deposits. An alternative interpretation of this could be that the deposits have been uplifted, and exposed for subaerial conditions at a later stage. This could be a possibility considering the extensive amount of caliche formation in the overlying strata, it is not impossible that the deposits in the Fruholmen Formation have been affected by the same conditions as the overlying Stø formation, favorable for caliche formation. It is also worth mentioning that there is a hiatus between the Fruholmen Formation and the Stø Formation, and it is therefore no unreasonable that these deposits could have been exposed to the air, deposition of coastal deposits above also strengthens this interpretation. The Stø Formation also corresponds well with previous studies done on the formation of both Worsley et al. (1988) and Bugge et al. (2002). These studies interpreted Stø to comprise two different depositional environments, inner shelf/delta front slope and fluvial coastal/delta plain deposits.

The different facies affects the maturity of the deposits, and a lack of sandstones suited for modal analysis above and below the formation boundaries in the two cores made it challenging to do any direct comparisons of the mineralogical maturity in the formations. For that reason a lateral comparison was done, rendering the possibility of a vertical comparison. The modal analysis in this paper show no great difference in mineralogical maturity between the Snadd Formation (7430/07-U-01) at the Bjarmeland Platform and Fruholmen Formation

(7230/05-U-03) in the Nordkapp Basin. However, a great difference in maturity between the underlying Triassic formations, Snadd and Fruholmen, to the Jurassic deposits in the Stø Formation. The sandstones in Snadd are classified as arkosic arenite, which correspond well with previous observations done on Svalbard in the DeGeerdalen Formation (Mørk, 1999; Riis et al., 2008). The Fruholmen Formation is also classified as arkosic arenite, and plots in the same area in the QFL-plot (Fig. 5-22). The sandstones in the Stø Formation are classified as sublitharenites, and quartz arenite. This agrees with the findings of Bugge et al. (2002), who reported a mineralogical shift and a dramatic drop in the feldspar content in the underlying Triassic sandstones from 20-30% to approximately zero in the overlying Jurassic formation, while the quartz content increases. When comparing with the modal analysis conducted in the DeGeerdalen-Snadd formations further north in the Barents Sea it is evident that the analyses conducted in the Nordkapp Basin in this analysis have higher quartz content, and a lower fraction of lithic fragments. This could be due to local variations, or possibly a consequence of the difficulties described in section 2.2. The deposits above and below the Snadd-Fruholmen formation boundary both have facies that are typically rich in feldspar, proximal deposits that have not undergone a lot of reworking. The fluvial deposits in the lower part of the Stø Formation in core 7227/08-U-01, however, show a very different facies. Fluvial deposits are exposed for a lot of reworking, and the constant water flow breaks down the feldspar leaving quartz rich, mature sandstone. Fluvial deposits are not typically found in the Stø Formation, and the Nordkapp Basin has the only reported incidences of deltaic deposits (Bugge et al., 2002). The upper part of Stø in 7227/08-U-01 and the Stø deposits in 7230/05-U-02 have been interpreted to have the same depositional environment as Fruholmen in core 7227/08-U-01 due to similar facies, raising the question as to why the two formations do not have the same maturity. One possible reason for the distinct shift in textural maturity between Fruholmen and Stø, despite similar facies could be extensive reworking in connection with regional transgression and changing environments following the main transgression that took place in the late Jurassic (Mørk, 1999; Bugge et al., 2002). It is also worth noting that rounding of the grains in both Snadd and Fruholmen is poor, and persistence of cherty rock fragments and angular feldspar implies that both sedimentary and felsic igneous rocks continued to be eroded from provenance areas throughout the Late Triassic (Mørk, 1999). Another possibility is a shift in provenance. Mørk (1999) suggests that there could be some additional influences due to a change in the erosion product from the east, with a relative increase in siliceous and differentiated igneous components. There is also the possibility of a local change in provenance for the Nordkapp Basin as the shift in maturity

appears at a later stage in the rest of the Barents Sea. Climatic changes could also have affected the mineralogical maturation in the sediments. A warmer and more humid climate would affect weathering on the provenance areas and deposition of more quartz-rich rocks (Mørk, 1999).

Overall the mineralogical maturity increases in the early Jurassic succession, which is slightly later than reported by Bergan and Knarud (1992) who suggests that already in the Middle and Upper Triassic successions in the Barents Sea the mineralogical maturity shows a tendency to increase, but that the most dramatic shift is found between the Triassic and the Jurassic deposits.

6.2.2 Mudstones

The clay mineralogy has also been analyzed in order to investigate any mineralogical shift in the clay composition above and below the Snadd- Fruholmen formation boundary. From XRD analyses it was apparent that the clay mineralogy was quite similar above and below the formation boundary, with kaolinite content between 10-21% and illite content between 9-18%. There is no apparent trend of increased illite content or higher abundance of kaolinite in any of the cores. Smectite was also detected in both cores, and in both formations, further investigation of the smectite contents could have provided more information of the paleoenvironment as illite/smectite (I/S) ratios have been widely studied. To identify the smectite in the sample further analyses should have been carried out, ethylene glycolation would make the smectite expand and give a 17.2\AA peak, it also often gives a 002 peak at 8.5\AA which would not occur in air-dried samples of smectite (Kristian Drivenes). Low illite content in the clay also implies that the sediments have not been buried very deep.

6.2.3 Burial Diagenesis

When doing XRD analyses the illite% in the mixed layer I/S would increase progressively with burial depth, and the kaolinite may decrease (Elslinger and Pevear, 1988). Illitization of kaolinite has a low kinetic precipitation rate and is not significant at temperatures below 120–140 °C, given availability of potassium in the sediments (Bjørlykke et al., 1995). Age-elevation patterns suggest that the Mesozoic geothermal gradient was 10-15°C/km higher than the present day 20°C/km (Rohrman et al., 1995), by assuming a geothermal gradient of about 30°C/km this means that the sediments would have had to be buried 4-5km. The lack of illitization despite the presence of potassium in the pore water from mica and K-feldspar indicate that the sediments cannot have been buried this deep, also looking at Figure 6-1 it is apparent that the sediments cannot have reached temperatures that high, as the maximum

burial is less than 1500 meters. Another conclusion that can be drawn is that the two formations must have undergone a similar burial history, as there are no great differences across the formation boundary.

The clay content is also highly dependant on the environment and latitude at the time of deposition. The small variations in the clay content could imply that climatic changes might have happened at a later stage, as the clay does not show any trace of a climatic transition.

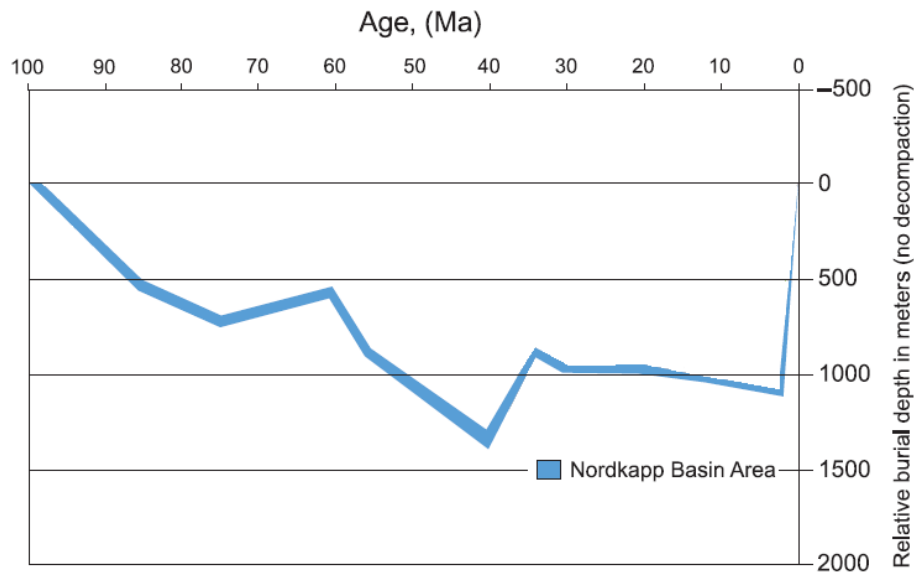


Figure 6-1: Subsidence curve for the Nordkapp Basin Area, with three periods of uplift, 60 Ma, 35 Ma and present. From this curve it is apparent that the maximum level of burial has been approximately 1400 meter. Modified from Ohm et al. 2008.

One apparent difference, however, that can be seen in the mudstone deposits in the two formations is the appearance of environmentally dependant diagenetic structures. The sphaerosiderite have formed in subaerial conditions and further analyses of this phenomenon could possibly reveal more about the ground water, palaeoclimate, and the influence of meteoric water, by analyzing the $\delta^{18}\text{O}$ content in the samples. Most of the evaporation takes place at low latitudes and the water vapour in the air has a progressively lower ^{18}O -content towards higher latitudes as the air cools and it rains (Bjørlykke, 2010). The presence of subaerialstructures in the delta front deposits in the upper part of Fruholmen (7227/08-U-01) present something of a puzzle. These have been interpreted to have undergone the calcrete forming processes after being uplifted, or during a longer period of regression.

6.2 Further work

The core selected for this study comprised only short sections with sandstone suitable for thin section analysis, and for the Snadd Formation sandstones from a different location needed to be used in order to compare the maturity of the sandstones. The poor quality of the thin sections used in the study also made it problematic to obtain optimal results. In order to map the feldspar content in the samples more accurately the thin sections could be treated with sodium cobaltinitre, which colors the K-feldspar yellow, this would make it easier to distinguish between the different types of feldspar present in the samples despite the dissolution.

Due to time constraints only six XRD analyses were conducted. In order to further map the composition above and below the Snadd-Fruholmen boundary more samples should be analyzed. It would also be interesting to do some analyses in the Stø Formation to investigate if there has been a shift in the composition of the clay, in addition to the mineralogical shift in the sandstone.

The spaerosiderite analysed in this study showed very high levels of manganese, these siderites could be further investigated and studied by analyzing the $\delta^{18}\text{O}$ content in the samples. The $\delta^{18}\text{O}$ could tell more about the latitude at which these sediments were deposited, as most of the evaporation takes place at low latitudes and the water vapor in the air has a progressively lower ^{18}O -content towards higher latitudes (Bjørlykke, 2010).

It would also be interesting to combine the findings in this thesis with the findings of other unpublished studies conducted in the same area. Hege W. Porten have recently handed in her MSc. And Hege Stensland who is currently working on her MSc., which is based on studies of the same cores used in this thesis.

7. Conclusion

Core 7227/08-U-01 and core 7230/05-U-03 comprise shale, sandstone, siltstone and conglomerates, and represent an overall transgressive trend throughout the Snadd, Fruholmen and Stø formations. The deposits have been interpreted to go from delta plain, through shoreface to inner shelf, with exception of the deposition of fluvial deposits in the lower part of the Stø Formation overlaying inner shelf deposits in the Fruholmen Formation in core 7227/08-U-01. These breaks with the transgressive pattern seen in the rest of the succession, and these fluvial deposits have been interpreted to represent a local variation in the Nordkapp Basin.

The diagenetic processes differ in the three formations due to dissimilar depositional environment. In both cores the Snadd Formation displays some sphaerosiderites with very high levels of manganese, and over 90% iron. High levels of manganese and iron in sphaerosiderites are typically found in subaerial sediments influenced by fresh-water. Some of the siderite is interpreted to be rhizcretions which is directly associated with soil-forming processes. This supports the sedimentological interpretation of the deposits, and fits with the model of the westward prograding paleo coastline stretching from the south-western part of the Barents Sea, across the Bjarmeland Platform and up to Svalbard.

There are no great mineralogical changes to detect across the Snadd-Fruholmen formation boundary. The largest compositional variation is seen between the Fruholmen and Stø formations, and has been reported to be the most important compositional shift in the Barents Sea. This change in maturity has previously been reported to take place in the Upper Triassic deposits, however, in this study the shift appears in the transition between Triassic and Jurassic sandstones, in accordance with other studies conducted in the Nordkapp Basin. The distinct increase in maturity may be due to extensive reworking connected with a regional transgression and sea-level rise causing changes in the depositional environment leading to the mineralogical shift in the Nordkapp Basin. The deposits seen in the Stø Formation are interpreted to be more distal, and thoroughly reworked by coastal processes. By looking at the overlying deposits it is likely that the sediments deposited in Stø have developed through delta front environment up to tidal plain with distributary channels and mouth bar complexes.

XRD analyses showed no great compositional differences between the mudstones in the Snadd and Fruholmen formations, supporting the observations from the sandstone compositions of similar provenance and environment above and below the formation

boundary. The high levels of kaolinite also indicate that the sediments have not been buried deeper than 4 km as potassium was available in the sediments the high temperatures would have led to illitization of the kaolinite. This is substantiated by the subsidence history of the Nordkapp Basin Area.

References

- Adams, L.K., Macquaker, J.H.S. and Marshall, J.D., 2006, Iron(III)-Reduction in low organic-carbon brackish-marine system: *Journal of Sedimentary Research* , v. 76, p. 919-925.**
- Amorosi, A., 1995, Glaucony and Sequence Stratigraphy: A Conceptual Framework of Distribution in Siliciclastic Sequences: in *Journal of Sedimentary Research*, v. B65, no.4, p. 419-425.**
- Auset, M., 2011, Sedimentological study of Upper Triassic core samples, 7430/07-U-01- Barents Sea (Project thesis), *Department of Geology and Mineral Resources Engineering*, NTNU, p. 72.**
- Bergan, M., and Knarud, R., 1992, Apparent changes in clastic mineralogy of the Triassic-Jurassic succession, Norwegian Barents Sea: possible implications for paleodrainage and subsidence, in Vorren, T.O., Bergsager, E., Dahl-Stamnes, Ø.A., Holter, E., Johansen, B., Lie, E., and Lund, T.B., eds., *Arctic Geology and Petroleum Potential: Norwegian Petroleum Society, Special Publication 2*, Amsterdam, Elsevier, p. 481–493.**
- Berner, R.A., 1970, Sedimentary pyrite formation: *American Journal of Science*, v. 268, p. 1–23**
- Bjørngen, T., 1985, A sedimentological study of the cored Lower/Middle Jurassic successions in wells: 7120/6-1, 7120/9-1 and 7120/12-2 (*Unpublished Cand scient thesis*), *University of Bergen*.**
- Bjørlykke, K., A. Elverhøi, and A. O. Malm, 1979, Diagenesis in Mesozoic sandstones from Spitsbergen and the North Sea-a comparison: *Geologische Rundschau*, v. 68, p. 1152-1171.**
- Bjørlykke, K., Aagaard, P., Egeberg, P.K. and Simmons, S.P., 1995, Geochemical constraints from formation water analyses from the North Sea and Gulf Coast Basin on quartz, feldspar and illite precipitation in reservoir rocks: in *Geological Society London Special Publication* 86, p. 33-50.**
- Bjørlykke, K., A., 2010, Petroleum Geoscience-From Sedimentary Environments to Rock Physics, *Springer-Verlag*, p. 87-111.**
- Boggs Jr, S., 2006, Principles of sedimentology and stratigraphy, 4th edition, *Person Education*, p. 774.**
- Bugge, T., Elvebakk, G., Fanavoll, S., Mangerud, G., Smelror, M., Weiss, H.M., Gjelberg, J., Kristensen, S.E. and Nilsen, K., 2002, Shallow stratigraphic drilling applied in hydrocarbon exploration of the Nordkapp Basin, Barents Sea: *Marine and Petroleum Geology*, v. 19, p. 13-37.**

- Curtis, C.D.**, and Spears, D.A., 1968, The formation of sedimentary iron minerals: *Economic Geology*, v. 63, p. 257–270
- Dimakis, P.**, Braaten, B.I., Faleide, J.I., Elverhøi, A., and Gudlaugsson, S.T., 1998, Cenozoic erosion and the ore-glacial uplift of the Svalbard-Barents Sea region: in *Tectonophysics*, v. 300, p. 311-327.
- Doré, A.G.**, 1995: Barents Sea geology, petroleum resources and commercial potential: in *Arctic*, v. 48, no. 3, p. 207-221.
- Dott, R. H.**, 1964, Wacke, Graywacke and matrix-what approach to immature sandstone classification: *Journal of Sedimentary Petrology*, v. 34, p. 625-632
- Faleide, J.I.**, Gudlaugsson, S.T., and Jacquart, G., 1984, Evolution of the western Barents Sea: in *Marine and Petroleum Geology*, v. 01, p. 123-128.
- Faleide, J.I.**, Vågnes, E. and Gudlaugsson, S.T., 1993, Late Mesozoic-Cenozoic evolution of the south-western Barents Sea in regional rift-shear tectonic setting: in *Marine and Petroleum Geology*, v. 10, p. 186-214.
- Flügel, E.**, 2009, *Microfacies of Carbonate Rocks: Analysis, Interpretation and Application*: Springer, p. 984
- Fossen, H.**, Dallman, W., and Andersen, T.B., 2006, Fjellkjeden går til grunne. Kaledonidene brytes ned; 405-359 millioner år: in Ramberg, I.B., Bryhni, I., Nøttvedt, A. (eds.), *Landet blir til-Norges geologi, Norsk geologisk forening*, p. 230-257.
- Gabrielsen, R.H.**, Færseth, R.B., Jensen, L.N., Kalheim, J.E., and Riis, F., 1990, Structural elements of the Norwegian continental shelf; Part I: The Barents Sea Region: in *Norwegian Petroleum Directorate (NPD), Bulletin*, 6, p. 10-16.
- Glørstad-Clark, E.**, Faleide, J.I., Lundshien, S.E., and Nystuen, J.P., 2011, Triassic seismic sequence stratigraphy and paleogeography of the western Barents Sea area: in *Marine and Petroleum Geology*, v. 27, p. 1448-1475.
- Gudlaugsson, S.T.**, Faleide, J.I., Johansen, S.E., and Breivik, A.J., 1998, Triassic seismic sequence stratigraphy and paleogeography of the south-western Barents Sea: in *Marine and Petroleum Geology*, v. 15, p. 73-102.

Hjelen, J., 1989, Scanning Electron Microscope (Compendium), *NTNU*.

Jensen, L.N., and Sørensen, K., 1992, Tectonic framework and halokinesis of the Nordkapp Basin, Barents Sea: in R.M. Larsen, H. Brekke, B.T. Larsen and E. Talleraas (Eds.), Structural and tectonic modeling and its application to petroleum geology, *Norwegian Petroleum Society (NPF) Special publication 1*, p. 109-120.

Johannessen, E.P., and Nøttvedt, A., 2007, Norge omkranses av kystsletter og deltaer: in I.B. Ramberg, I. Bryhni, and A. Nøttvedt (Eds.), *Landet blir til-Norges geologi, Norsk geologisk forening*, p. 354-381.

Johansen, S. E., Ostistiy, B.K., Birkeland, Ø., Fedorovsky, Y.F., Marirosjan, V.N., Christensen, O.B., Cheredeev, S.I., Ignatenko, E.A., and Magulis, L.S., 1992, Hydrocarbon potential in the Barents Sea region: play distribution and potential, in Vorren, T.O., Bergsager, E., Dahl-Stammes, Ø.A., Holter, E., Johansen, B., Lie, E., and Lund, T.B., eds., *Arctic Geology and Petroleum Potential: Norwegian Petroleum Society, Special Publication 2*, Amsterdam, Elsevier, p. 273–320.

Ketzer, J.M., Morad, S., and Amorosi, A., 2003, Predictive diagenetic clay-mineral distribution in siliciclastic rocks within a sequence of stratigraphic framework, *International Association of Sedimentologists, Special Publication 34*, p. 43-61

Klappa, C.F., 1980, Rhizoliths in terrestrial carbonates: Classification, recognition, genesis and significance: *Sedimentology*, v. 27, p. 613–629.

Leeder, M.R., 1973, Pedogenic carbonate and flood sediment accretion rates: a quantitative model for alluvial, arid-zone lithofacies: in *Geological Magazine* 112, p. 257-270.

Mozley, P.S., 1989, Relationship between depositional environment and the elemental composition of early diagenetic siderite: *Geology*, v. 17, p. 704-706.

Mørk, M.B.E., 1999, Compositional variations and provenience of Triassic sandstones from the Barents Shelf, in *Journal of Sedimentary Research*, v. 69, no. 3, p. 690-710.

Nystuen, J.P., Mørk, A., Müller, R., and Nøttvedt, A., 2006, Fra ørken til elvesletter- fra land til hav; 251-200 millioner år: in Ramberg, I.B., Bryhni, I., Nøttvedt, A. (eds.), *Landet blir til-Norges geologi, Norsk geologisk forening*, p. 328-353.

Nøttvedt, A., and Worsley, D., 2006, Vidstrakte sletter, kull og salt. Karbon og perm i nord; 359-251 millioner år: in Ramberg, I.B., Bryhni, I., Nøttvedt, A. (Eds.), *Landet blir til-Norges geologi*, Norsk geologisk forening, p. 258-283.

Ohm, S. E., Karlsen, D. A., and Austin, T. J. F., 2008, Geochemically driven exploration models in uplifted areas: Examples from the Norwegian Barents Sea: in The American Association of Petroleum Geologists Bulletin, v. 92, no. 9, p. 1191-1223.

Pettijohn, F.J., 1954, Classification of Sandstones, *The Journal of Geology*, v. 62, no. 4, p. 360-365.

Pettijohn, F.J., Potter, P.E. and Siever, R., 1972, Sand and Sandstone. *New York - Heidelberg - Berlin, Springer-Verlag*, p. 618

Reading, H.G., 1978, Sedimentary environments and facies, 2nd edition, *Alden press*, Oxford, p. 615.

Riis, F., Lundschieen, B.A., Høy, T., Mørk, A., and Mørk, M.B.E., 2008, Evolution of the Triassic shelf in the northern Barents Sea region: in *Polar Research*, v. 27, no. 3, p. 218-338.

Reineck, H.E., and Singh, I.B., 1980, Depositional sedimentary environments, 2nd edition, *Springer-Verlag*, Berlin, p. 549

Rohrman, M., Beek, P.V.D., Andriessen, P., and Cloetingh, S., 1995, Meso-Cenozoic morphotectonic evolution of southern Norway: Neogene domal uplift inferred from apatite fission track thermochronology: in *Tectonics*, v. 14, no. 3, p. 704-718.

Smelror, M., Petrov, O.V., Larssen, G.B., and Werner, S.C., 2009, Geological history of the Barents Sea: in *Geological Survey of Norway*, Trondheim, p. 135.

Thornhild, M., 2011, Analytical Methods-XRD: Course material in TGB4145 Analytical Methods in Geology, NTNU

Ufnar, D.F., Gonzalez, L.A., Ludvigson, G.A., Brenner, R.L., and Witzke, B.J., 2001, Stratigraphic implications of meteoric sphaerosiderite $\delta^{18}\text{O}$ values in paleosols of the Cretaceous (Albian) Boulder Creek Formation, NE British Columbia foothills, Canada: *Journal of Sedimentary Research*, v. 71, p. 1017–1028.

Ufnar, D.F., Gonzalez, L.A., Ludvigson, G.A., Brenner, R.L., and Witzke, B.J., 2004, Diagenetic overprinting of the sphaerosiderite paleoclimate proxy: are records of pedogenic groundwater $\delta^{18}\text{O}$ values preserved?: International Association for Sedimentologists, *Sedimentology*, v. 51, p. 127-144.

Vorren, T.O., and Mangerud, J., 2006, Istider kommer og går. Sein pliocen og pleistocen (kvartær); 2.7 Ma-11500 år: in Ramberg, I.B., Bryhni, I., Nøttvedt, A. (eds.), *Landet blir til-Norges geologi*, Norsk geologisk forening, p. 478-531.

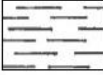


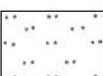





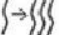






Worsley, D., Aga, O.J., Dalland, A., Elverhøi, A., and Thon, A., 1986, The geological history of Svalbard- Evolution of an arctic archipelago, *Statoil, Aske Trykkeri*, Stavanger, p. 120.



Worsley, D., Johansen, R., and Kristensen, S.E., 1988, The Mesozoic and Cenozoic succession of Tromsøflaket: in *Norwegian Petroleum Directorate (NPD) Bulletin*, 4, p.42-65.

Appendix A

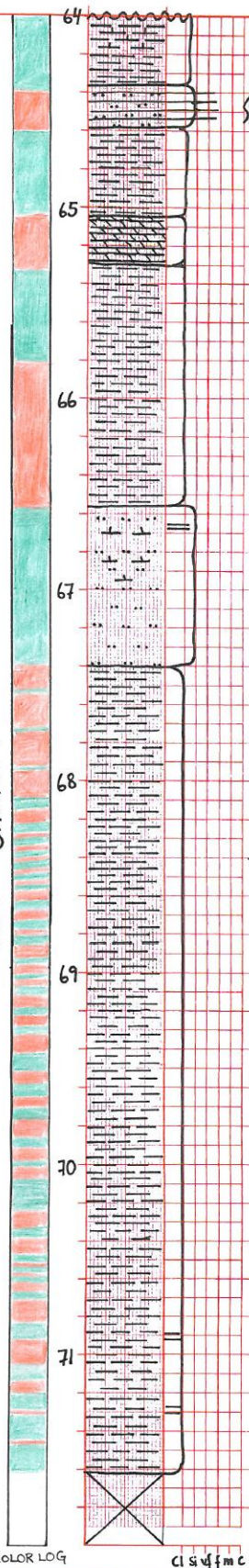
Core 7227/08-U-01

Core 7227/08-U-01 was drilled in the central part of the southwestern basin segment.

Legend	
	Shale
	Sandstone
	Limestone
	Siltstone
	Conglomerate
	Coal
	Pyrite
	Wood fragments
	Roots
	Bioturbation
	Ripple lamination
	Wavy bedding
	Horizontal bedding
	Calcite cement
	Siderite cement
	Bivalves

Color log	
	Red coloration in sediments
	Green coloration in sediments

THE SNADD FORMATION



Calcite cemented

Alternating silt and sandstone
Burrows filled with coarser material

Siderite cemented

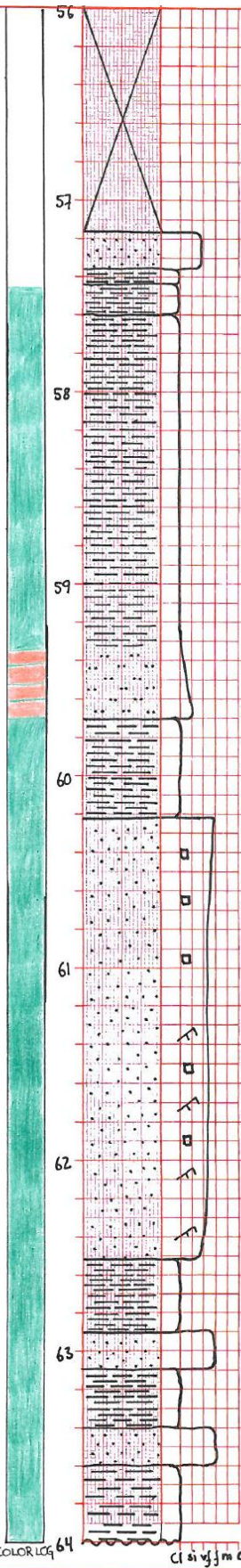
Alternating coloration due to differences in the
reduction caused by variations in permeability

Horizontal lamination in the lower part
of the core

COLOR LOG

CLASSIFICATION

THE FRUHOLMEN FORMATION



Brown color

Very contorted, no visible structures

Red coloration in the sediments

Not many structures in the upper part of the layer

Wavy/flaser bedding

Ripples, flaser bedding, fine-grained sandstone with a light color.

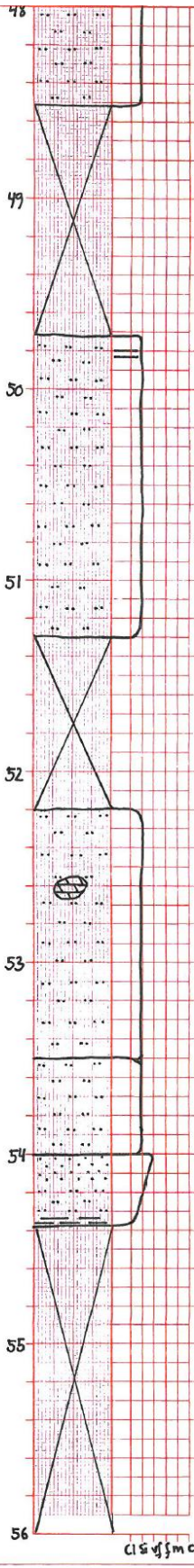
Contorted layer

No characteristic depositional structures

COLOR LOG 64

cl s i v j m c

THE FRUHOLMEN FORMATION



Synaeresis structures



Shrinking structures

Horizontal lamination



Alternating silt and clay mixed by bioturbation. Can see both vertical and horizontal burrows

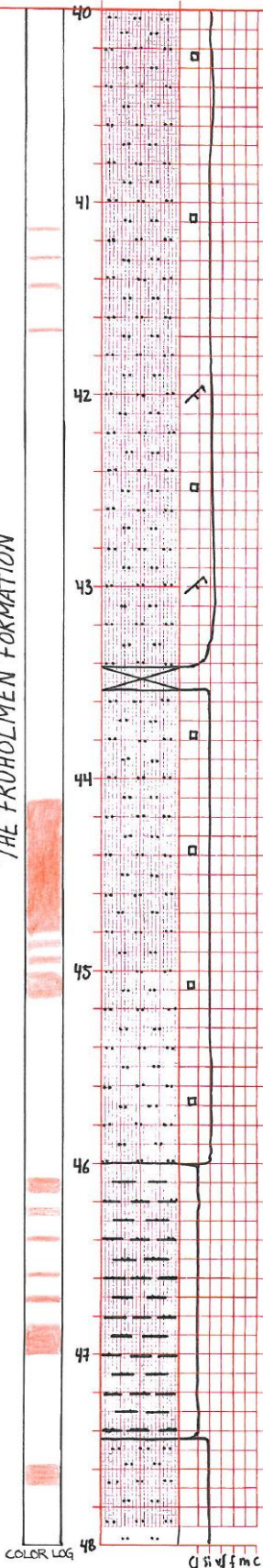
Siderite concretion

Synaeresis structures } Some bioturbation, both vertical and horizontal burrows.

Brown coloration

cl s y f m c

THE FRUHLIHMEN FORMATION



Horizontal burrows

Some preserved ripples

Patches of pyrite cement can be seen in the whole layer

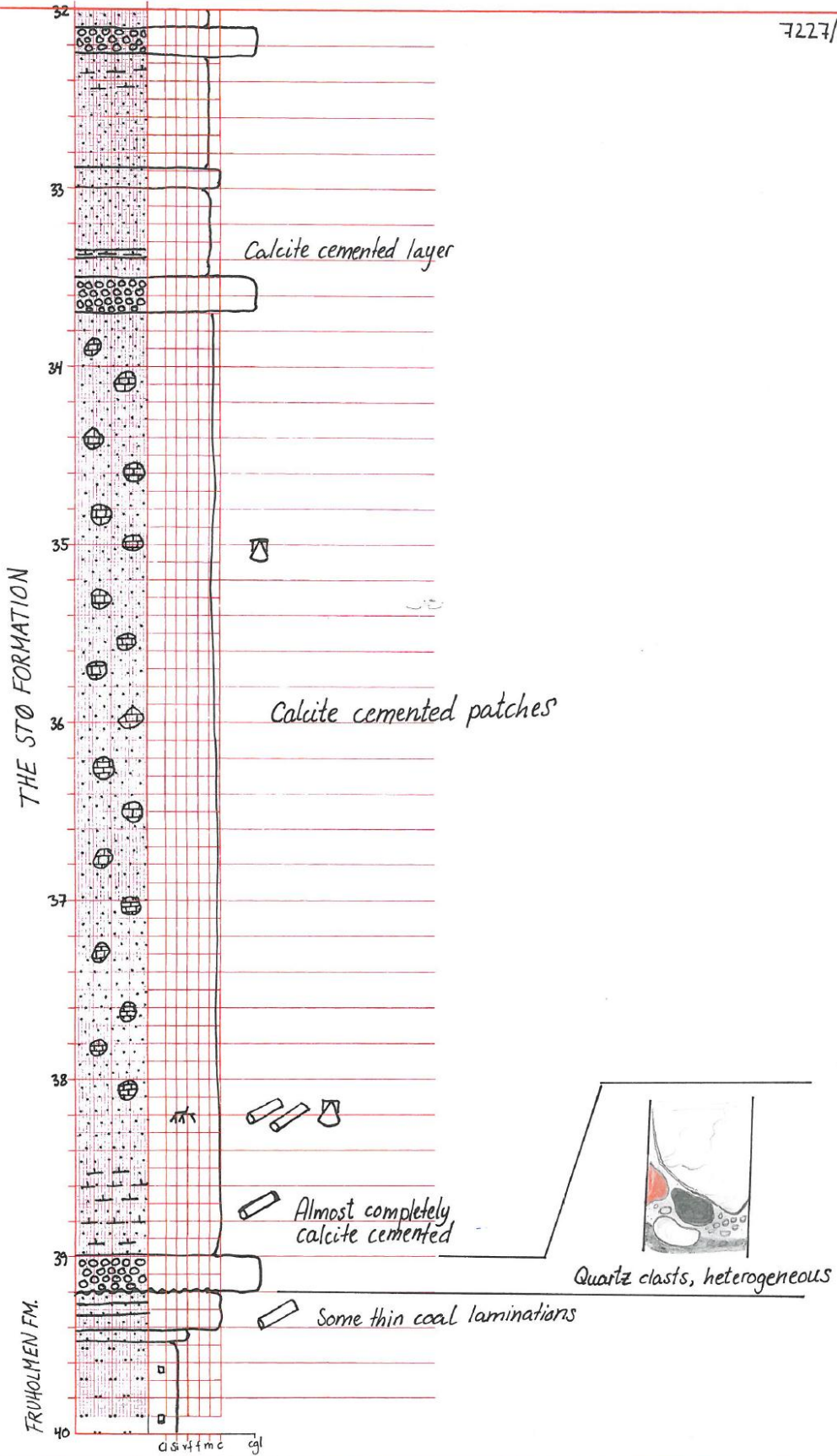
This section has a rusty red color

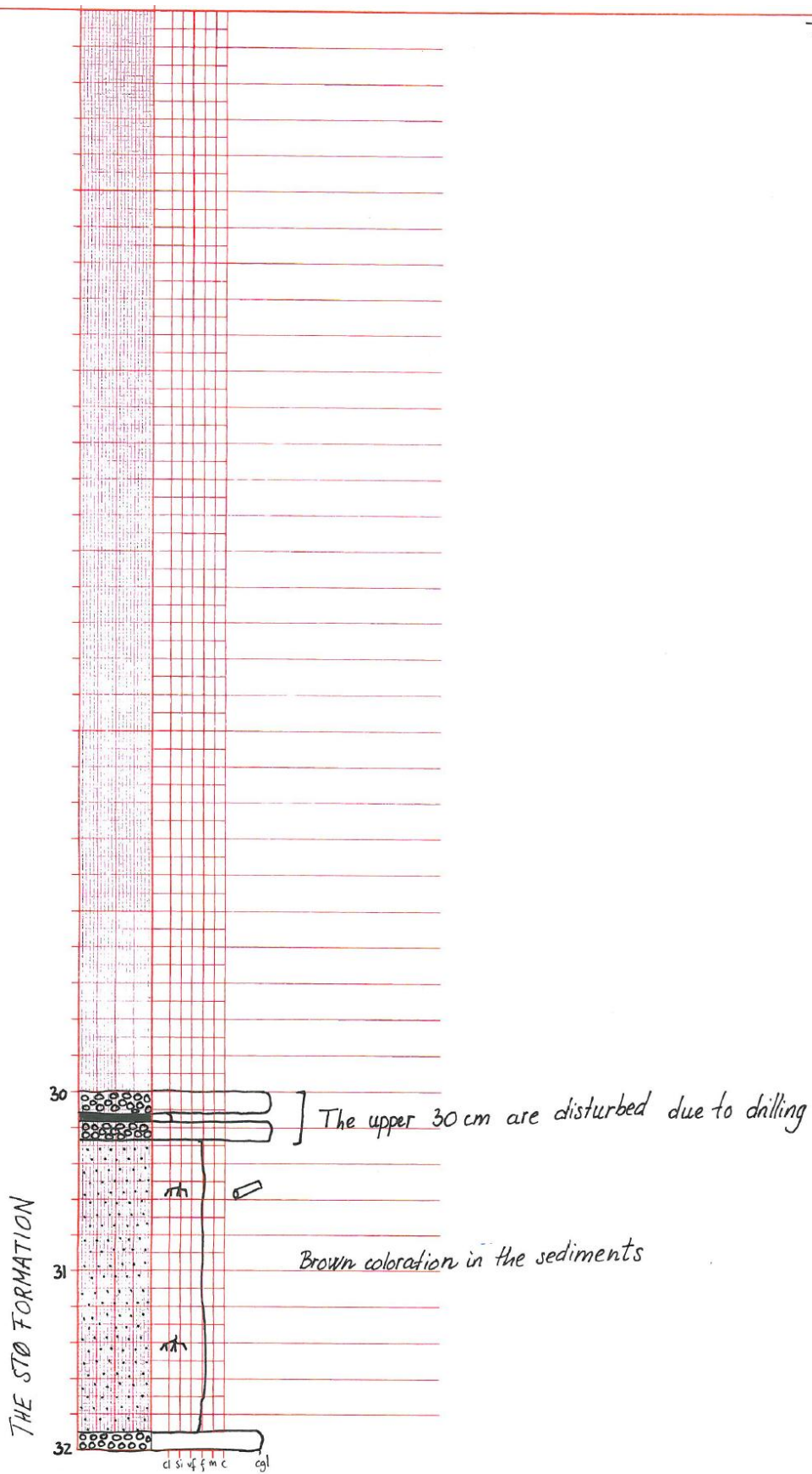
Horizontal burrows

Dark color with red coloration in some patches

COLOR LOG

Classification

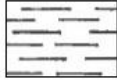
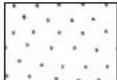

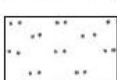
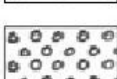





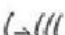










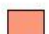

Core 7227/08-U-01

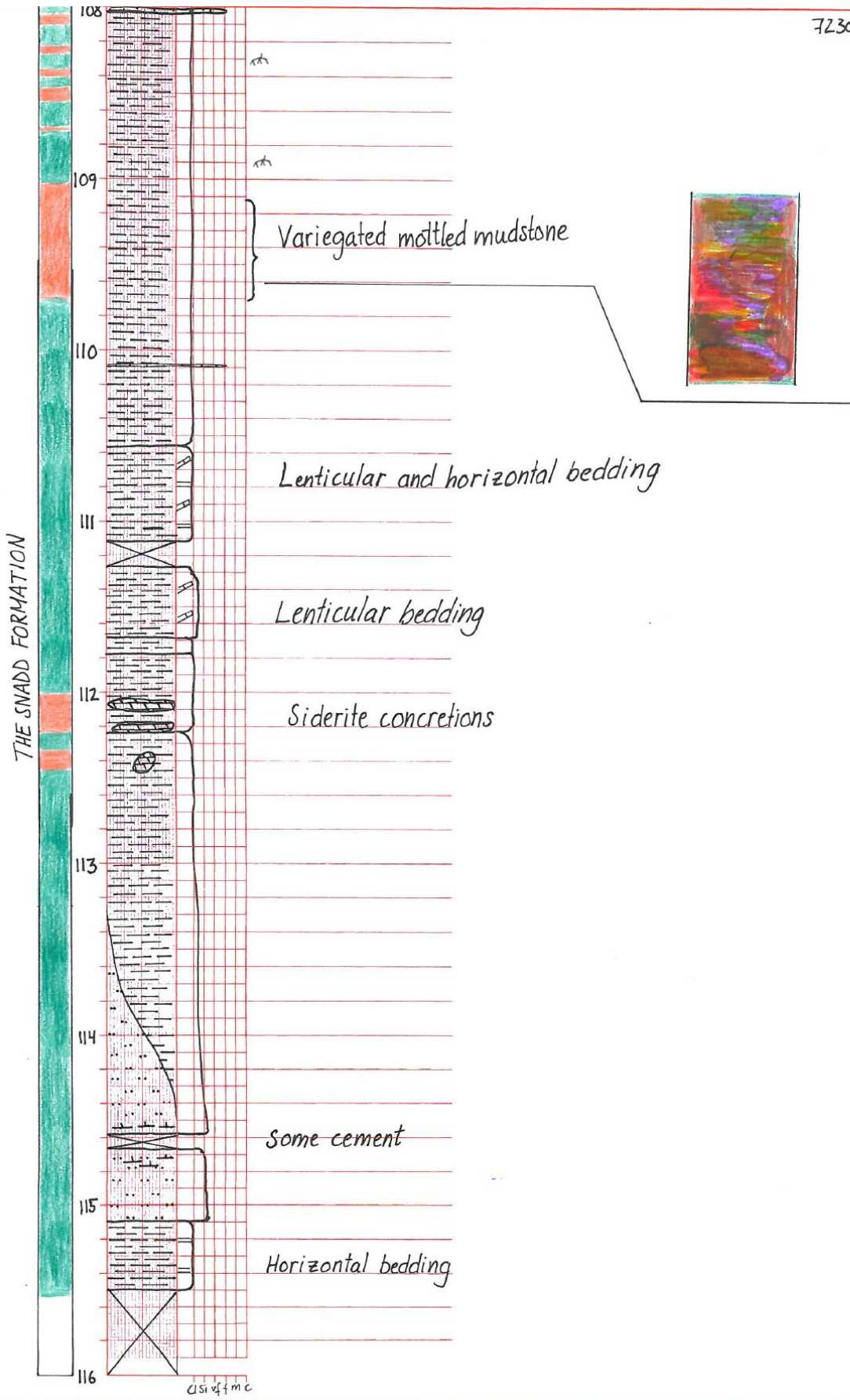
Core 7230/05-U-03 was drilled in the central eastern segment of the basin.

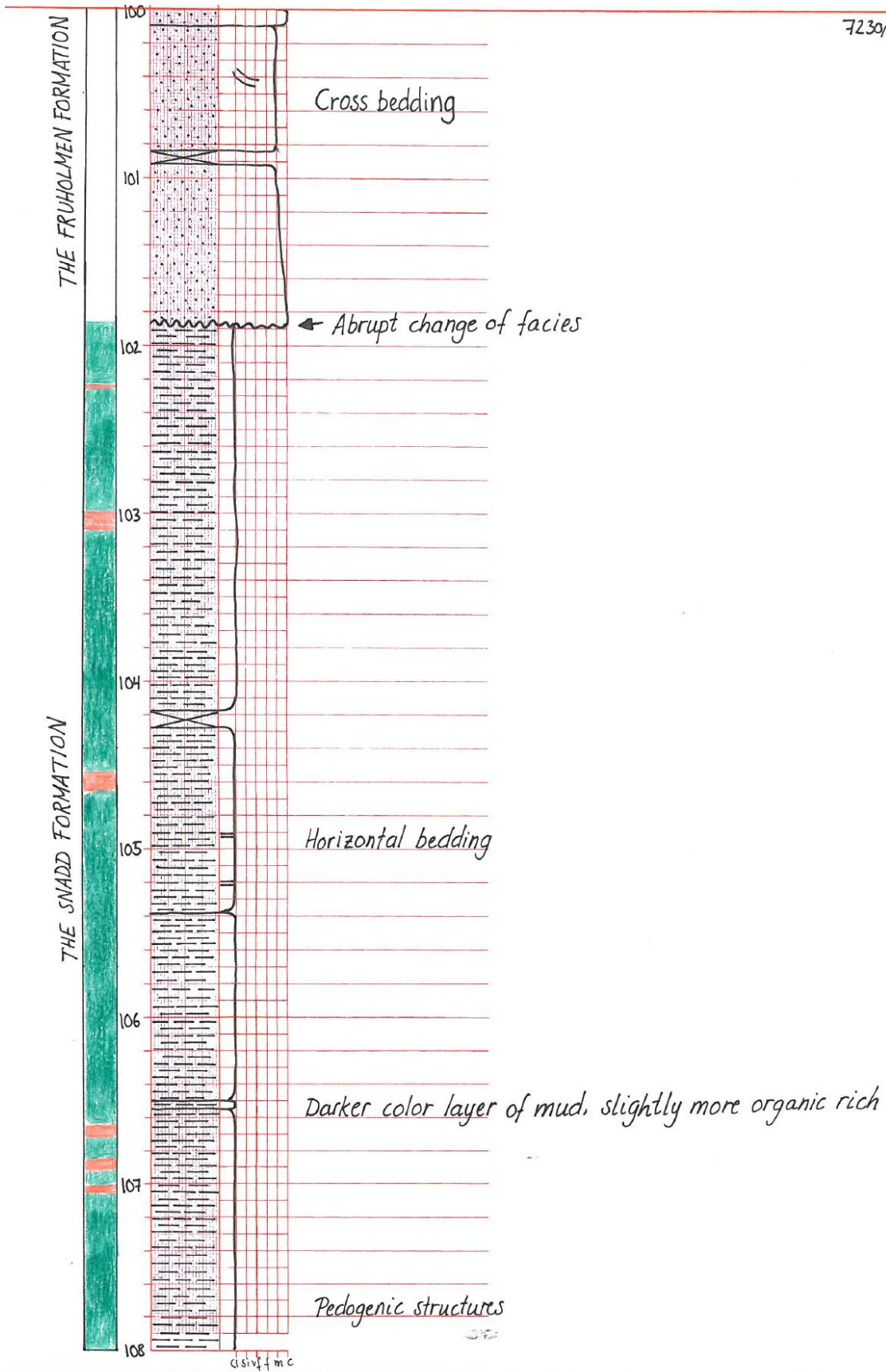
Legend

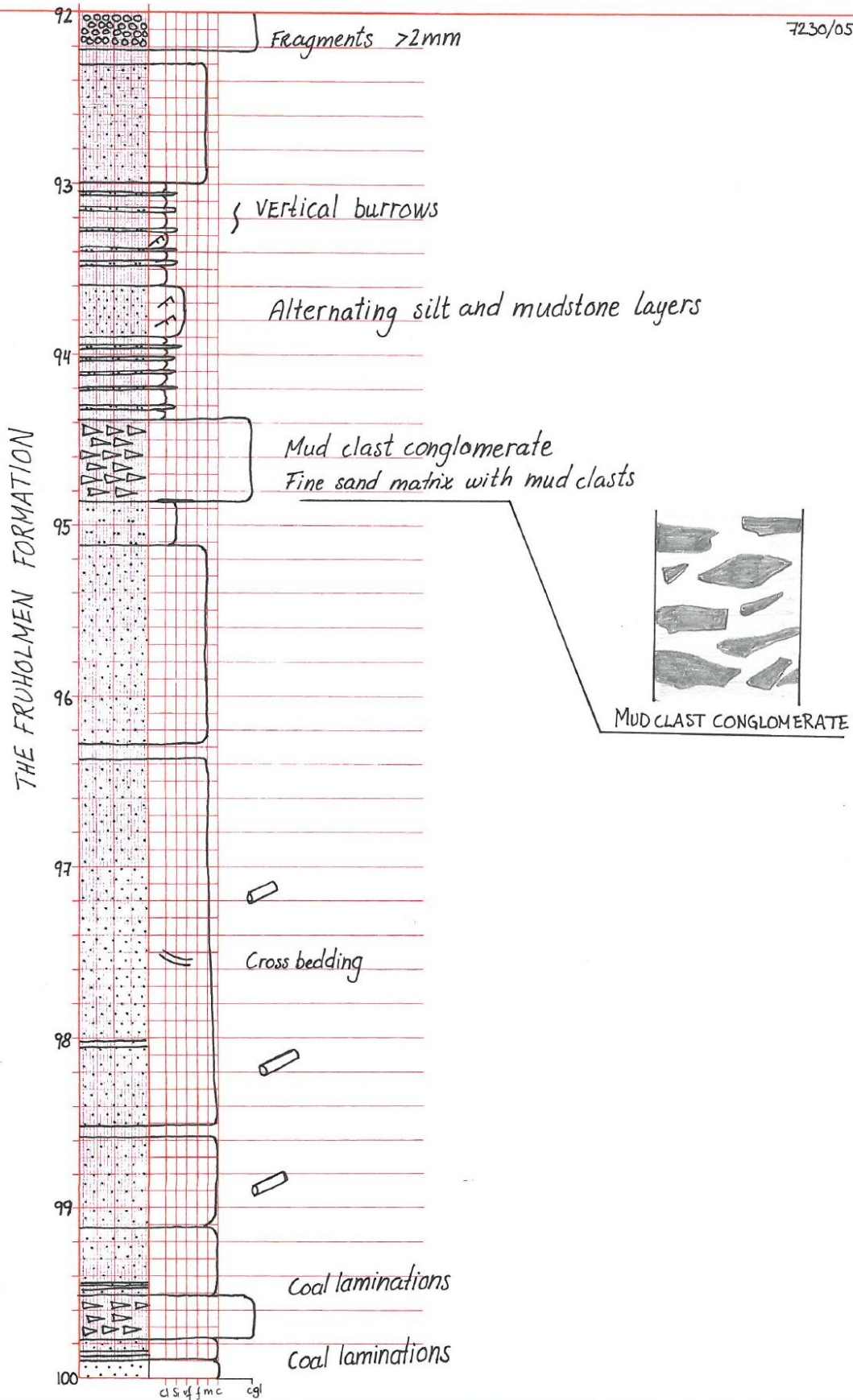
	Shale
	Sandstone
	Limestone
	Siltstone
	Conglomerate
	Coal
	Mudclast conglomerate
	Pyrite
	Wood fragments
	Roots
	Bioturbation
	Ripple lamination
	Wavy bedding
	Horizontal bedding
	Calcite cement
	Siderite cement
	Cross bedding

Color log

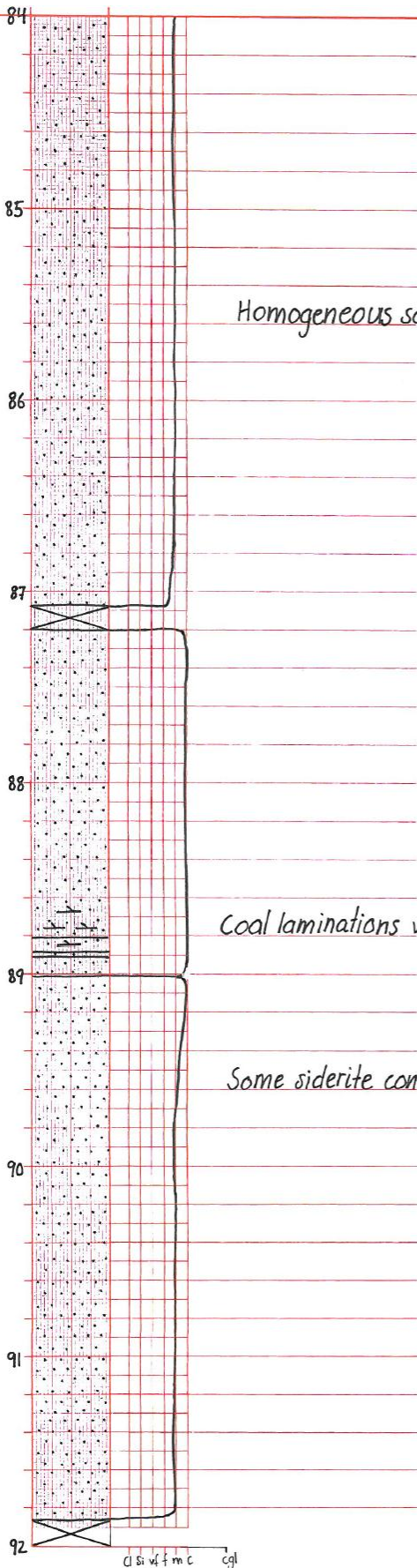
	Red coloration in sediments
	Green coloration in sediments







THE FRUHOLMEN FORMATION



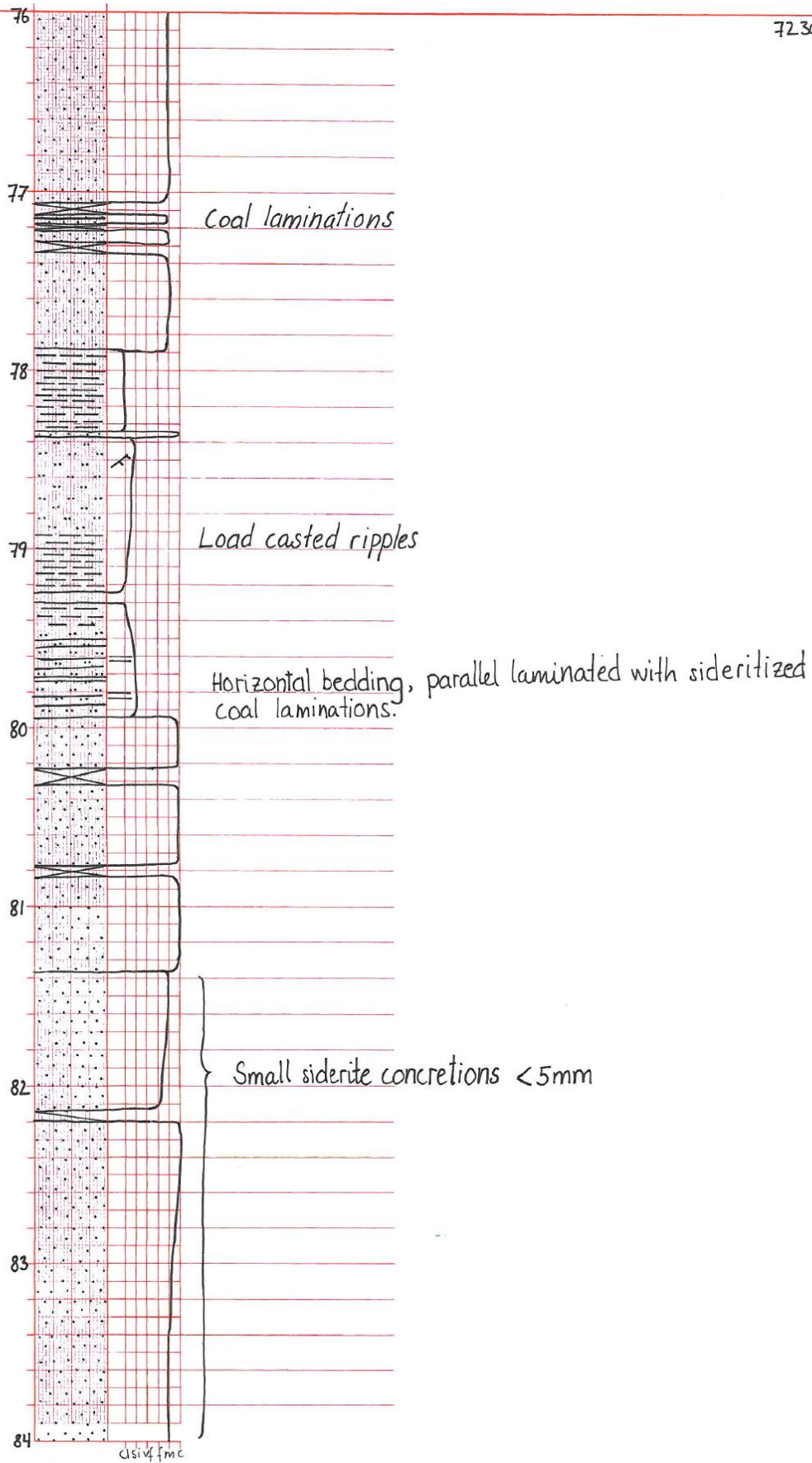
Homogeneous sand, some siderite concretions

Coal laminations with slightly red rims

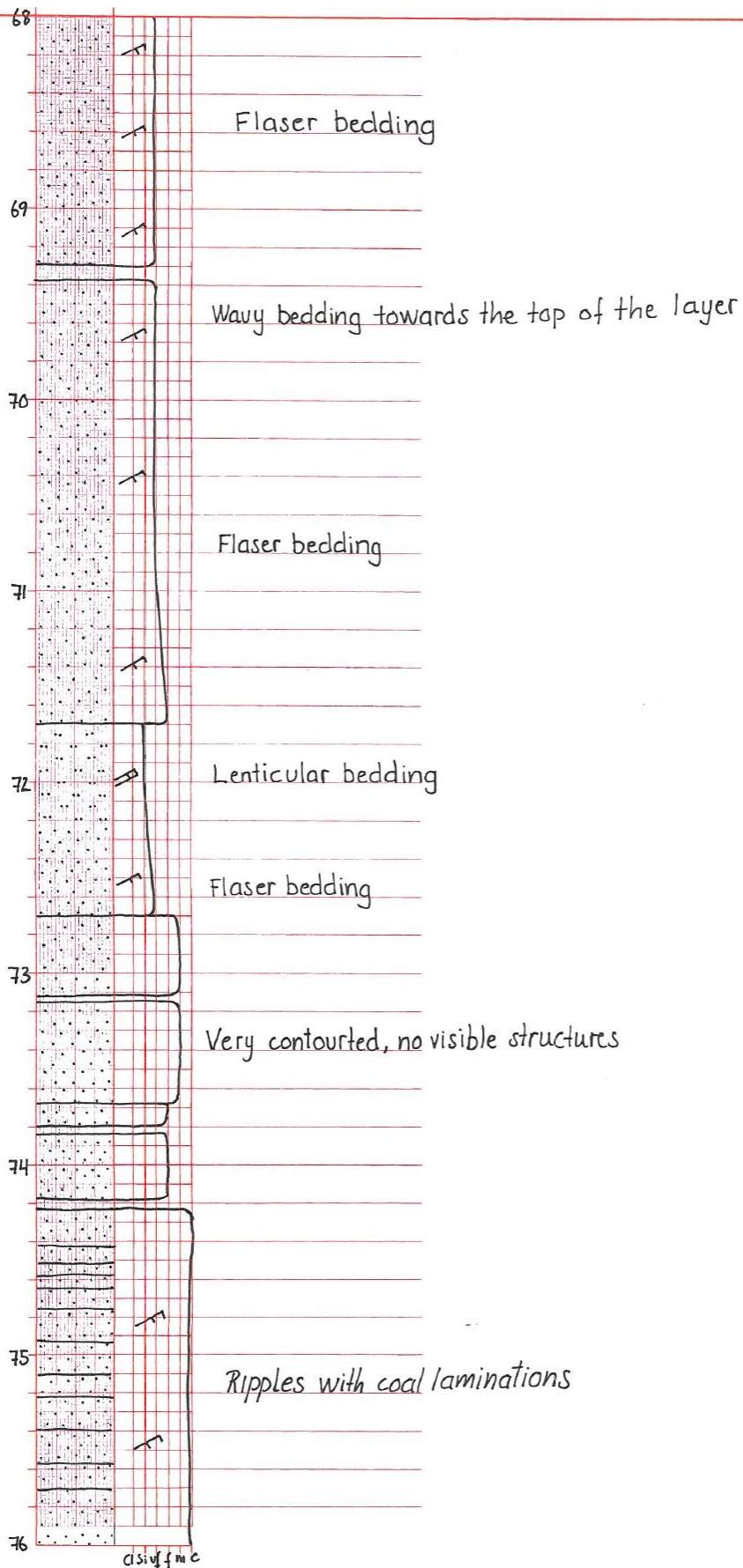
Some siderite concretions < 5mm

cl silt v. f. m. c
cgl

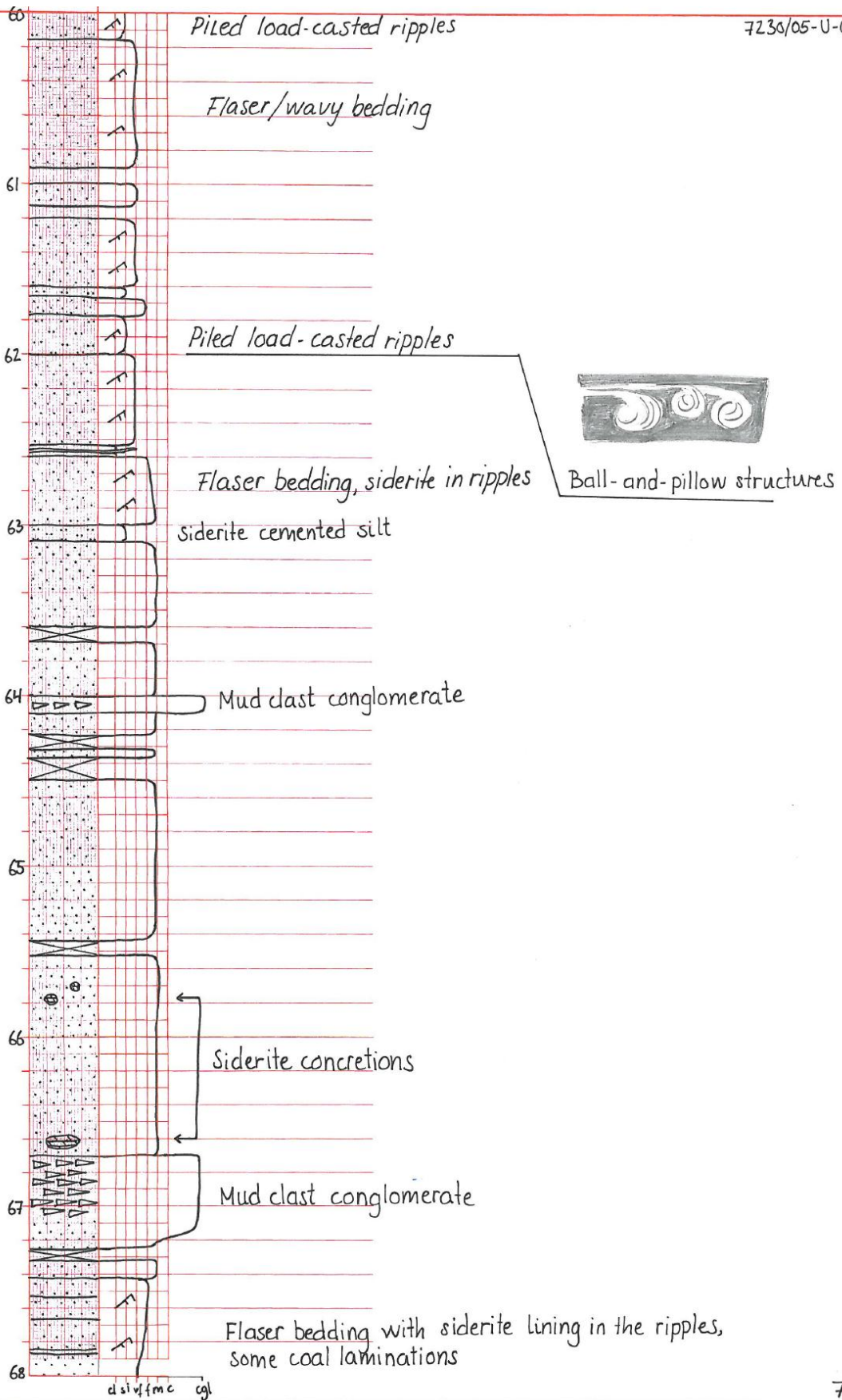
The Fruholmen Formation



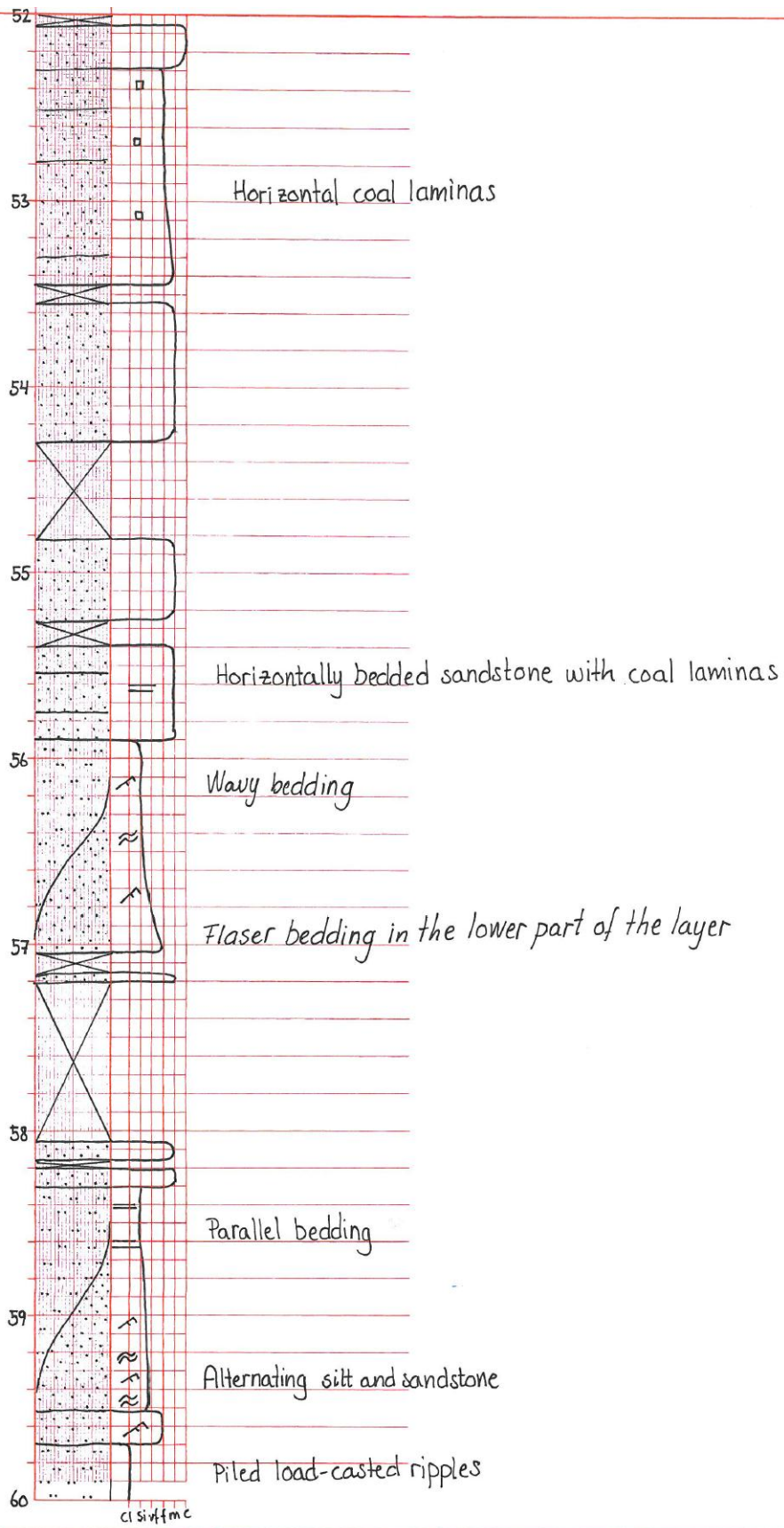
THE FRUHOLMEN FORMATION



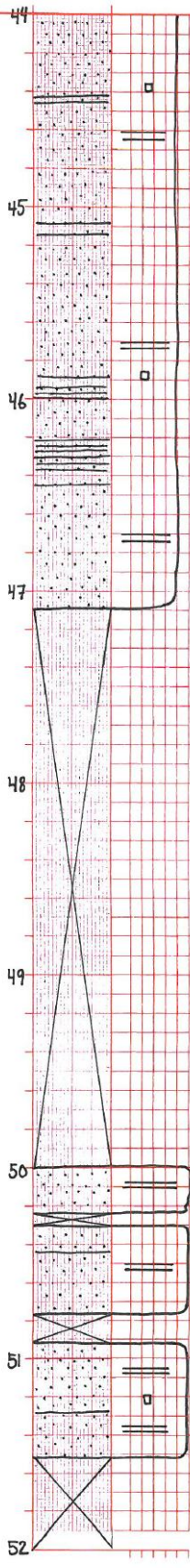
THE FRUHHOLMEN FORMATION



THE FRUHLIMEN FORMATION



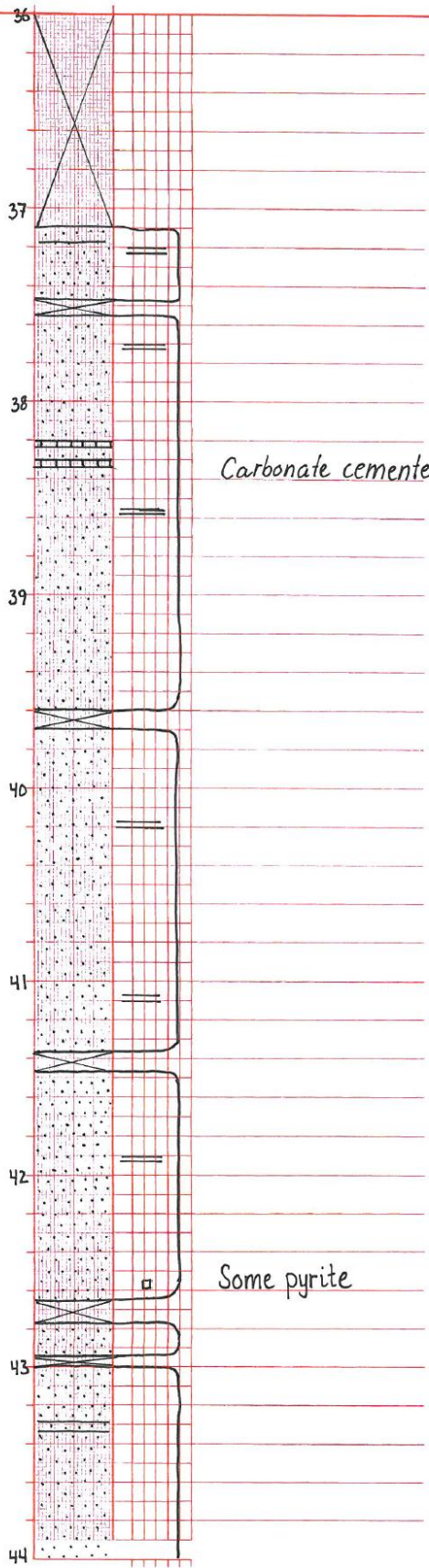
THE FRUHOLMEN FORMATION



A lot of horizontal coal laminas
Pyrite can be observed in near proximity to the laminations

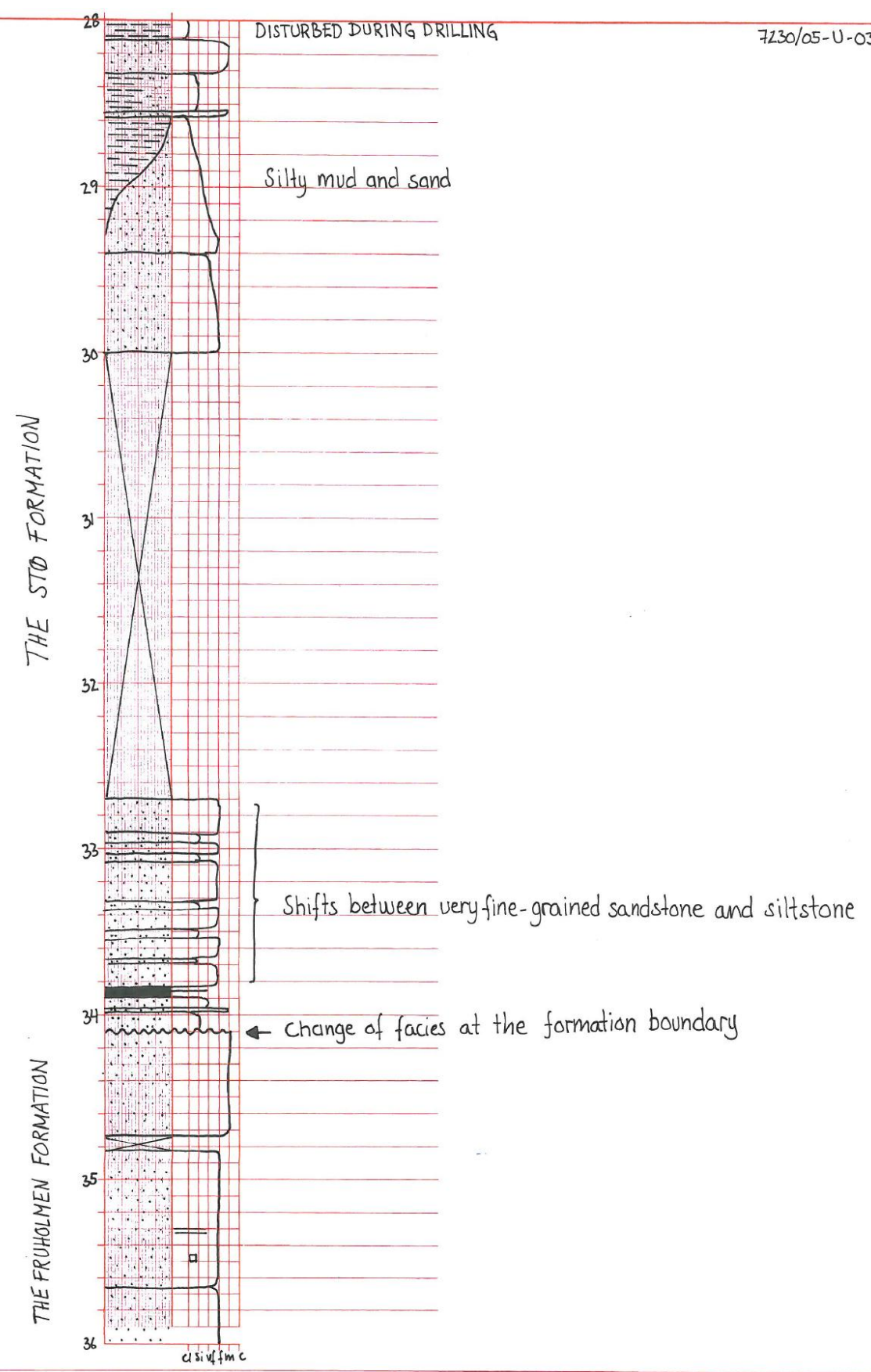
Thin horizontal coal laminas

The FRUHOLMEN FORMATION



Carbonate cemented laminae, calcite.

Some pyrite



Appendix B

Energy dispersive spectra (EDS)

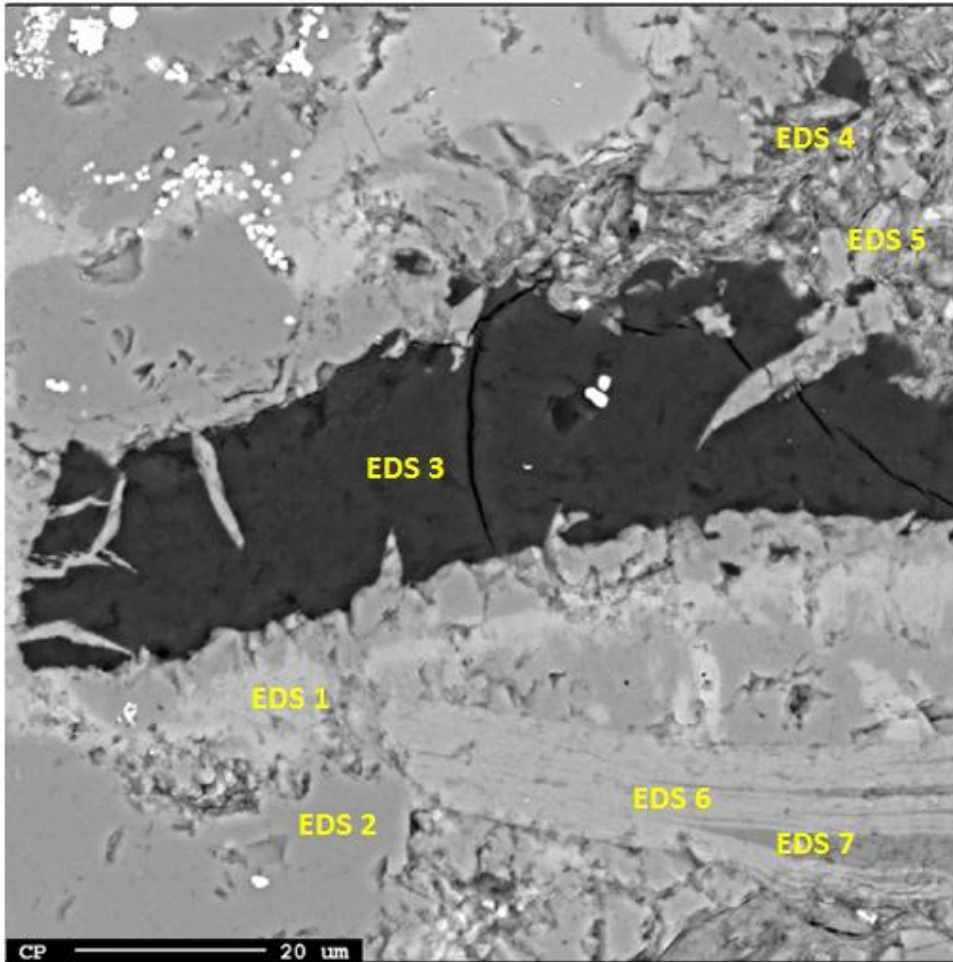
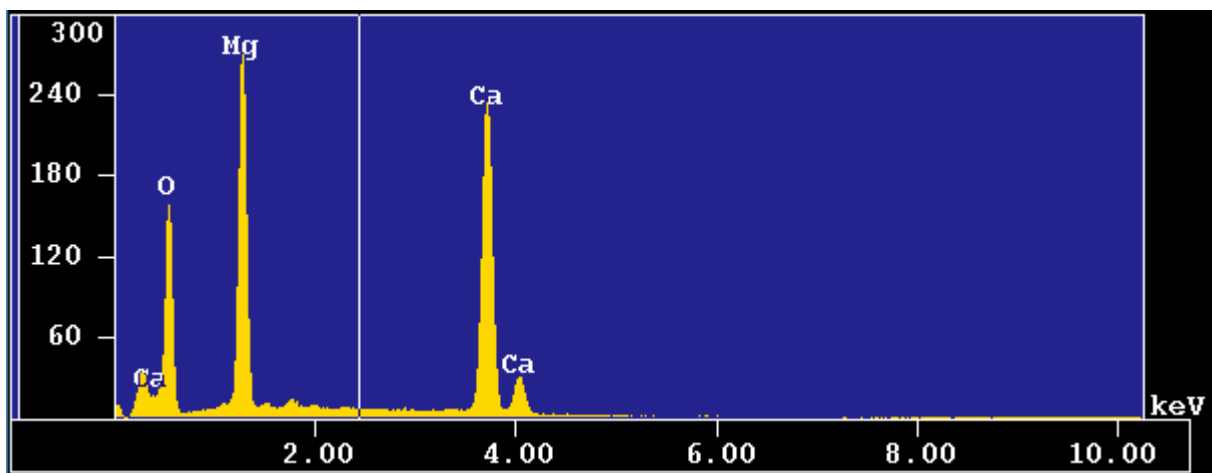


Figure B-1: Overview of the EDS analyses taken at 38.10 meters depth (7227/08-U-01).



FigureB-2: EDS1 shows a high Magnesium and Calcium content characteristic for Dolomite ($\text{CaMg}(\text{CO}_3)_2$)

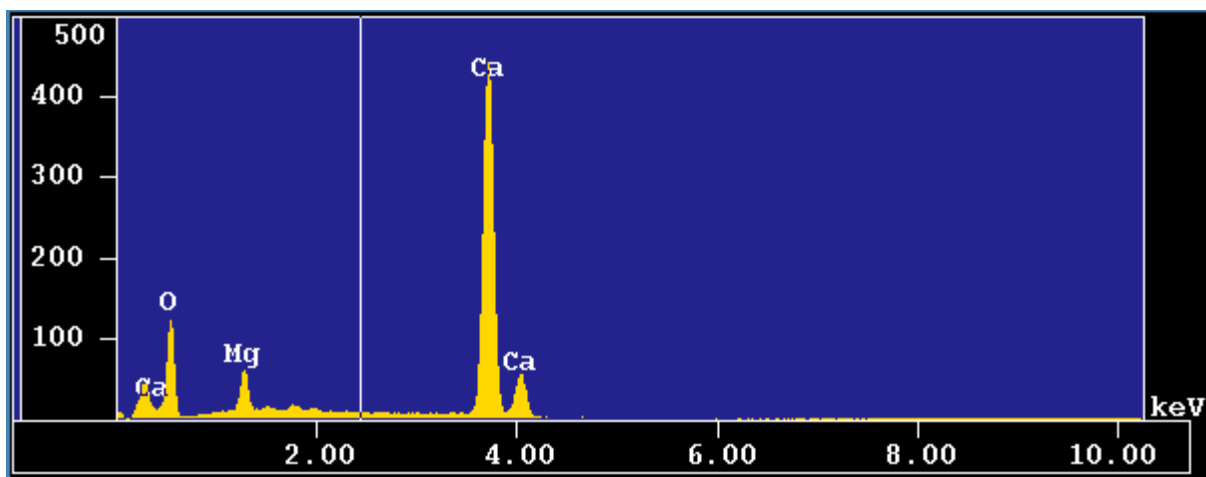


Figure B-3: The EDS2 spectra show a high Calcium content indicating that this could be Calcite (CaCO_3)

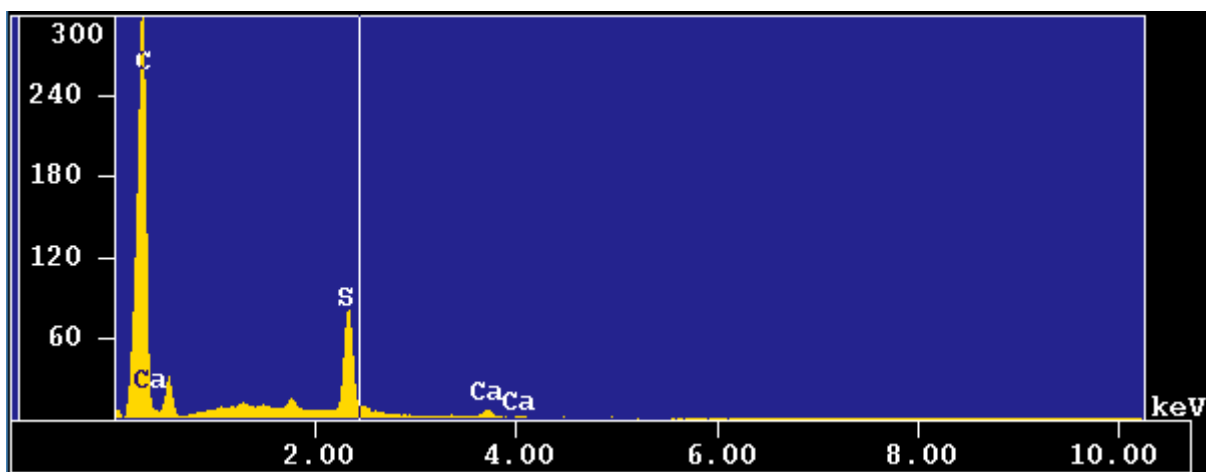


Figure B-4: This EDS3 spectra shows a high Carbon peak, and also a moderate level of Sulphur, this is probably Sulphur rich organic matter.

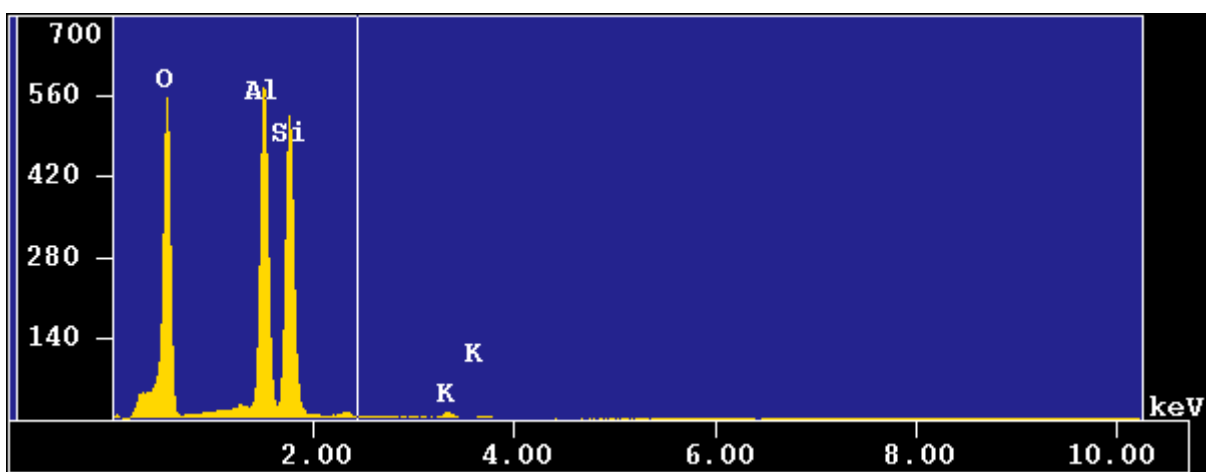


Figure B-5: The EDS4 spectra shows the fingerprint of Kaolinite.

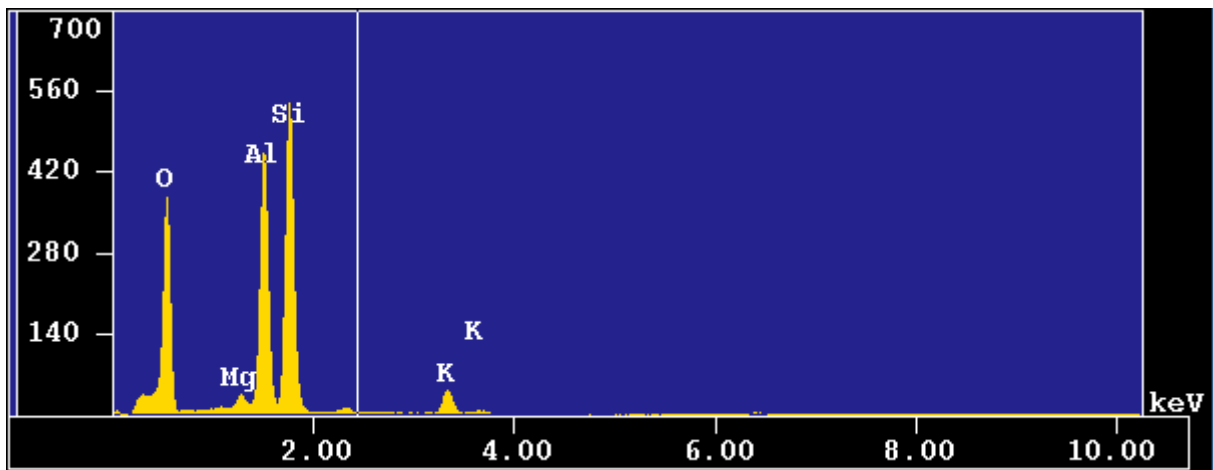


Figure B-6: This EDS5 spectra shows a higher Kalium content indicating that it is Illite.

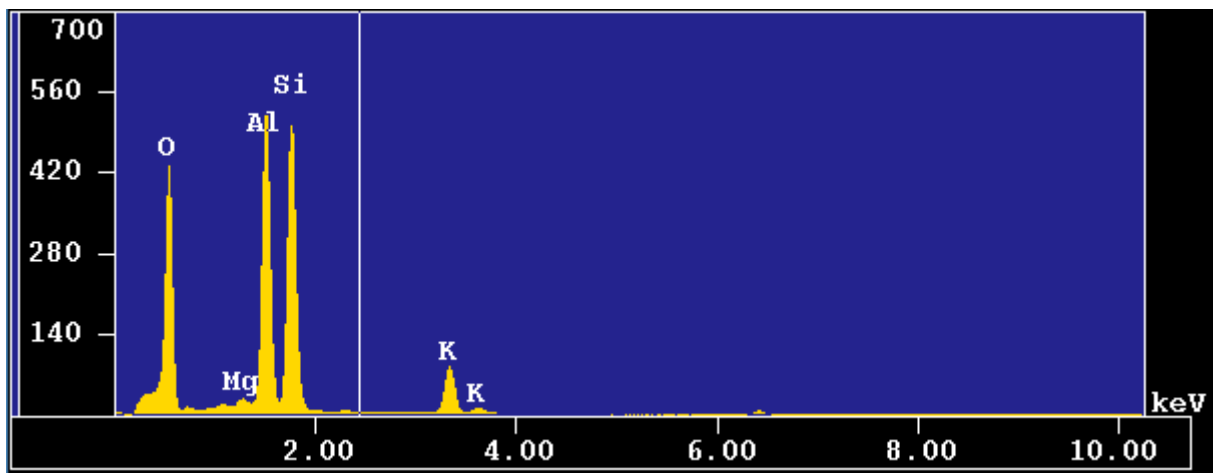


Figure B-7: A higher Aluminium content, and high Kalium content typical for Muscovite in EDS6.

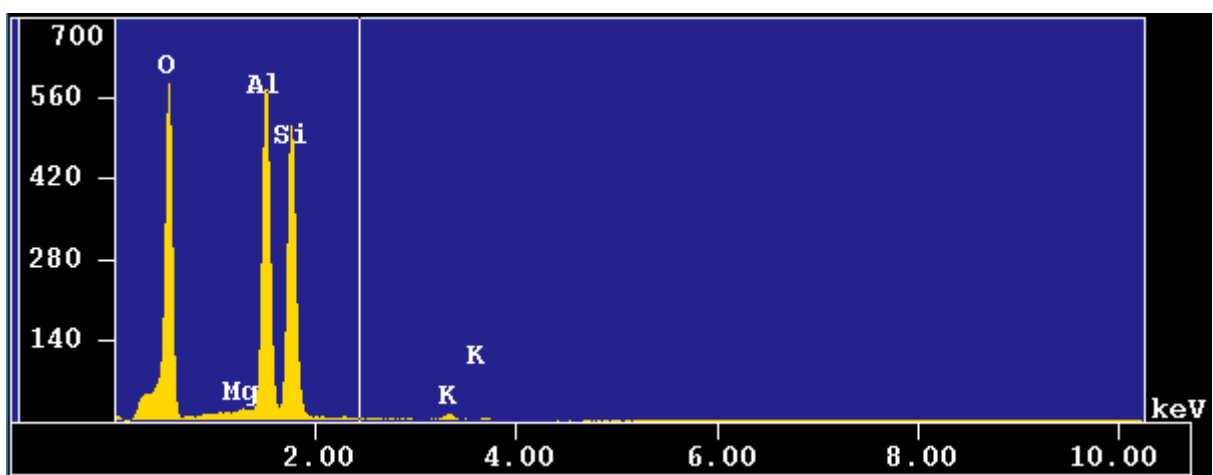


Figure B-8: The EDS7 spectra show the Kaolinite fingerprint.

Appendix C

The analysis was conducted with D8 ADVANCE. The DIFFRAC^{plus} SEARCH software in combination with the PDF-2 database suggests the following contents in the samples, sums higher than 100 are due to rounding. Due to limited opportunities only a total of six samples were analyzed in order to check for any differences above and below the formation boundary.

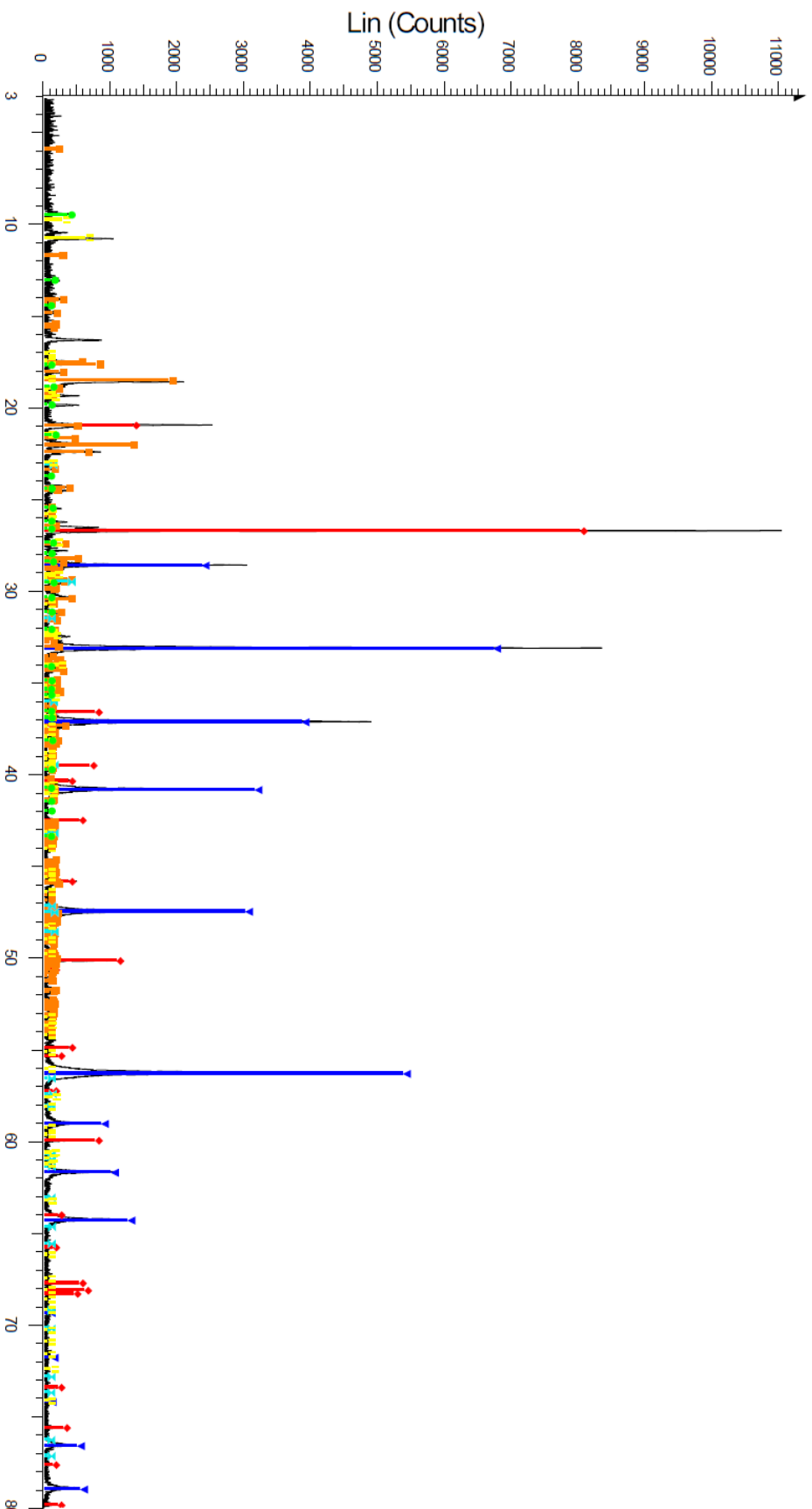
Table C-1: The quantitative XRD analysis of mudstones from the Snadd and Fruholmen formations

Sample		1	2	3	4	5	6
Journal number		120267	120268	120269	120270	120271	120272
Formation		Fruholmen Fm.	Fruholmen Fm.	Snadd Fm.	Fruholmen Fm.	Snadd Fm.	Snadd Fm.
Depth		50.50 m	58.52 m	70.25 m	79.10 m	105.98 m	112.15 m
Core		7227/08-U-01	7227/08-U-02	7227/08-U-03	7230/05-U-03	7230/05-U-04	7230/05-U-05
Mineral group	Mineral	Semi quantification (%)					
Quartz	Quartz	34	54	48	52	67	49
Mica	Biotite						
	Muscovite						
	Illite		13	12	9	15	18
Feldspar	K-feldspar		10	9	14	8	10
	Plagioclase			12	7		13
Kaolinite-Serpentinite	Kaolinite		21	11	11	10	11
Calcite	Calcite	2					
	Anatase		2	2			
Chlorite	Clinocllore			7	7		
Pyrite	Pyrite	36					
	Romerite	24					
Zeolite	Laumonite	2					
Amphibole	Cummingtonite	2					
Sum		100	100	101	100	100	101

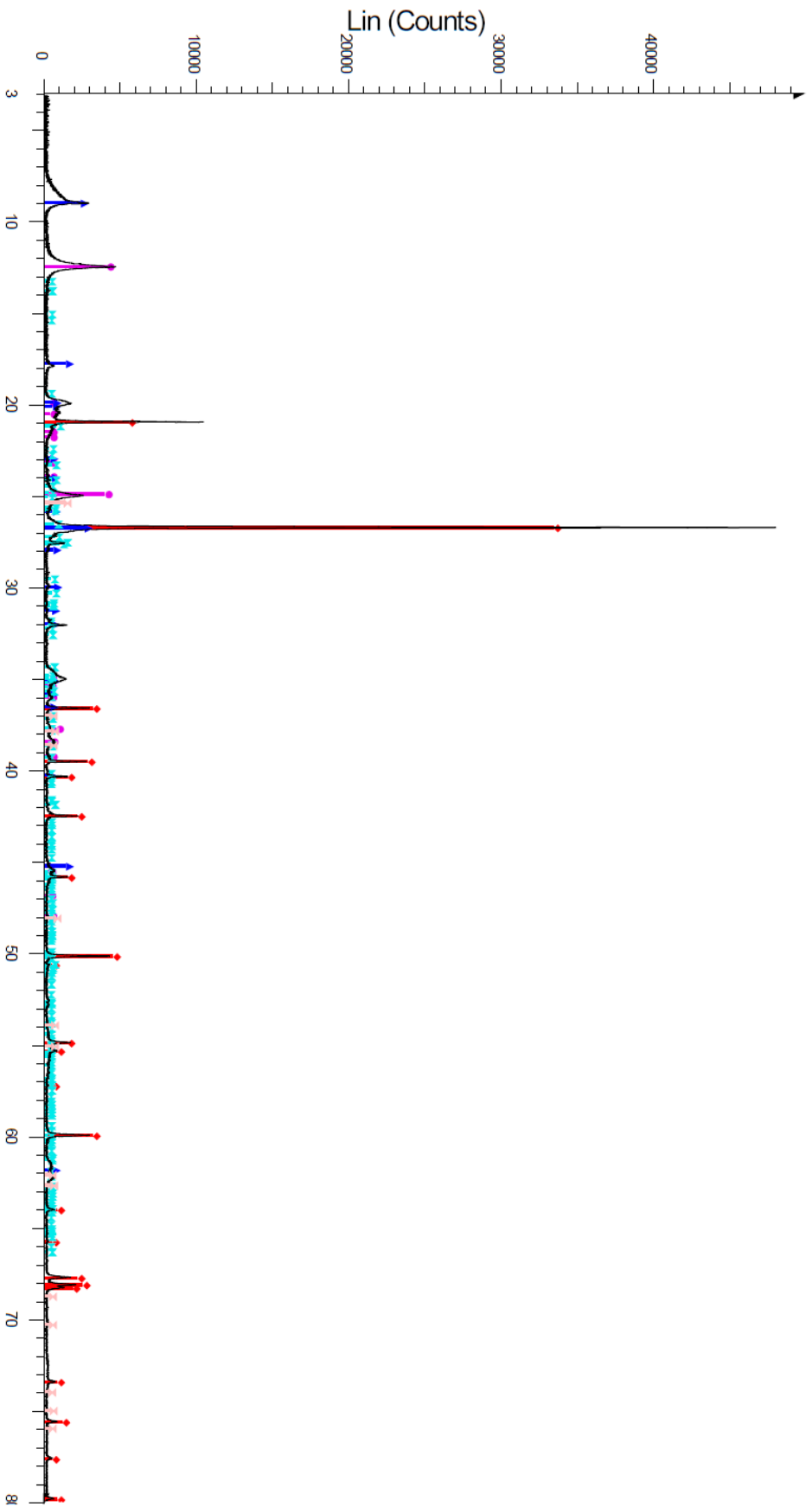
Sample 1 was taken from the concretion described in section 4.1.1, Fruholmen Formation (Fig. 4-4, b) and is therefore not directly comparable with the other samples. XRD was applied in order to identify the content in the concretion. In sample 1 the secondary peak does not match Cummingtonite perfectly, but it is in the amphibole area and has been found to be the closest match. In this sample there are also two unidentified peaks. Romerite has also been identified in this sample as it is an oxidation product of iron sulphide and therefore a probable match in this setting.

The remaining samples are collected from similar facies above and below the formation boundaries in both cores.

1 - Jnr 120267



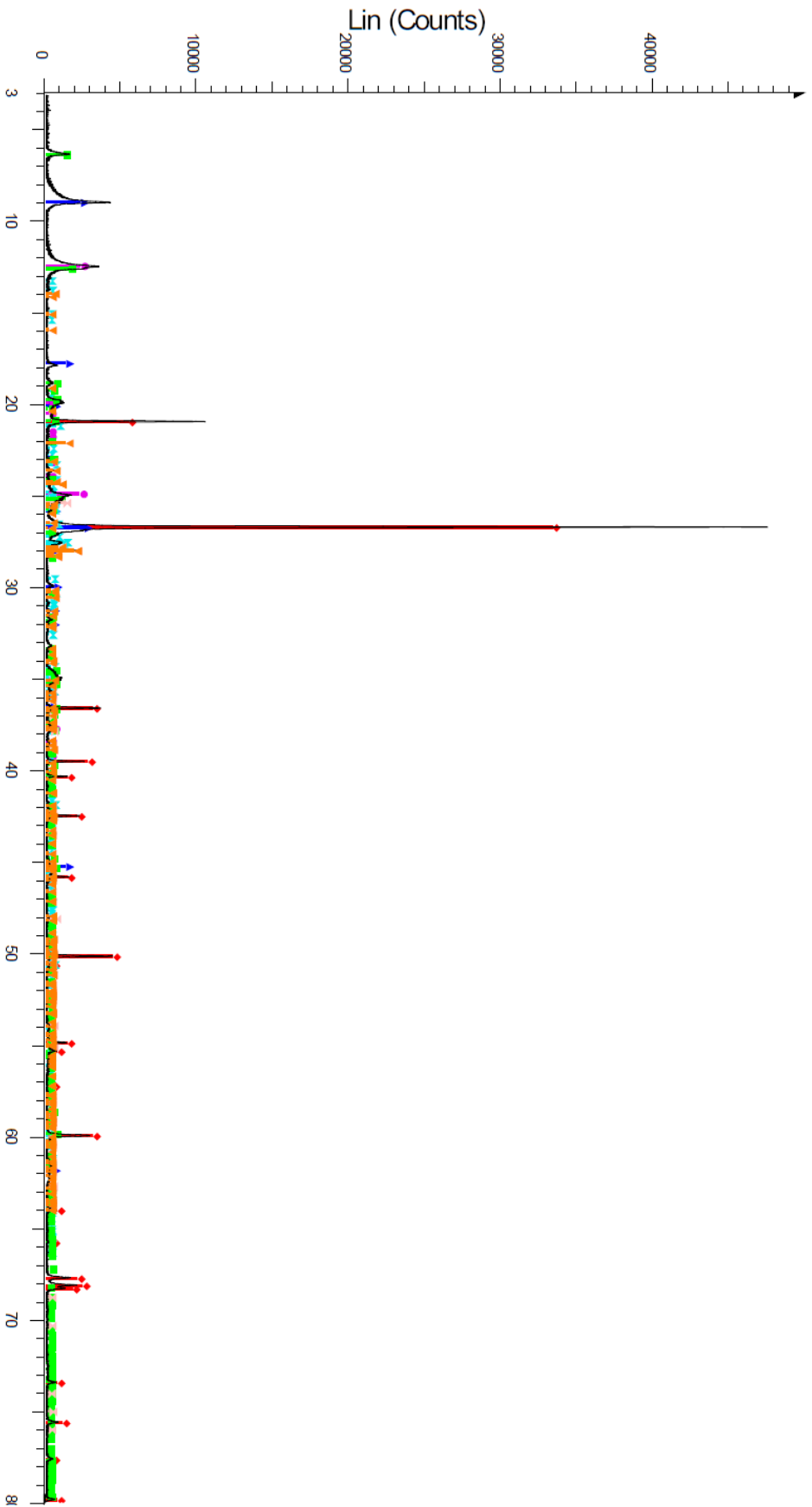
2 - Jnr 120268



KJ 120268wr - File: 120268wr.raw - Type: 2Th/T θ locked - Start: 3.000 ° - End: 80.000 ° - Step: 0.009 ° - Step time: 174. s - Temp.: 25 °C (Room) - Time Started: 18 s - 2-Theta: 3.000 ° - Theta: 1.500 ° - Chi
Operations: Strip kAlpha2 0.5001 Background 0.977, 1.0001 Import

- ◆ 00-046-1045 (*) - Quartz, syn - SiO₂ - S-Q 53.5 %
- ◆ 00-058-2004 (I) - Kadirite-1A - Al₂Si₂O₅(OH)₄ - S-Q 21.4 %
- ◆ 00-026-0911 (I) - Ilite-2M1 (NR) - (K,H₃O)Al₂Si₃AlO₁₀(OH)₂ - S-Q 13.4 %
- ◆ 01-072-1114 (*) - Microcline - KAlSi₃O₈ - S-Q 10.0 %
- ◆ 00-021-1272 (*) - Anatase, syn - TiO₂ - S-Q 1.7 %

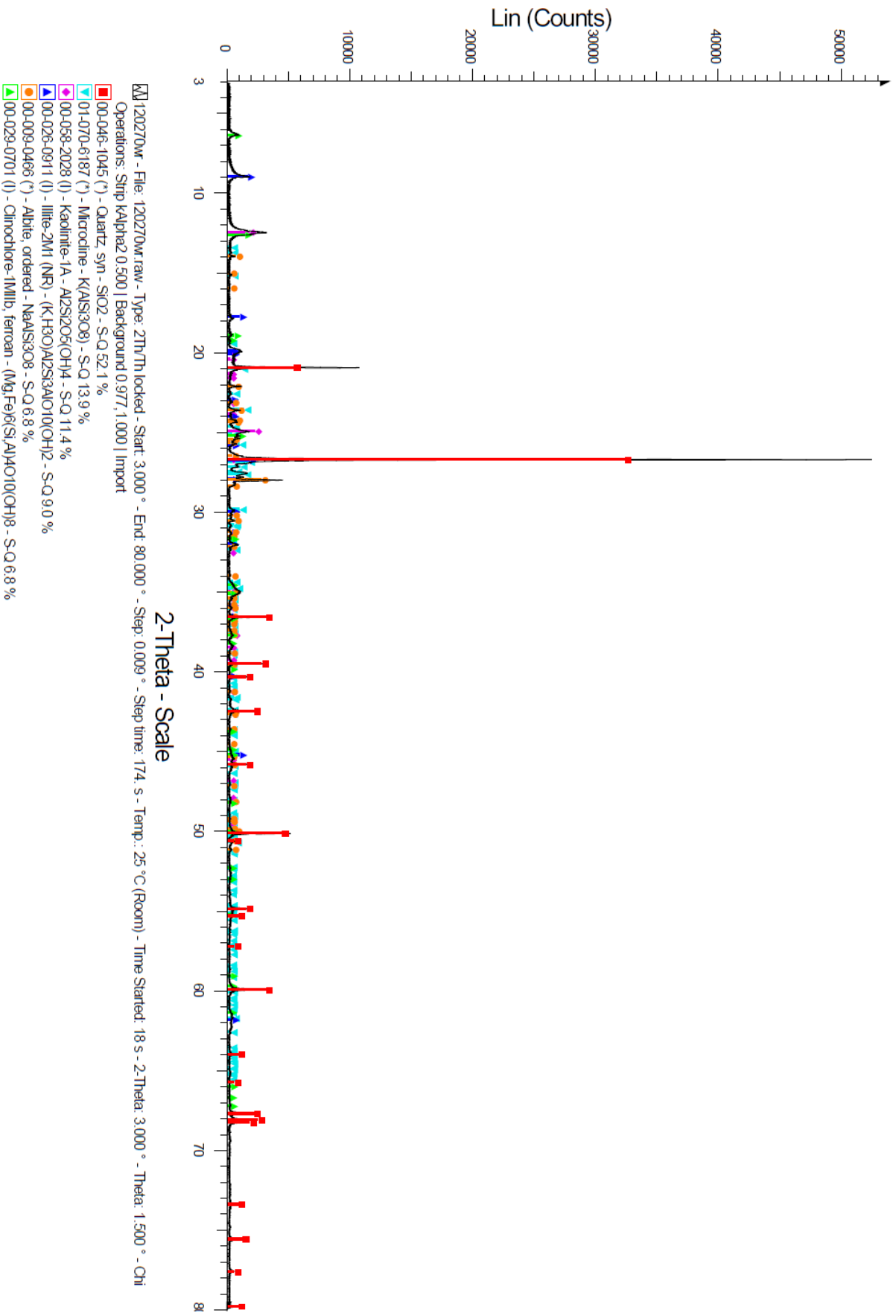
3 - Jnr 120269



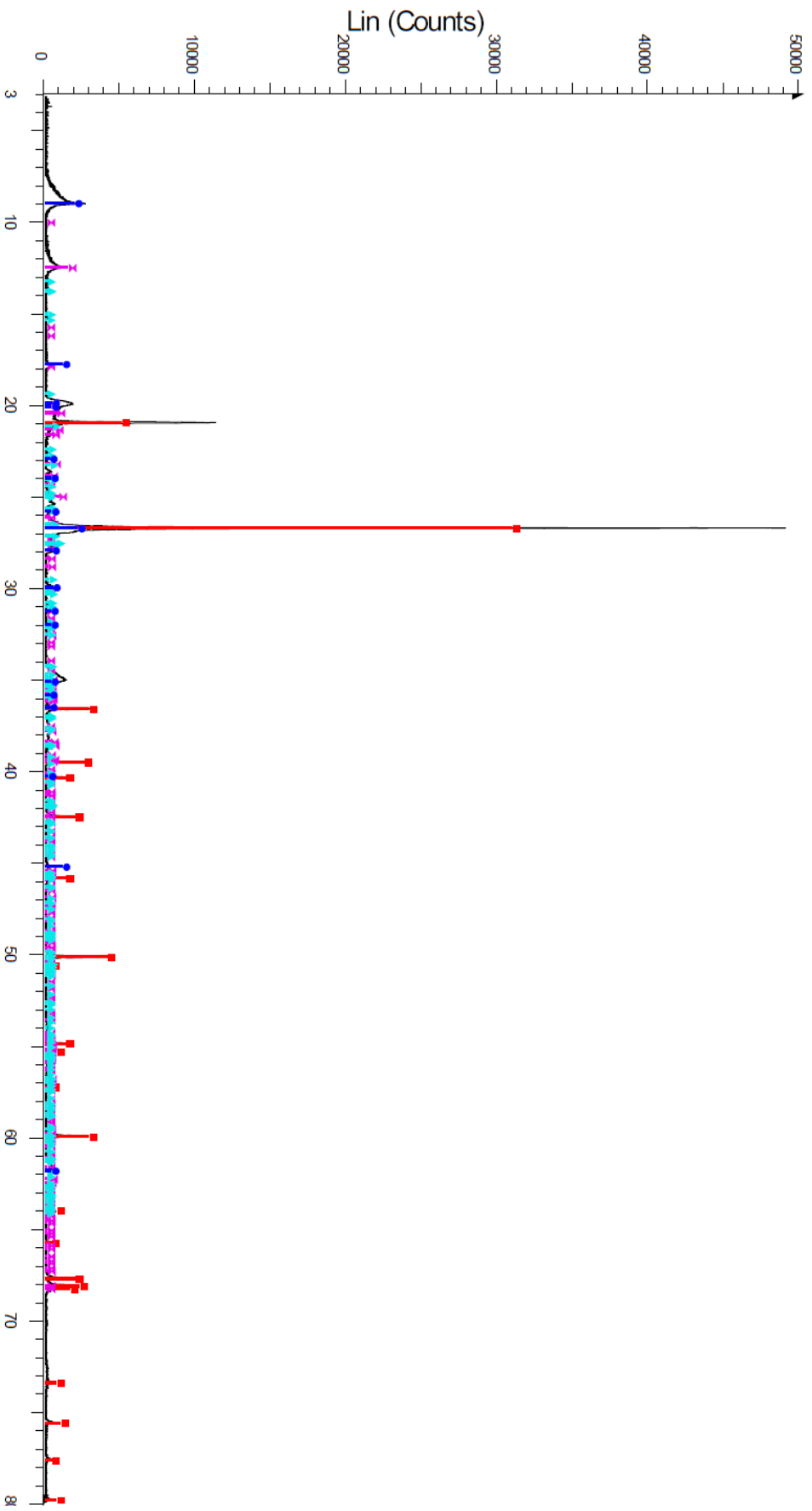
File: 120269w.raw - Type: 2Th/Th locked - Start: 3.000 ° - End: 80.000 ° - Step: 0.009
Operations: Strip kAlpha2 0.500 | Background 0.977, 1.000 | Import

- 00-046-1045 (*) - Quartz - SiO₂ - S-Q 47.8 %
- 01-070-3752 (I) - Albite - (Na₀98Ca₀02)(Al₁02Si₂98O₈) - S-Q 12.3 %
- 00-026-0911 (I) - Illite-2M1 (NR) - (K₁H₃O)Al₂Si₃AlO₁₀(OH)₂ - S-Q 11.9 %
- 00-068-2004 (I) - Kaolinite-1A - Al₂Si₂O₅(OH)₄ - S-Q 10.8 %
- 01-072-1114 (*) - Microcline - KAlSi₃O₈ - S-Q 8.9 %
- 01-079-1270 (*) - Clinocllore - (Mg₂96Fe₁55Fe₁36Al₁27Si₂622Al₁376O₁₀)(OH)₈ - S-Q 6.6 %

4 - Jnr 120270



5 - Jnr 120271



KJ 120271.wr - File: 120271.wr.raw - Type: 2Th/Th locked - Start: 3.000 ° - End: 80.000 ° - Step: 0.009 ° - Step time: 174. s - Temp.: 25 °C (Room) - Time Started: 18 s - 2-Theta: 3.000 ° - Theta: 1.500 ° - Chi

Operations: Strip KAlpha2 0.500 | Background 0.977, 1.000 | Import

00-046-1045 (*) - Quartz, syn - SiO2 - S-Q 67.2 %

00-026-0911 (I) - Illite-2M1 (NR) - (K,H3O)Al2Si3AlO10(OH)2 - S-Q 15.0 %

01-080-0886 (I) - Kaolinite-1A - Al2(Si2O5)(OH)4 - S-Q 9.7 %

01-084-1455 (*) - Microcline - (K,95Na,05)AlSi3O8 - S-Q 8.1 %

6 - Jnr 120272

